0008-7114

Caryologia

2023
Vol. 76 - n. 2

International Journal of Cytology, Cytosystematics and Cytogenetics

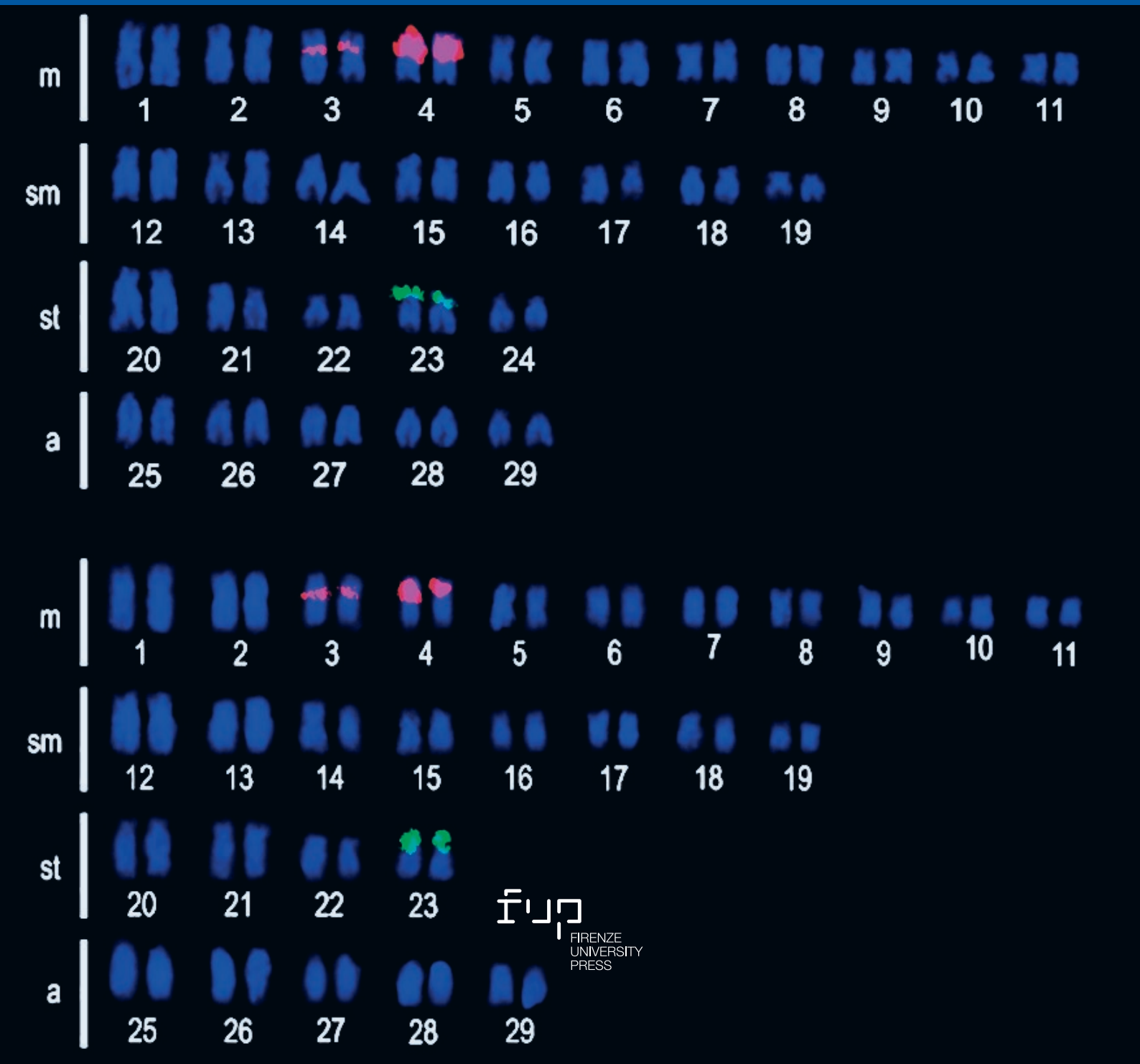

FIRENZE UNIVERSITY PRESS

Caryologia. International Journal of Cytology, Cytosystematics and Cytogenetics

Caryologia is devoted to the publication of original papers, and occasionally of reviews, about plant, animal and human karyological, cytological, cytogenetic, embryological and ultrastructural studies. Articles about the structure, the organization and the biological events relating to DNA and chromatin organization in eukaryotic cells are considered. *Caryologia* has a strong tradition in plant and animal cytosystematics and in cytotoxicology. Bioinformatics articles may be considered, but only if they have an emphasis on the relationship between the nucleus and cytoplasm and/or the structural organization of the eukaryotic cell.

Cover: figure from the article inside by Mauricio Barros Fernandes, Jamille de Araújo Bitencourt, Joandson Calixto dos Santos, José Henrique Galdino, Paulo Roberto Antunes de Mello Affonso. Cytogenetic analysis in *Tetragonopterus franciscoensis* (Characiformes): another piece to the karyoevolutionary puzzle of tetra fishes.

Caryologia

International Journal of Cytology, Cytosystematics and Cytogenetics

Volume 76, Issue 2 - 2023

Firenze University Press

***Caryologia*. International Journal of Cytology, Cytosystematics and Cytogenetics**
Published by
Firenze University Press – University of Florence, Italy
Via Cittadella, 7 - 50144 Florence - Italy
http://www.fupress.com/caryologia

Caryologia
International Journal of Cytology, Cytosystematics and Cytogenetics

Firenze University Press
www.fupress.com/caryologia

OPEN ACCESS

Citation: Fatima Omari Alzahrani, Sami Asir Al-Robai (2023). Molecular classification of Barbeyaceae (*Barbeya oleoides* Schweinf.) using four different DNA barcodes. *Caryologia* 76(2): 3-13. doi: 10.36253/caryologia-1857

Received: October 3, 2022

Accepted: July 3, 2023

Published: December 31, 2023

Data Availability Statement: All relevant data are within the paper and its Supporting Information files.

Competing Interests: The Author(s) declare(s) no conflict of interest.

Molecular classification of Barbeyaceae (*Barbeya oleoides* Schweinf.) using four different DNA barcodes

Fatima Omari Alzahrani, Sami Asir Al-Robai

Department of Biology, Faculty of Science, Al-Baha University, Al-Baha, Saudi Arabia
E-mail: drfatimaomari@gmail.com, dr.alrobai@gmail.com; ,fsalomari@bu.edu.sa, sal-robai@bu.edu.sa

Abstract. Despite many efforts to determine the phylogenetic relationship between Barbeyaceae and other families of Rosales, the sister relationship of this family has remained unclear. *Barbeya oleoides*, which is currently the only species in the family Barbeyaceae, and native to Somalia, Ethiopia, and the Arabian Peninsula were collected from Wadi Turbah Zahran northwestern of Al-Baha City, southwestern Saudi Arabia (20°14'N, 41°15'E). To study the sister relationship of Barbeyaceae and the other families of Rosales, the complete chloroplast sequences were used for phylogenetic analysis. In addition, four standard DNA barcodes (the internal transcribed spacer 2 (ITS2), ribulose 1,5-biphosphate carboxylase (rbcL), maturase K (matk), the intergenic spacer region (trnH-psbA)) were used to test for their quality in identifying phylogenetic relationship of the studied families. Sequence analysis of the complete chloroplast sequences showed that Rosales clade has two subclades and clearly discriminated all families within this order. This is the first report of a partial ITS2 locus sequence in *B. oleoides*. The partial ITS2, rbcL, matk, and gene sequences discriminate *B. oleoides* of the Barbeyaceae family from the closely related plant families: Cannabaceae, Rosaceae, Rhamnaceae, Urticaceae, Moraceae, Elaeagnaceae, Dirachmaceae, and Ulmaceae. In contrast, the partial trnH-psbA sequence of *B. oleoides* did not show any homology to the available DNA sequence of plant families in GenBank, suggesting that it is more suitable as DNA barcode for variations within one species.

Keywords: DNA barcoding, phylogenetic analysis, ITS2, rbcL, matK, trnH-psbA.

Abbreviations:

B. oleoides: Barbeya oleoides Schweinf.
ITS2: the internal transcribed spacer 2
rbcL: ribulose 1,5-biphosphate carboxylase
matk: maturase K
trnH-psbA: the intergenic spacer region
w/v: wight/volume
IUCN: The International Union for Conservation of Nature

1. INTRODUCTION

Barbeya oleoides Schweinf. (*B. oleoides*) is the only species in the family Barbeyaceae and considered one of the smallest families in the plant kingdom (Dickison and Sweitzer, 1970, Chaudhary, 1999). Barbeyaceae belongs to the order Rosales, which comprises eight families besides Barbeyaceae: Cannabaceae, Dirachmaceae, Elaeagnaceae, Moraceae, Rhamnaceae, Rosaceae, Ulmaceae, and Urticaceae (Angiosperm Phylogeny Group (APG), 1998, 2003, 2009). *B. oleoides* is a small olea-like tree, reaching a height of up to 5 m, and can be found as a bushy shrub. The plant is characterized by dense hairs that cover the lower surfaces of the leaves. It is widely distributed in southwestern Saudi Arabia, including the Al-Baha region and locally known as kathah in Arabic–(Dickison and Sweitzer, 1970). In Al-Baha region, the plant was reported only in seven locations between 1454 and 1768 masl on drainage lines facing the southwest and northeast (Namazi et al., 2021).

B. oleoides is considered a medicinal plant in Saudi Arabia and used as a folkloric remedy for the treatment of diseases such as infection, edema, or related inflammatory diseases (Baka, 2010). Few local studies have evaluated the medicinal effects of different plant parts, including leaves and stems (Ahmed et al., 2002; Khojah et al., 2021). The International Union for Conservation of Nature (IUCN) categorized *B. oleoides* as the least concerned taxon. However, it represents a monotypic taxon, implying the importance of taxonomic and phylogenetic studies on this plant (Rana and Ranade, 2009; Sarwar and Araki, 2010).

DNA barcoding is widely used as an effective tool to identify species and to make the obtained data publicly available to help understand, conserve, and utilize biodiversity. DNA barcodes in plants are usually located in the chloroplast genome, either within coding sequences (such as maturase K (matK) and ribulose bisphosphate carboxylase (rbcL)) or in intergenic regions (such as the chloroplast trnH-psbA spacer region), or located at nuclear loci (such as the internal transcribed spacer of ribosomal DNA2 (ITS2)) (CBOL Plant Working Group, 2009; China Plant BOL Group, 2011: Li et al., 2015). The combination of these markers is important to achieve the highest discriminatory power and molecular identification of species.

The aim of this study was to investigate the phylogenetic relationship and molecular identification of *B. oleoides* using the whole chloroplast genome and four different barcodes of plant DNA. The sequences of rbcL, matk, and trnH-psbA loci were compared to those available for *B. oleoides* in the NCBI GenBank database; however, the current study is considered the first report on the amplification and sequencing of the ITS2 region of the *B. oleoides* genome.

2. MATERIALS AND METHODS

2.1 Plant materials and DNA extraction

The plant samples were collected from Wadi Turbah Zahran, northwestern Al-Baha City, southwestern Saudi Arabia (20°14'N, 41°15'E). Total genomic DNA was extracted from 50 mg of fresh leaves using the CTAB extraction method described by Aboul-Maaty and Oraby (2019). The 3× CTAB extraction buffer contained 3% CTAB (w/v), NaCl, 0.8 M Tris-HCl pH 8.0), and EDTA (0.5 M EDTA pH 8.0). Compound 2 was preheated to 65 °C and 3% 2-β-mercaptoethanol was added to 3× CTAB extraction buffer immediately before use. Then, 800 μL of this buffer was added to the plant samples, which were ground into a powder using liquid nitrogen. The mixture was incubated in a water bath at 60–65 °C for 1 h and mixed gently every 20 min by inverting each tube 20 times. After cooling the mixture to room temperature, an equal volume of chloroform was added. The mixture was centrifuged at 13,000 rpm for 15 min at room temperature. The upper aqueous phase was then transferred to a new 1.5-mL Eppendorf tube. NaCl (6 M) with a volume equal to half the volume of the upper aqueous phase and 3 M potassium acetate (1/10 the volume of the upper aqueous phase) were added and simultaneously mixed with ice-cold 100% isopropyl alcohol (approximately two-thirds of the volume of the aqueous phase).

The extracted DNA was quantified using a UV spectrophotometer (NanoDrop 2000 Spectrophotometer; Thermo Scientific, UK).

2.2 PCR amplification and sequencing

The sequences of the primers used for amplification of the investigated regions are shown in Table 1. Amplifications were performed in 50-μL reactions. DNA amplification was carried out using PCR TECHNE (GMI, USA) and the conditions were as follows: pre-denaturation at 94 °C for 3 min followed by 34 cycles of denaturation at 94 °C for 30 s, annealing for 40 s, extension at 72 °C for 50 s, and one cycle of final extension at 72 °C for 5 min. The annealing temperatures for each primer are listed in Table 1. The PCR products were separated by 1.0% agarose gel electrophoresis. For DNA purification, Expin PCR purification kit (Gene ALL, Korea) was used.

Amplicons were sequenced by Macrogen (Seoul, South Korea).

Table 1. List of primers used for the investigated DNA barcoding loci.

DNA locus	Primer name	Primer sequence	Annealing temperature
rbcL	rbcLaF	ATGTCACCACAAACAGAGACTAAAGC	60.6 °C
	rbcLarev	GTAAAATCAAGTCCACCRCG	57.5 °C
matk	matK-KIM1	ACCCAGTCCATCTGGAAATCTTGGTTC	66.1 °C
	matK-KIM3	CGTACAGTACTTTTGTGTTTACGAG	56.8 °C
trnH-psbA	psbAF	CGCGCATGGTGGATTCACAATCC	65.7 °C
	t-rnH2	GTTATGCATGAACGTAATGCTC	54.8 °C
ITS2	ITS-S2F	ATGCGATACTTGGTGTGAAT	55 °C
	ITS4rev	TCCTCCGCTTATTGATATGC	55.8 °C

2.3 Sequence analysis

For the phylogenetic analysis of *B. oleoides*, the resultant sequences were compared with reference sequences in the NCBI GenBank database (http://www.ncbi.nlm.nih.gov). To query for highly similar sequences, Basic Local Alignment Search Tool (BLAST) (http://blast.ncbi.nlm.nih.gov/Blast.cgi) was used. The retrieved sequences were aligned, trimmed, and analyzed using the MEGA11 program (Tamura et al., 2021). A phylogenetic tree was constructed after finding the best DNA models using MEGA11, and models with the lowest Bayesian Information Criterion (BIC) scores were considered the best model to describe the substitution pattern.

The maximum likelihood method (based on the best model obtained) was used to construct the phylogenetic tree with default parameters, except that the test of phylogeny was modified to the bootstrap method (Felsenstein, 1985). Therefore, the confidence levels for the individual branches of the resulting tree were assessed by the bootstrap test in which 1,000 replicate trees were generated from resampled data, and statistical support for each constructed tree was also provided by pairwise distance estimated using the best-fit model.

To infer phylogenetic relationships within Rosales, the seven plastid genomes were compared to *Barbeya oleoides*. All plastid genome sequences were aligned using MAFFT v7.402 (Katoh and Standley 2013) . Maximum likelihood analyses were conducted using raxmlGUI (Silvestro and Michalak 2012) with GTR+G, and 1000 bootstrap replicates.

3. RESULTS

The amplification and sequence success rates of ITS2, rbcL, matk, and trnH-psbA from specimens of *B. oleoides* were 100%. The lengths of the ITS2, rbcL, matk, and trnH-psbA sequences used for the analysis were 356, 555, 783, and 498, respectively. Sequences of the ITS2, rbcL, matk, and trnH-psbA loci were submitted to the NCBI GenBank database under the following accession numbers: OP023315, OP094675, OP094676, and OP094677, respectively. The obtained sequences were used as query sequences in BLAST at NCBI to find similar sequences in the order Rosales. For the ITS2 loci the species included in the analysis are shown in Fig. 1.

The nucleotide sequences of all selected species were analyzed using MEGA11 which revealed that the Tamura 3-parameter model had the lowest BIC scores (Tamura, 1992). As a result, evolutionary history was inferred using the maximum likelihood method and Tamura 3-parameter model (Fig. 1).

In addition, by blasting the sequence of rbcL loci, the most highly similar identity sequences obtained from GenBank were the Rosaceae family, For the rbcL loci the species included in the analysis are shown in Fig 2. The nucleotide sequences of all selected species were analyzed by MEGA11, which revealed that the Jukes-Cantor model is the best model to describe the substitution pattern (Jukes and Cantor, 1969). Therefore, evolutionary history was inferred using the maximum likelihood method and the Jukes-Cantor model (Fig. 2).

The matK loci sequence showed that the most highly similar identity sequences obtained from GenBank were from the Rhamnaceae family. For the matK loci the species included in the analysis are shown in Fig 3. The nucleotide sequences of all selected species were analyzed using MEGA11 which revealed that the Tamura 3-parameter model had the lowest BIC scores (Tamura, 1992). As a result, evolutionary history was inferred using the maximum likelihood method and Tamura 3-parameter model (Fig. 3).

In contrast, the trnH-psbA loci of the investigated *B. oleoides* did not show any similarity to any other plant family in the BLAST search at NCBI, and the present identity to the available data of *B. oleoides* (only two accessions: NC_040984 and MG880221) was 89.39%

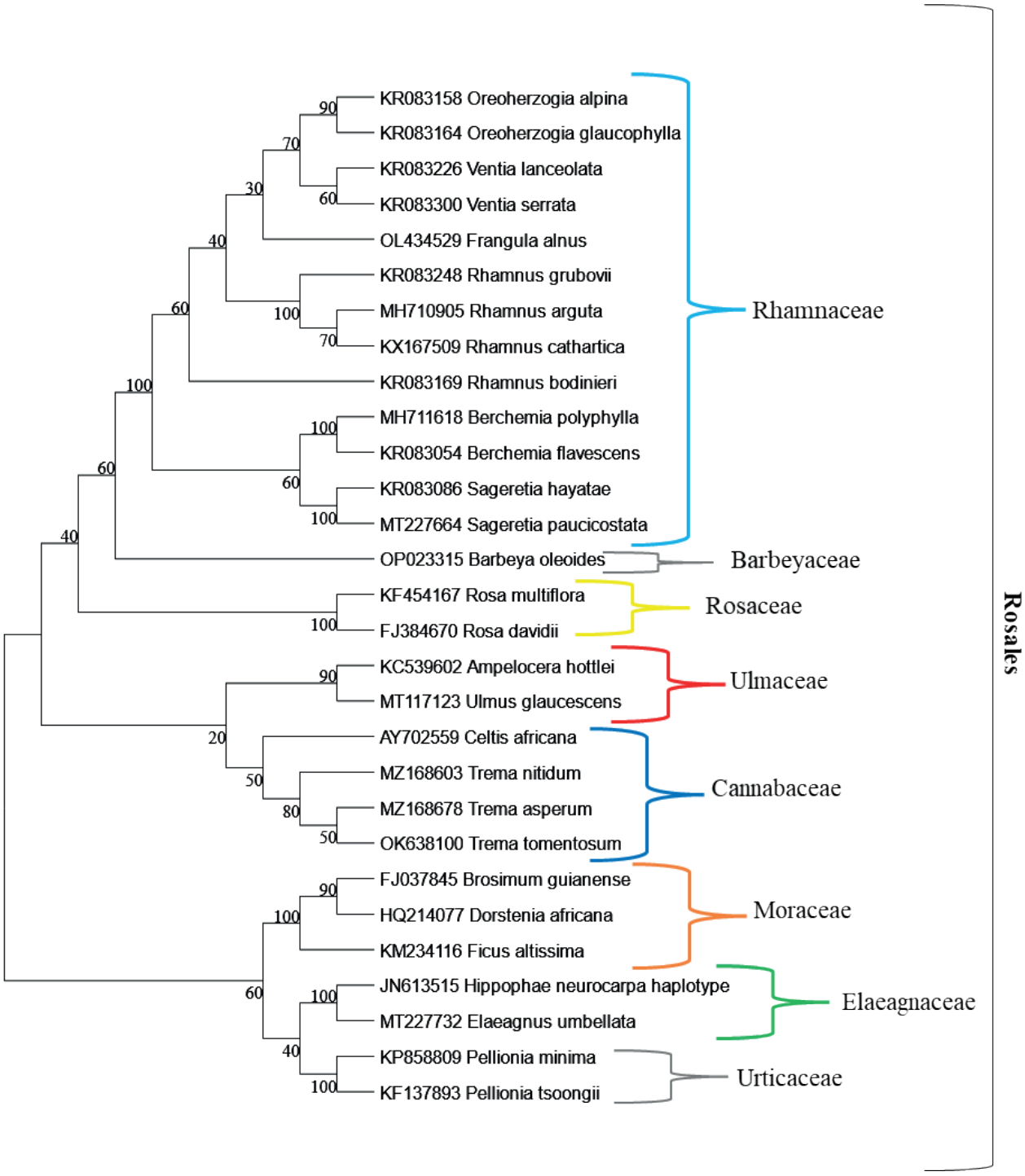

Figure 1 Phylogram based on ITS2 locus for *B. oleoides* and the retrieved species from NCBI using the maximum likelihood tree method. The evolutionary history and phylogenetic relationship were inferred using the maximum likelihood method and the Tamura 3-parameter model (Tamura, 1992). The tree with the highest log-likelihood is shown. The analysis involved 16 nucleotide sequences. The codon positions included were 1st+2nd+3rd+ noncoding. There were 364 positions in the final dataset. Evolutionary analyses were conducted in MEGA11 (Tamura et al., 2021).

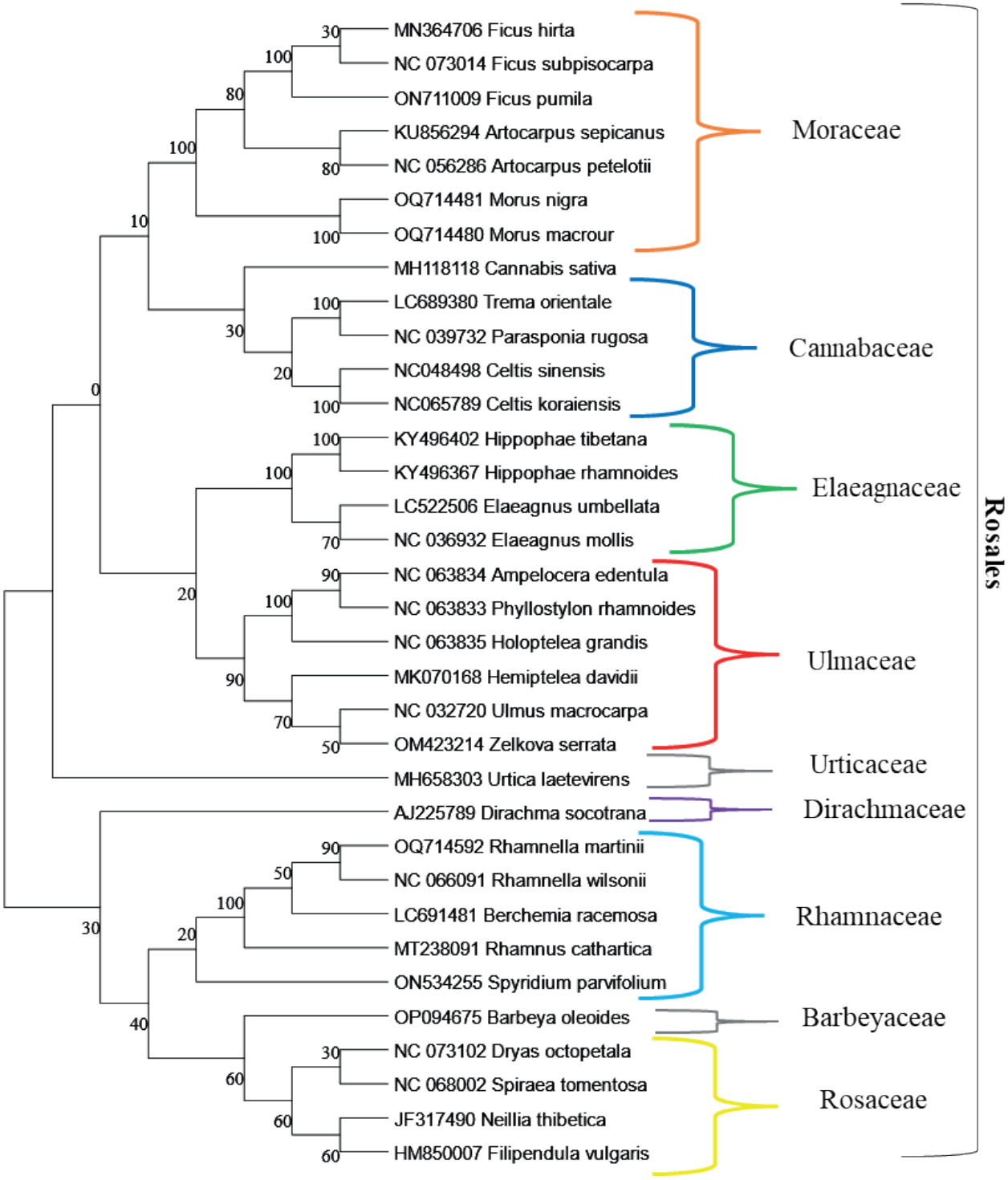

Figure 2 Phylogram based on rbcL locus for *B. oleoides* and the retrieved species from NCBI using the maximum likelihood tree method. The evolutionary history and phylogenetic relationship were inferred using the maximum likelihood method and the Tamura 3-parameter model (Tamura, 1992). The tree with the highest log-likelihood is shown. The analysis involved 16 nucleotide sequences. The codon positions included were 1st+2nd+3rd+ noncoding. There were 364 positions in the final dataset. Evolutionary analyses were conducted in MEGA11 (Tamura et al., 2021).

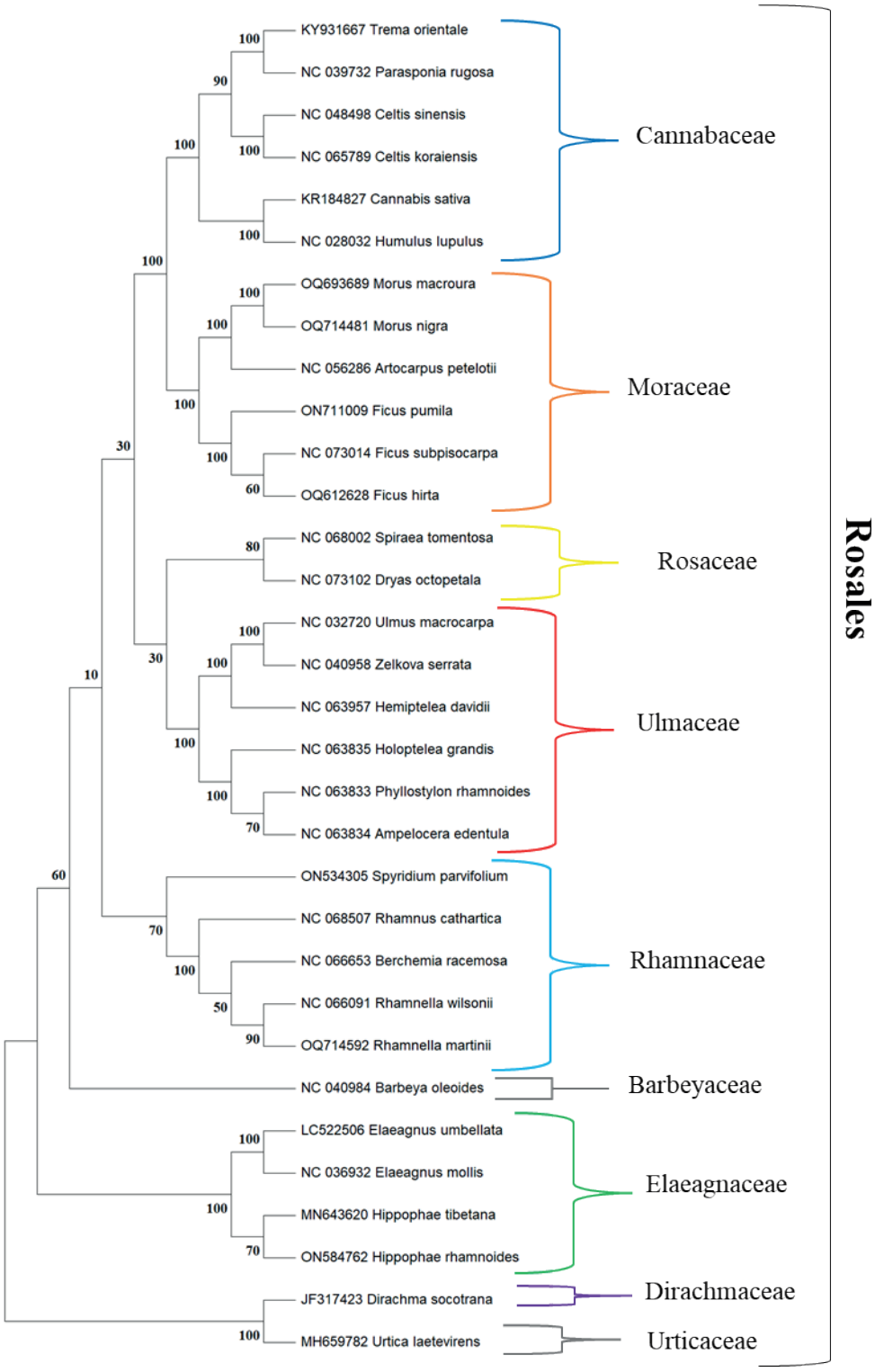

Figure 3 Phylogram based on matK locus for *B. oleoides* and the retrieved species from NCBI using the maximum likelihood tree method. The evolutionary history and phylogenetic relationship were inferred using the maximum likelihood method and the Tamura 3-parameter model (Tamura, 1992). The tree with the highest log-likelihood is shown. The analysis involved 16 nucleotide sequences. The codon positions included were 1st+2nd+3rd+ noncoding. There were 364 positions in the final dataset. Evolutionary analyses were conducted in MEGA11 (Tamura et al., 2021).

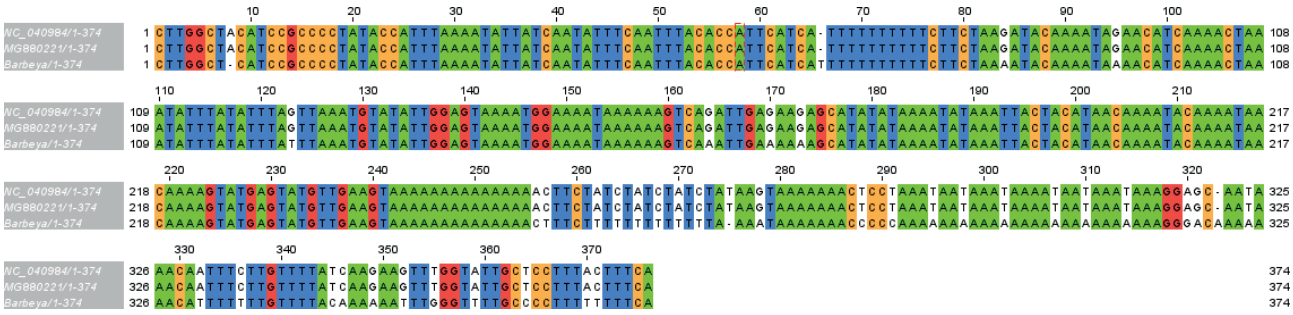

Figure 4 Variable sites between aligned sequence of trnH-psbA locus for *B. oleoides* and the retrieved sequence of *B. oleoides* from NCBI

with a very low E value (E-value =1e-127). The length of the aligned sequence was 374 bp and the percentage of variable sites within this sequence was 10% (Fig. 4).

The completed sequences of chloroplast of the families within Rosales (except Dirachmaceae not yet sequenced and instead available plastid sequences were used) were included for phylogenetic analysis using raxmlGUI (Silvestro and Michalak 2012). The result showed that the Rosales clade contains two subclades Fig. 5. The first subclade includes Rhamnaceae, Barbeyaceae, Elaeagnaceae, and Rosaceae. The Second subclade includes Ulmaceae, Cannabaceae, Moraceae, and Urticaceae. However, due to the absence of the completed chloroplast sequence of Dirachmaceae species, the family appeared as an outgroup taxon.

4. DISCUSSION

DNA barcoding is an important tool for species and family identification. Combining nuclear and chloroplast DNA barcodes is a good approach for DNA barcoding in plants (Kress et al., 2010). Not all DNA barcodes exhibit the same performance and efficiency across all plant species (Liu et al., 2011). In 2009, matK and rbcL barcodes were suggested to be the core sequences of plant DNA barcodes, while ITS and trnH-psbA are complementary plant DNA barcodes (CBOL Plant Working Group, 2009). The karyotype characteristic that is commonly utilized in cytotaxonomic analyses is the count of chromosomes. However, the complete sequencing of Barbeya oleoides has not been accomplished, thus preventing the utilization of chromosome number as a means of facilitating its classification. Chen et al. (2010) attempted to develop a practical and standardized tool for authenticating medicinal plants using DNA barcodes. In their study, the phylogeny of 4,800 species from 193 families across seven phyla (angiosperms, gymnosperms, ferns, mosses, liverworts, algae, and fungi) was analyzed, including different DNA barcodes. Their results proposed the use of ITS2 as a core DNA barcode to identify medicinal plants at different taxonomic levels. The results of the ITS2 sequence BLAST and phylogenetic relationship inferred by using the maximum likelihood method discriminate Barbeyacea from the Cannabaceae family, which is represented by two highly similar genera: *Aphananthe* and *Celtis*. Thus, the power of ITS2 for species identification was confirmed in the current study, and it was also documented to be a useful DNA marker for phylogenetic reconstructions at both the genus and species levels by several studies (Schultz and Wolf, 2009; Schultz et al., 2005). The applicability of different DNA barcode regions for species identification within Rosaceae has been tested, and the results indicate that ITS2 is the best of all loci tested for barcoding Rosaceae (Pang et al., 2011).

The matK barcode alone was not suggested to be a suitable universal barcode. This is due to the low success rate of species identification (Fazekas et al., 2008) and the different discrimination rates in different taxonomic groups; for example, the matK discrimination rate was more than 90% for species in the family Orchidaceae (Kress and Erickson, 2007) but less than 49% in the nutmeg family (Newmaster et al., 2008). In contrast to these previous studies, our study presents a strong case for the matK region as a good DNA barcode for authenticating *B. oleoides* and discriminating the Barbeyaceae family from other closely related families, such as the Rhamnaceae family, which is represented in the analysis by the genera *Ventilago* and *Berchemia*.

Although the rbcL region is not recommended for use as a candidate plant barcode based on several limitations, such as its modest discriminatory power at the species level (CBOL Plant Working Group, 2009; Chen et al., 2010; Fazekas et al., 2008; Lahaye et al., 2008) and the length of the gene, this study evaluated the rbcL barcode, and the results indicate accurate identification of *B. oleoides*. In addition, consistent with the current study, both rbcL and matK barcodes have the ability to discriminate among Cannabaceae, Rosaceae, and Rham-

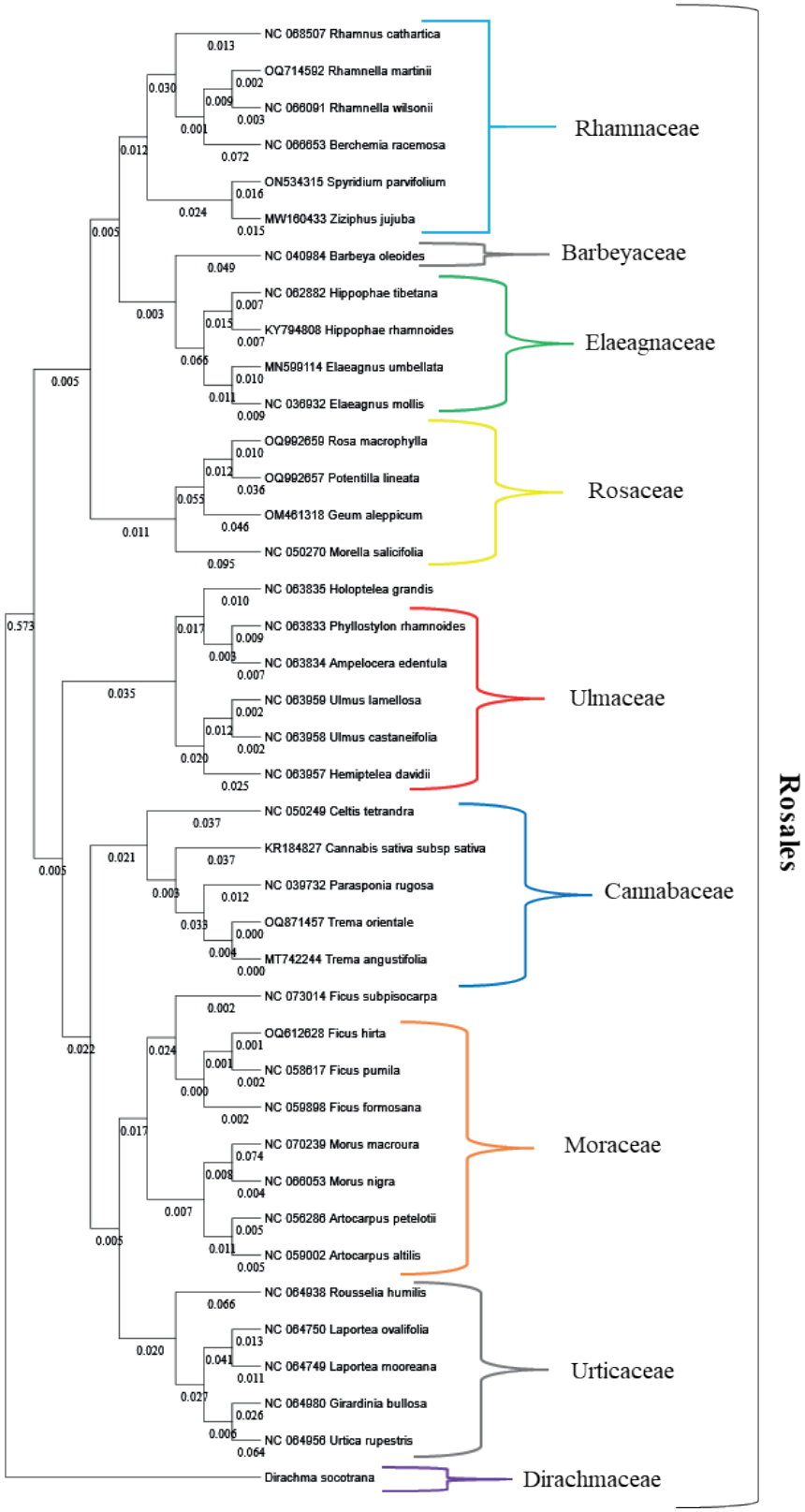

Fig. 5 Phylogenetic relationships of Barbeyaceae family with related families within Rosales based on the whole chloroplast genomes by maximum likelihood (ML) with bootstrap values above the branches.

naceae families within the order Rosales (Muhammad and Siddiqui, 2022).

Although the ITS2, matk, rbcL, and trnH-psbA loci of *B. oleoides* were efficient in the identification of this plant species, only ITS2, rbcL, and matk could discriminate the Barbeyaceae family from other closely related families. A phylogenetic evolutionary tree was constructed for *B. oleoides* species for each rbcL, matK, and ITS2, which was supported by the values of nodes on most branches being higher than 90%, indicating that the evolutionary relationships between *B. oleoides* and other closely related families are highly reliable. This result was supported by the ability of the trees constructed to differentiate clearly between the Barbeyaceae family and other closely related families, such as Cannabaceae, Rosaceae, and Rhamnaceae (fig. 1,2,3).

The weak discriminatory power of trnH-psbA compared to ITS2 at low taxonomic levels has been widely studied and has been suggested as a complementary barcode for the identification of medicinal plant species (Chen et al., 2010; Kress et al., 2005; Kress and Erickson, 2007). Our results indicated that the trnH-psbA locus was efficient in the identification of *B. oleoides*, but failed to distinguish between closely related families. This may be attributed to the high substitution rate within the chloroplast trnH-psbA spacer region (Whitlock et al. 2010). Therefore, as the trnH-psbA region accumulates more variation, it may offer more resolution at lower levels of taxa such as species and cultivars (Kress et al., 2010; Kress et al., 2005; Kress and Erickson, 2007, Chen et al., 2010).

The complete chloroplast sequence analysis considers a strong and informative tool for phylogenetic relationship analysis (Moore et al. 2007; Do et al. 2013). The analysis showed thar the Rosales clade includes two subclades, which agreed with previous studies (Zhang et al. 2011). In addition, it showed that Barbeyaceae is sister to Elaeagnaceae. Other previous studies placed Elaeagnaceae in the same clade with Barbeyaceae, Dirachmaceae and Rhamnaceae (Soltis et al. 2007; Savolainen et al. 2000; Richardson et al. 2000a), hence, confirming the result of completed chloroplast phylogenetic analysis. Additionally, morphological studies confirmed the close relationship of Barbeyaceae, Dirachmaceae, Elaeagnaceae and Rhamnacea (Richardson et al. 2000b; Wang et al. 2009).

5. CONCLUSIONS

This study is the first to assess molecular marker-based identification and classification of *B. oleoides*. This study produced DNA sequences from ITS2, matK, rbcL, and trnH-psbA barcoding loci in *B. oleoides* collected from Al-Baha, Saudi Arabia. It is concluded that the three barcode markers, ITS2, matK, and rbcL, worked reasonably well in the differentiation of Barbeyaceae from closely related families of order Rosales. In addition, the study reported a low resolution of the trnH-psbA marker for the identification of families within the order Rosales. Thus, it is suggested to be used to differentiate among variations within *B. oleoides* plants, or variations within one species. Finally, the present study provides data to aid in the correct identification and conservation of this medicinally important plant species.

DATA AVAILABILITY

Sequences of the ITS2, rbcL, matk, and trnH-psbA loci were submitted to the NCBI GenBank database under the following accession numbers: OP023315, OP094675, OP094676, and OP094677, respectively

REFERENCES

Aboul-Maaty, N.A.F., Oraby, H.A.S., 2019. Extraction of high-quality genomic DNA from different plant orders applying a modified CTAB-based method. Bull. Natl Res. Cent. 43, 1–10.

Ahmed, B., Al-Rehaily, A.J., Mossa, J.S., 2002. Barbeyol: A NewPhenolic indane Type Component from Barbeya oleoides. Z. Naturforsch. C J. Biosci. 57, 17–20.

Angiosperm Phylogeny Group (APG), 1998. An ordinal classification for the families of flowering plants. Ann. Mo. Bot. Gard. 85, 531–553.

Angiosperm Phylogeny Group (APG), 2003. An update of the Angiosperm Phylogeny Group classification for the orders and families of flowering plants: APG II. Botan. J. Linn. Soc. 141, 399–436.

Angiosperm Phylogeny Group (APG), 2009. An update of the Angiosperm Phylogeny Group classification for the orders and families of flowering plants: APG III. Bot. J. Linn. Soc. 161, 105–121.

Baka, Z.A.M., 2010. Antifungal activity of six Saudi medicinal plant extracts against five phyopathogenic fungi. Arch. Phytopathol. Plant Prot. 43, 736–743.

CBOL Plant Working Group, 2009. A DNA barcode for land plants. Proc. Natl Acad. Sci. U. S. A. 106, 12794–12797.

Chaudhary, S.A., Al Jowaid, A.A., 1999. Vegetation of the Kingdom of Saudi Arabia. Ministry of Agriculture and Water Kingdom of Saudi Arabia 1, 222–223.

Chen, S., Yao, H., Han, J., Liu, C., Song, J., Shi, L., Zhu, Y., Ma, X., Gao, T., Pang, X., Luo, K., Li, Y., Li, X.,

Jia, X., Lin, Y., Leon, C., 2010. Validation of the ITS2 region as a novel DNA barcode for identifying medicinal plant species. PLOS ONE. 5, e8613.

China Plant, B.O.L., 2011. Group, Li DZ, Gao LM, Li HT, Wang H, Ge XJ, et al. Comparative analysis of a large dataset indicates that internal transcribed spacer (ITS) should be incorporated into the core barcode for seed plants. *Proc Natl Acad Sci USA*, *108*, pp.19641-19646.

Dickison, W.C., Sweitzer, E.M., 1970. Morphology and relationships of Barbeya oleoides. Am. J. Bot. 57, 468–476.

Do HDK, Kim JS, Kim J. 2013. Comparative genomics of four Liliales families inferred from the complete chloroplast genome sequence of Veratrum patulum O. Loes.(Melanthiaceae). Gene 530(2):229-235.

Fazekas, A.J., Burgess, K.S., Kesanakurti, P.R., Graham, S.W., Newmaster, S.G., Husband, B.C., Percy, D.M., Hajibabaei, M., Barrett, S.C.H., 2008. Multiple multilocus DNA barcodes from the plastid genome discriminate plant species equally well. PLOS ONE. 3, e2802.

Felsenstein, J., 1985. Confidence limits on phylogenies: An approach using the bootstrap. Evolution. 39, 783–791.

Jukes, T.H., Cantor, C.R., 1969. Evolution of protein molecules, in: Munro, H.N. (Ed.), Mammalian Protein Metabolism. Academic Press, New York, pp. 21–132.

Katoh K, Standley DM. 2013. MAFFT multiple sequence alignment software version 7: improvements in performance and usability. Molecular biology and evolution 30(4):772-780.

Khojah, A.A., Padilla-González, G.F., Bader, A., Simmonds, M.J.S., Munday, M., Heinrich, M., 2021. Barbeya oleoides leaves extracts: In vitro carbohydrate digestive enzymes inhibition and phytochemical characterization. Molecules. 26, 6229.

Kress, W.J., Erickson, D.L., 2007. A two-locus global DNA barcode for land plants: The coding rbcL gene complements the non-coding trnH-psbA spacer region. PLoS One. 2, e508.

Kress, W.J., Erickson, D.L., Swenson, N.G., Thompson, J., Uriarte, M., Zimmerman, J.K., 2010. Advances in the use of DNA barcodes to build a community phylogeny for tropical trees in a Puerto Rican Forest Dynamics Plot. PLOS ONE. 5, e15409.

Kress, W.J., Wurdack, K.J., Zimmer, E.A., Weigt, L.A., Janzen, D.H., 2005. Use of DNA barcodes to identify flowering plants. Proc. Natl Acad. Sci. U. S. A. 102, 8369–8374.

Lahaye, R., Van Der Bank, M., Bogarin, D., Warner, J., Pupulin, F., Gigot, G., Maurin, O., Duthoit, S., Barraclough, T.G., Savolainen, V., 2008. DNA barcoding the floras of biodiversity hotspots. Proc. Natl Acad. Sci. U. S. A. 105, 2923–2928.

Li, X.W., Yang, Y., Henry, R.J., Rossetto, M., Wang, Y., Chen, S., 2015. Plant DNA barcoding: From gene to genome. Biol. Rev. Camb. Philos. Soc. 90, 157–166.

Liu, J., Möller, M., Gao, L.M., Zhang, D.Q., Li, D.Z., 2011. DNA barcoding for the discrimination of Eurasian yews (Taxus L., Taxaceae) and the discovery of cryptic species. Mol. Ecol. Resour. 11, 89–100.

Moore MJ, Bell CD, Soltis PS, Soltis DE. 2007. Using plastid genome-scale data to resolve enigmatic relationships among basal angiosperms. Proceedings of the National Academy of Sciences 104(49):19363-19368.

Muhammad, S., Siddiqui, M.F., 2022. Taxonomic reaffirmation of some members of family Cannabaceae, Moraceae, Rhamnaceae, Rosaceae and Urticaceae of order Rosales using DNA bar-coding markers. Pak. J. Bot. 54, 231–241.

Namazi, A.A., Al-Khulaidi, A.W.A., Algarni, S., Al-Sagheer, N.A., 2021. Natural plant species inventory of hotspot areas in Arabian Peninsula: Southwest Al-Baha region, Saudi Arabia. Saudi J. Biol. Sci. 28, 3309–3324.

Newmaster, S.G., Fazekas, A.J., Steeves, R.A.D., Janovec, J., 2008. Testing candidate plant barcode regions in the Myristicaceae. Mol. Ecol. Resour. 8, 480–490.

Pang, X., Song, J., Zhu, Y., Xu, H., Huang, L., Chen, S., 2011. Applying plant DNA barcodes for Rosaceae species identification. Cladistics. 27, 165–170.

PLoS ONE 2: e508

Rana, T.S., Ranade, S.A., 2009. The enigma of monotypic taxa and their taxonomic implications. Curr. Sci. 96.

Richardson JE, Fay MF, Cronk QC, Bowman D, Chase MW. 2000a. A phylogenetic analysis of Rhamnaceae using rbcL and trnL-F plastid DNA sequences. American Journal of Botany 87(9):1309-1324.

Richardson JE, Fay MF, Cronk QC, Bowman D, Chase MW. 2000b. A phylogenetic analysis of Rhamnaceae using rbcL and trnL-F plastid DNA sequences. American Journal of Botany 87(9):1309-1324.

Sarwar, A.K.M.G., Araki, H., 2010. Monotypic taxa, their taxonomic implications and conservation needs in Bangladesh. Proc. of International Conference on Environmental Aspects of Bangladesh. Japan, Sept. 2010, (p. ICEAB10).

Savolainen V, Fay MF, Albach DC, Backlund A, van der Bank M, Cameron KM, Johnson SA, Lledo MD, Pintaud J, Powell M. 2000. Phylogeny of the eudicots: a nearly complete familial analysis based on rbcL gene sequences. Kew Bulletin:257-309.

Schultz, J., Maisel, S., Gerlach, D., Müller, T., Wolf, M., 2005. A common core of secondary structure of the internal transcribed spacer 2 (ITS2) throughout the Eukaryota. RNA. 11, 361–364.

Schultz, J., Wolf, M., 2009. ITS2 sequence-structure analysis in phylogenetics: A how-to manual for molecular systematics. Mol. Phylogenet. Evol. 52, 520–523.

Silvestro D, Michalak I. 2012. raxmlGUI: a graphical front-end for RAxML. Organisms Diversity & Evolution 12:335-337.

Soltis DE, Gitzendanner MA, Soltis PS. 2007. A 567-taxon data set for angiosperms: the challenges posed by Bayesian analyses of large data sets. International journal of plant sciences 168(2):137-157.

Tamura, K., 1992. Estimation of the number of nucleotide substitutions when there are strong transition-transversion and G + C-content biases. Mol. Biol. Evol. 9, 678–687.

Tamura, K., Stecher, G., Kumar, S., 2021. MEGA11: Molecular Evolutionary Genetics Analysis Version 11. Mol. Biol. Evol., version 11. 38, 3022–3027. https://doi.org/10.1093/molbev/msab120.

Wang H, Moore MJ, Soltis PS, Bell CD, Brockington SF, Alexandre R, Davis CC, Latvis M, Manchester SR, Soltis DE. 2009. Rosid radiation and the rapid rise of angiosperm-dominated forests. Proceedings of the National Academy of Sciences 106(10):3853-3858.

Whitlock, B.A., Hale, A.M., Groff, P.A., 2010. Intraspecific inversions pose a challenge for the trnH-psbA plant DNA barcode. PLOS ONE. 5, e11533.

Zhang S, Soltis DE, Yang Y, Li D, Yi T. 2011. Multigene analysis provides a well-supported phylogeny of Rosales. Molecular phylogenetics and evolution 60(1):21-28.

Caryologia
International Journal of Cytology, Cytosystematics and Cytogenetics

Firenze University Press
www.fupress.com/caryologia

OPEN ACCESS

Citation: Asma Mahmoud Hamza, Sumaya Hussein Elboshra (2023). Mitotic metaphase karyotype of the mosquito *Anopheles arabiensis* Patton (Diptera: Culicidae) from Kassala State, eastern Sudan. *Caryologia* 76(2): 15-21. doi: 10.36253/caryologia-2095

Received: October 3, 2022

Accepted: July 3, 2023

Published: December 31, 2023

Data Availability Statement: All relevant data are within the paper and its Supporting Information files.

Competing Interests: The Author(s) declare(s) no conflict of interest.

Mitotic metaphase karyotype of the mosquito *Anopheles arabiensis* Patton (Diptera: Culicidae) from Kassala State, eastern Sudan

Asma Mahmoud Hamza[1,*], Sumaya Hussein Elboshra[2]

[1] *Departement of Biology, Faculty of Education, University of Kassala, Kassala, Sudan*
[2] *Departement of Biology, Faculty of Science, University of Kassala, Kassala, Sudan*
*Corresponding author. E-mail: asmakassala@gmail.com

Abstract. The mosquito *Anopheles arabiensis* Patton is the most important malaria vector in Sudan. The study was conducted for the first time to describe numerically the karyotype of *An. arabiensis* from Kassala State, eastern Sudan. Adults *An. arabiensis* were caught from human dwellings during the rainy season of 2022. We examined for the first time the utility of brain ganglia tissues of adult mosquitoes for mitotic chromosomal preparations using Giemsa stain - spreading technique. High-quality chromosomal preparations were examined and photographed. Chromosome measurements were carried out using computer software and analyzed statistically using SPSS® software. The diploid mitotic chromosome complement of *An. arabiensis* consists of three pairs of chromosomes, two pairs of metacentric autosomes (chromosome II and chromosome III) and one acrocentric dot-shaped pair, sex chromosome, which is homomorphic in females (XX) and heteromorphic in males (XY). Chromosome II was described as the longest (2.61±0.07) of the complement and constitute 44.39% of the total length (5.88 µm) of the haploid chromosomes set, while chromosome I (X=1.39 ±0.04; Y=1.04±0.04) as the shortest chromosome. Chromosome X appears in the males significantly larger than chromosome Y (P = 0.00). Chromosome III has an intermediate length (1.88±0.06) compared with the other chromosomes. Comparison of the average lengths of the three chromosome pairs by ANOVA test revealed highly statistical significant differences between them (P < 0.00). The study establishes a strong cytogentic data, which can contribute to accurate identification of the mosquito *An. arabiensis* and to planning human malaria vector control programs in Kassala State, eastern Sudan.

Keywords: *Anopheles arabiensis*, karyotype, brain ganglia, mitotic chromosomes, chromosome measurements, Sudan, Kassala.

1. INTRODUCTION

Of the nine recognized sibling species of the *Anopheles gambiae* complex (Barron et al 2019), *Anopheles arabiensis* Patton (Diptera: Culicidae) is one of the most significant malaria vectors globally (WHO 2018). It is considered the most efficient malaria vector in Kassala State, eastern Sudan and it has

been reported from Kassala town by (Hamza et al. 2014; Mustafa et al. 2021).

Chromosomes are the critical carrier of genetic information in eukaryotic cell nuclei, and their characteristics are typically stable within species (Vimala et al 2021). The karyotype is a fundamental characteristic of the chromosome complement (Marinho et al. 2016; Dehury et al 2021) and it represents the phenotype of the chromosomes including chromosome number, size, shape and position of the centromere (Tjong et al. 2012; Astuti et al. 2017). Cytogenetics is usually based on the examination of the fixed mitotic chromosomes during the analysis of metaphase of cell cycle, in which the DNA is folded up and chromatin is strongly condensed (Tüzün and Yükse 2009). In karyotype (ideogram) construction, the chromosomes are arrange on the basis of homologous chromosome pairs and sort out by chromosome size and centromere position from the longest to the shortest (Tjong et al. 2012) and can either be developed in haploid or diploid organism's cells. An ideogram construction following chromosome measurements is a versatile tool for cytogenetic studies (Kirov et al. 2017).

In the past chromosome measurements were carried out using classical karyological measurement methods (e.g. Anil et al 1970; Robert et al. 1986). Recently with advance in computer science, different computer software were developed for image processing and can be used for chromosome measurements from microphotographs (e.g. Image J, Rasband and Eliceiri 2012). In addition, others software beside chromosome measurements can be used in karyotype analysis (e.g. KaryoType, Altınordu et al. 2016). These software allow efficient, precise and rapid chromosome measurements.

Chromosomes cytologic information can be used for many purposes; such as, to study cytotaxonomy, phylogenetic relationships, karyotypic evolution (Felip et al. 2009; Guerra 2012), chromosomal aberrations and cellular function (Zhao et al. 2013) and chromosomal structural variation (Marinho et al. 2016; Dehury 2021). Karyotype analysis can serve as an additional tool in the species level identification of the species, which have morphological similarity and require additional identification methods. Using morphological, molecular, and karyotypic data, more precise species identification can be performed (Alekseeva et al. 2020).

The chromosome complement of *Anopheles* mosquitoes consists of three pairs of chromosomes (Baimai et al. 1996), two pairs of generally metacentric autosomal chromosomes of unequal size and one pair of heteromorphic sex chromosomes (XX in females and XY in males) (White 1980). Many workers carried out cytogenetic studies of *An. arabiensis* e.g: Coluzzi and Sabatini (1967) described the karyotype of *An. arabiensis* using larval mitotic and polytene chromosomes. Coosemans et al. (1989) investigated the frequencies of inversion polymorphisms in polytene autosomal chromosomes of *An. arabiensis*. Ayala et al. (2017) investigated the role of chromosome inversion polymorphisms in environmental adaptation from a macro-ecological perspective. Sharma et al. (2020) analyzed the metaphase chromosomes in *An. arabiensis* using fluorescence in situ hybridization techniques.

The objective of the present study is to provide for the first time a base line data of the karyotype of the mosquito *An. arabiensis* from Kassala State, eastern Sudan. We examined for the first time the utility of brain ganglia tissues of adult female and male *An. arabiensis* for description of mitotic karyotype based on chromosome measurements using computer software program. This type of data is important for improving the cytogenetic identification of this species and for planning human malaria vector control programs in Kassala State, eastern Sudan.

MATERIALS AND METHODS

Mosquitoes used in the study

Adult *Anopheles* mosquitoes were collected from Kassala town, eastern Sudan. The town is located between 15°: 28″ N and 36°: 24″ E. in semi-arid climate with rainfall of varying intensity and duration.

Indoor resting wild adult *An. arabiensis* mosquitoes were caught from human dwellings by hand capture using sucking tube, aspirator (WHO 1975) during the rainy season of 2022. The collected samples were fixed alive in the field and preserved in freshly prepared modified Carnoy's solution (3 absolute ethanol: 1 glacial acetic acid by volume). Then the collected samples were transported to the laboratory and kept at -20C° for prolong storage. The processing of the materials for this study was carried out at the Molecular Biology Laboratory of Tuberculosis and Endemic Diseases' Center of Kassala University, Kassala town, Sudan.

The collected specimens were identified morphologically using morphological identification keys described by Gillies and De-Mellion (1968) and Gillies and Coetzee (1987) with the aid of the dissecting microscope.

Preparation of mitotic chromosomes

Brain ganglia tissues of adult females and males of *An. arabiensis* were dissected out and used for mitotic

slide chromosome preparations, following the karyotyping spreading technique described by Barker (1970) using giemsa stain, with minor modifications. For mitotic karyotype analysis, 48 chromosomal slide preparations derived from 4 specimens females and 4 specimens males (6 slides per specimen) were studied.

Chromosomal slide preparations were viewed under 40 X objective of A. X. L- GERMANY EGLASS light compound microscope with DG CAM 1600 equipped digital camera. The microscopic images were projected into a *hp* intel core i 2 computer screen and preparations with well spread chromosomes were selected and photographed using the S eye software package.

Chromosome measurements and karyotype

Metaphase images with the best chromosomes spreading; fewest overlaps and sharpest were selected for mitotic karyotype description. For chromosome measurements, an image of 1mm, Erma- Tokxc, micrometer stage having a linear scale of 100 divisions was taken at the same magnification as that of the chromosome preparations. This was used as a scale to measure the lengths of individual chromosomes - with a clear centromere - and their arms (in micrometer, µm) from the chromosome preparations. Chromosome measurements were made from about 84 metaphase images using Image J computer software version16 for Windows (Rasband and Eliceiri 2012).

Measurements were taken from male chromosomal preparations as follows: long arm length of chromosome (L), short arm length of chromosome (S), centromere length of chromosome (C) and total chromosome length (TCL) = [L + S+ C]. Then parameters were calculated based on chromosome measurements, which include: arm ratio of chromosome (AR) = [L / S], centromeric index (CI) = [S / (L + S) × 100] (Eroğlu et al. 2017) and relative length (RL%) = [TCL / Total length of all the chromosomes in haploid genome size x100]. Arm ratio was used to classify chromosomes according to classical method of Levan et al. (1964).

Computer imaging system Photoshop version 7.0 was used for image editing. First, the images were processed minimally by adjusting brightness and contrast. Then, the karyotype (ideogram) was constructed by arranging the homologous chromosome pairs (by cutting and pasting) based on the averaged length, shape and centromere position. Chromosomes were named according to the classical nomenclature for chromosomal complement in the *An. gambiae* complex (Coluzzi and Sabatini 1967).

Statistical analysis of chromosome measurements:

The computer soft ware package SPSS® (Statistical package for Social Science) version 16.0 for windows was used for statistical aspects of the *An. arabiensis* chromosomes analysis. Descriptive statistics (means, standard error, maximum, and minimum) of all chromosome measurements were recorded. The mean lengths of all the autosomal and sex chromosomes were compared by analysis of variance (ANOVA). T-test was used to compare the mean lengths of the long and short arms of the same chromosome and the sex chromosomes.

RESULTS

Karyotype

Cytological observations of adult females and males brain ganglia tissues of *An. arabiensis* demonstrate a diploid mitotic chromosome complement consisting of three pairs of chromosomes (2n= 6), two pairs of autosomes (chromosome II and chromosome III) and one pair of sex chromosomes (chromosome 1), which is homomorphic in females (XX) and heteromorphic in males XY (Figure 1).

Chromosome analysis

Chromosome measurements and parameters calculated were used to describe the karyotype of *An. arabiensis* numerically. The measurement data of all chromosomes are given in Table 1. Chromosome lengths range between (2.61±0.07) µm and (1.04±0.04) µm from the longest to the shortest. Comparison of the average lengths of the three chromosome pairs by ANOVA test revealed highly statistically significant differences between them (f = 137.11; df. = 3; P = 0.00), as explained in details by the result of Scheffe Post Hoc Test.

From the analysis of chromosome length measurements, chromosomes were identified according to their length: chromosome II can be describe as the longest (2.61±0.07) of the complement, while chromosome III has an intermediate length (1.88±0.06) compared with the other chromosomes. Staining of chromosomes II and III by giemsa stain revealed a primary strong constriction, the centromere, so this allowed the estimating of the arm ratio of these two chromosomes and classify them according to the standard classification method of Levan et al. (1964). The calculated arm ratio of chromosomes II and III were 1.45 and 1.06, respectively and the centromeric index of the two chromosomes were 40.79

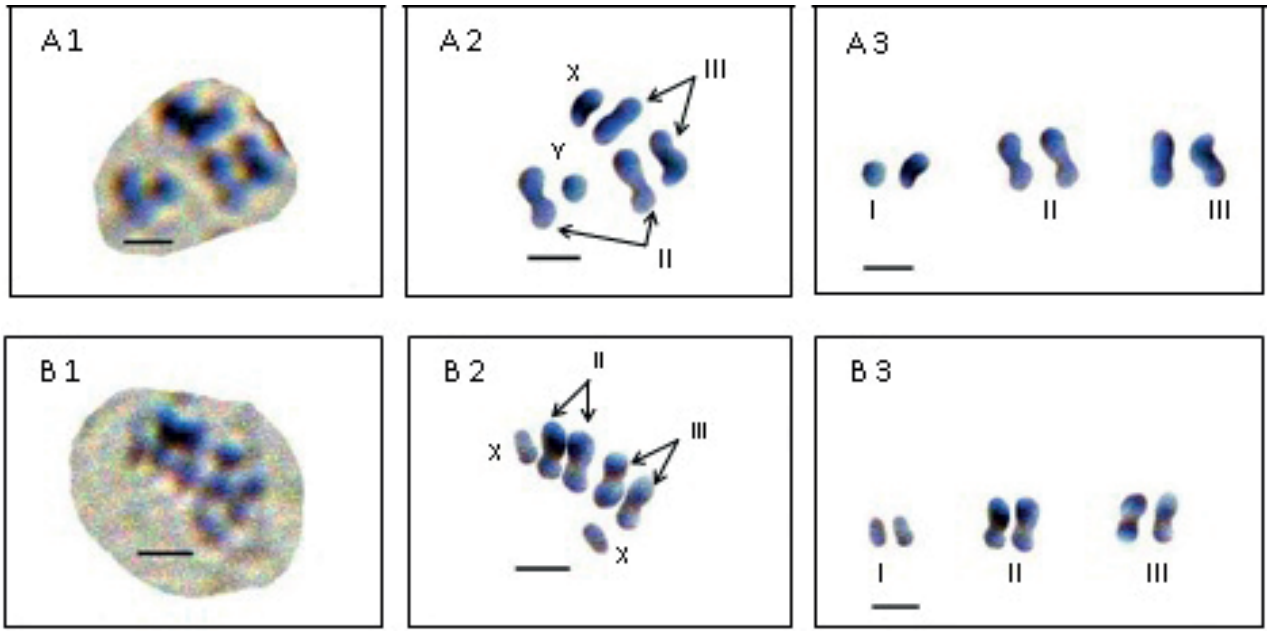

Figure 1. . Giemsa stained mitotic karyotype of adult female and male *Anopheles arabiensis* collected from Kassala town, eastern Sudan A: Male cell; A1- Plate of metaphase chromosomes. A2- Somatic pairing. A3- Karyotype B: Female cell; B1- Plate of metaphase chromosomes. B2 -Somatic pairing. B3- Karyotype Scale bar = 3 µm.

Table 1. Chromosome measurements of the mosquito *Anopheles arabiensis* from Kassala State, eastern Sudan.

Chromosome pair	No of chromosomes measured	Average length of long arm (L±SE) (µm)	Average length of short arm (S±SE) (µm)	Average length of centromere (C±SE) (µm)	Average total length (T±SE) (µm)	Arm ratio (r)	Centromeric index (SI) (%)	Relative length (%)	Chromosome type
X	15	-1,39 ±0.04 (1.17-1.58)	0	0	1,39 ±0.04 (1.17-1.58)	0	0	23.64	Telocentric
Y	19	1.04±0.04 (0.70-1.24)	0	0	1.04±0.04 (0.70-1.24)	0	0	17.69	Telocentric
2	29	1.35±0.04 (1.04-1.67)	0.93±0.04 (0.58-1.31)	0.33±0.02 (0.141-0.49)	2.61±0.07 (2.97-3.27)	1.45	40.79 Median	44.39	Metacentric
3	24	0.82±0.04 (048-1.13)	0.77±0.03 (0.55—1.10)	0.28±0.03 (0.12-046)	1.88±0.06 (1.38-2.52)	1.06	48.43 Median	31.97	Metacentric

Total length of the haploid genome: 5.88.
Number between two brackets represent the range of the measurement.
Chromosome type according to Levan et al. (1964).

and 48.43%, respectively, so the relative position of the centromere of the two autosomes meeting the parameters characteristic of metacentric chromosomes. However, the two chromosomes are metacentric, there was highly statistically significant difference (t = 8.00; df. = 56; P = 0.00) between the long arm and short arm of chromosome II, in contrast there was no statistically significant difference (t = 1.12; d.f. = 46; P > 0.05) between the long arm and short arm of chromosome III according to T- test analysis.

Chromosome I (X=1.39 ±0.04; Y=1.04±0.04) was described as the shortest chromosome, dot-shaped and with no obvious centromeric region, so it can be described as acrocentric. The X-chromosome appears in the males is larger than the Y-chromosome with highly statistically significant difference (t = 6.60; df. = 32; P = 0.00) between them.

The total haploid length (n, the two autosomes+ X chromosome) equal 5.88 µm, thus chromosome II constitutes 44.39% of the total length of the haploid chro-

mosomes set. Secondary constriction was not detected in chromosomal arms.

DISCUSSION

The karyotype information is important for understanding population differentiation and for the development of human malaria vector control programs (Rafael1 et al. 2005). In this study, the mosquito *An. arabiensis* has been cytologically investigated because of lack of information on karyotype of this important malaria vector in Kassala State, eastern Sudan.

The study demonstrates for the first time the utility of brain tissues of adult females and males *An. arabiensis* for mitotic chromosomes analysis using giemsa stain -spreading techniques. The protocol provides clear differential phases and visualized chromosomes in metaphase cell division. The techniques for chromosome preparation are always based on obtaining sources of dividing cells to produce high quality metaphase spreads with good chromosome definition (Felip et al. 2009). Most of the cytogenetic studies on *Anopheles* mosquitoes were performed on mitotic chromosomes from brain ganglia (Baimai et al. 1995; Salara, 1998; Rafael and Tadei 1998; Rafael et al. 2005, 2006) or leg and wing imaginal discs (Sharma et al. 2020) tissues of fourth instar larva and testis tissues of adult male (Salara 1998; Choochote 2011).

The computer software Image J allowed us to measure the length of chromosomes and their arms accurately as done by Bozek et al. (2012) and Sadílek et al. (2016). Here the description of the karyotype of *An. arabiensis* was updated numerically using chromosome measurements, so the chromosomes were identified and the characteristic features of each chromosome were described. The detailed study of *An. arabiensis* mitotic karyotype has confirmed a diploid number of six, agreeing with diploid numbers reported in other *Anopheles* species, e.g.: Brazilian *An. albitarsis* (Rafael et al. 2005, 2006), *An. darlingi* and *An. nuneztovari* (Rafael and Tadei 1998).

In the present study, chromosomes have been numbered according to the classical nomenclature for chromosomal complement in the *An. gambiae* complex (Coluzzi and Sabatini 1967) which was adopted by Sharma et al. (2020), in which the shortest chromosome is designated as chromosome I and the longest is II. In contrast, in other *Anopheles* mosquitoes, the chromosomes were numbered according to the nomenclature proposed by Rai (1963), in which the chromosomes were numbered in a descending order, i e the shortest chromosome is designated as chromosome I and the longest is III.

Our study revealed a karyotype consists of two pairs of metacentric autosomes (chromosome pair II and III) and acrocentric pair I, sex chromosome (X & Y). These findings differ with the findings of previous study of Coluzzi and Sabatini (1967) who described chromosome pair II in members of *An. gambiae* complex including *An. arabiensis* as submetacentric.

Secondary constriction that constitutes a satellite in chromosome arm was not detected in the study. Rafael and Tadei (1998) detected secondary constriction in chromosome II and chromosome III from different populations of the Brazilian *An. darlingi* and they stated that secondary constriction is an important aspect of chromosome morphology.

CONCLUSION:

The chromosomal measurements of the mosquito *An. arabiensis* from Kassala State, eastern Sudan were reported here for the first time. In the study, the mitotic chromosomes number, karyotype and ideogram of *An. arabiensis* were determined. The cytogenetic data of this study together with morphological characters could be used for accurate classification of *An. arabiensis* and other members of the *An. gambaie* complex.

AUTHORS' CONTRIBUTIONS

A. M. H. performed chromosome preparations and photographing, chromosome measurements, data analysis and wrote the draft manuscript. S. H. E. performed morphological identification of mosquitoes and participated in chromosome preparations and photographing. The two authors read and approved the final manuscript.

ACKNOWLEDGMENTS

The authors thank the Tuberculosis and Endemic Diseases' Center, University of Kassala, Sudan for providing infrastructure.

REFERENCES

Alekseeva SS, Andreeva YV, Wasserlauf IE, Sibataev AK, Stegniy VN. 2020. Analysis of the metaphase chromosome karyotypes in imaginal discs of *Aedes communis*, *Ae. punctor*, *Ae. intrudens*, and *Ae. rossicus* (Diptera: Culicidae) mosquitoes. *Insects*; 11: 63

Altınordu F, Peruzzi L, Yu Y, He XJ. 2016. A tool for the analysis of chromosomes: KaryoType. *Taxon*; 65: 586-592.

Anil BM, Don MR, Asit BM. 1970. A Comparative Study of the mosquito karyotypes. *Cytologica*, 35: 57-62

Astuti G, Roma-Marzio F, Peruzzi L. 2017. Traditional karyomorphological studies: can they still provide a solid basis in plant systematics?. *Flora Mediterranea*; 27: 91-98.

Ayala1 D, Acevedo P, Pombi M, Dia I, Boccolini D, Costantini C, Simard F, Fontenille D. 2017. Chromosome inversions and ecological plasticity in the main African malaria mosquitoes. *Evolution*; 71(3): 686–701.

Baimai V, Treesucon A, Kijchalao U. 1996. Heterochromatin variation in chromosome X in a natural population of Anopheles willmori (Diptera, Culicidae) of Thailand. *Genetics*; 97: 235-239

Baimai V, Rattanarithiku R, Kijchalao N. 1995. Metaphase karyotypes of *Anopheles* of Thailand and Southeast Asia: IV. The Barbirostris and Umbrosus species groups, Subgenus Anopheles (Diptera: Culicidae). *Journal of the American Mosquito Control Association*; ll (3): 323-328

Barker RJ. 1970. Karyotypic trends in bats "Biology of Bats". WA. Wimsatt (editor), Academic Press, New York and London; 66- 67

Barron MG, Paupy C, Rahola N, Akone-Ella O, Ngangue, MF, Wilson-Bahun TA, Pombi M, Kengne P, Costantini C, Simard F, et al. 2019. A new species in the major malaria vector complex sheds light on reticulated species evolution. *Sci. Rep*.; 9, 14753

Bozek M, Leitch AR, Leitch IJ, Drábková ZL, Kuta E. 2012. Chromosome and genome size variation in *Luzula* (Juncaceae), a genus with holocentric chromosome. *Botanical Journal of the Linnean Society*; 170: 529-541

Choochote W. 2011. Evidence to support karyotypic variation of the mosquito, Anopheles peditaeniatus in Thailand. *Journal of Insect Science*; 11:10

Coluzzi M, Sabatini A. 1967. Cytogenetic observations on species A and B of the *Anopheles gambiae* complex. *Parasitologia*; 9: 73-88

Coosemans M, Petrarca V, Barutwanayo M, Coluzzi M. 1989. Species of the *Anopheles gambiae* complex and chromosomal polymorphism in a rice-growing area of the Rusizi Valley (Republic of Burundi). *Parassitologia*; 31: 113-122

Dehury S, Dehery SK, Das, AB. 2021. Karyotype variation in eight cultivars of Indian Dessert Banana (*Musa acuminata* L.) of Section Eumusa from Odisha, India. *Caryologia*; 74: 23-31.

Eroğlu E H, Doğan H, Altay D, Budak Ü. 2017. The Medicinal Plant of Genus *Paronychia* and the karyotype analysis of *Paronychia adalia*. *Int. J. Sec. Metabolite*; 4: (3) 103-107

Felip A, Carrillo M, Herráez MP, Zanuy S, Basurco B. 2009. Protocol I - Preparation of metaphasic chromosomes [Practical guide of protocols: methods of verification of the ploidy]. Advances in fish reproduction and their application to brood stock management: a practical manual for sea bass. Zaragoza: CIHEAM / CSIC-IATS; 61-65 (Options Méditerranéennes: Série B. Etudes et Recherch es; n. 63

Gillies MT, De-Mellion B. 1968. The Anophelinae of Africa South of the Sahara. South African Institute for Medical Research, Johannesburg, South Africa

Gillies MT, Coetzee M. 1987. A supplement to the Anophelinae of Africa South of the Sahara (Afrotropical region). South African Institute for Medical Research, Johannesburg, South Africa

Guerra M. 2012. Cytotaxonomy: The end of childhood. *Plant Biosyst*; 146: 703-710.

Hamza AM, El-Rayah EL-A, Abukashawa SM. 2014. Molecular characterization of mosquitoes of *Anopheles gambiae* species complex (Diptera: Culicidae) from Sudan and Republic of Southern Sudan. *J Mosquito Res*; 4 (13): 1–10

Kirov I, Khrustaleva L, Van Laere K, Soloviev A, Meeus S, Romanov D, Fesenko I. 2017. DRAWID: user-friendly java software for chromosome measurements and ideogram drawing. *Comparative Cytogenetics*; 11(4): 747-757

Levan AK, Fredgaand KA, Sandberg A. 1964. Nomenclature for centromeric position on chromosomes. *Hereditas*; 52: 201-220

Marinho MAO, Sales-Melo, MRC, Melo de Oliveira MB, Maciel VEdO, de Carvalho R. 2016. Karyotype variation in 11 species of the Vernonieae Cass. tribe (Asteraceae Bercht. & J. Presl). Plant Biosyst. Int. *J. Deal. All Asp. Plant Biol*; 151: 291-303.

Mustafa MS, Jaal Z, Abu Kashawa S, Nor S M. 2021. Population genetics of *Anopheles arabiensis*, the primary malaria vector in the Republic of Sudan. *Malaria Journal*; 20: 469

Rafael MS and Tadei WP (1998). Metaphase karyotypes of *Anopheles* (*Nyssorhynchus*) *darlingi* Root and *A.* (*N.*) *nuneztovari* Gabaldón (Diptera; Culicidae). *Genet. Mol. Biol.* 21: 351-354.

Rafael MS, Santos-Jr IP, Tadei WP, Carvalho KA, Recco-Pimente SM, Sallum MAM, Forrattini OP. 2006. Cytogenetic study of *Anopheles albitarsis* (Diptera: Culicidae) by C-banding and in situ hybridization. *Hereditas*; 143: 62- 67

Rafael MS, Santos-Junior IP, Tadei WP, Sallum MAM, Forattini OP. 2005. Karyotype of Brazilian *Anopheles*

albitarsis complex. *Genetics and Molecular Research*; 4 (4): 684-690

Rai K. 1963. A comparative study of mosquito karyotypes. *Ann Entomol Soc Amer*; 56: 160-170

Rasband CA, W S, Eliceiri KW. 2012. NIH Image to Image J: 25 years of image analysis. Nature Methods; 9(7): 671–675.

Robert D, Hunter Jr, Keith WH. 1986. Observations on the mitotic chromosomes of the mosquito *Toxorhynchites amboinensis* (Doleschall). *Mosquito Systematics*; 18(Z):119-124.

Sadílek D, Angus RB, Šťáhlavský F, Vilímová J. 2016. Comparison of different cytogenetic methods and tissue suitability for the study of chromosomes in *Cimex lectularius* (Heteroptera, Cimicidae). *Comparative Cytogenetics*; 10(4): 731-752.

Sarala KS. 1998. Anopheline species complexes in South-East Asia. WHO, New Delhi. Technical Publication; SEARO No: 18.

Sharma A, Kinney NA, Timoshevskiy VA, Sharakhova MV, Sharakhov IV. Structural Variation of the X Chromosome Heterochromatin in the *Anopheles gambiae* Complex. *Genes* 2020; 11, 327: 1-20.

Tjong DH, Syaifullah Indra S, Amelia A. 2012. A complex *Rana chalconota* karyotype found in West Sumatra. *Biospecies*; 5213 - 19

Tüzün A, Yükse S. 2009. Insect chromosomes preparing methods for genetic researches. *African Journal of Biotechnology*; 0l. 8 (1), 001-003

Vimala Y, Lavania S, Lavania UC. 2021. Chromosome change and karyotype differentiation–implications in speciation and plant systematics. *Nucleus*; 64: 33–54.

White GB. 1980. Academic and applied aspects of mosquito cytogenetics. In: Insect cytogenetics (Blackman RL, Hewitt GM and Ashburner M, eds.). Blackwell Scientific Publications, London, England, 245-274

WHO, World Health Organization. 2018. World Malaria Report

WHO, World Health Organization. 1975. Manual on Practical Entomology in malaria: part II, Methods and techniques. WHO, offset publications, No: 13. Geneva, Switzerland

Zhao X, Fan R, Lin G, Wang X. 2013. Chromosome abnormalities in diffuse large B-cell lymphomas: analysis of 231 Chinese patients. *Hematological Oncology*; 3 (31): 127-135

Caryologia
International Journal of Cytology, Cytosystematics and Cytogenetics

Firenze University Press
www.fupress.com/caryologia

OPEN ACCESS

Citation: Gousia Jan, Asim Iqbal Bazaz, Azra Shah, Saima Andleeb, Irfan Ahmad, Durdana Qazi, Oyas Asimi, Bilal A. Bhat, Anayitullah Chesti (2023). Karyotypic analysis of Crucian carp, *Carassius carassius* (Linnaeus, 1758) from cold waters of Kashmir Himalayas. *Caryologia* 76(2): 23-30. doi: 10.36253/caryologia-2112

Received: April 14, 2023

Accepted: October 29, 2023

Published: December 31, 2023

Data Availability Statement: All relevant data are within the paper and its Supporting Information files.

Competing Interests: The Author(s) declare(s) no conflict of interest.

Karyotypic analysis of Crucian carp, *Carassius carassius* (Linnaeus, 1758) from cold waters of Kashmir Himalayas

Gousia Jan[1], Asim Iqbal Bazaz[2], Azra Shah[1], Saima Andleeb[1], Irfan Ahmad[1,*], Durdana Qazi[1], Oyas Asimi[3], Bilal A. Bhat[5], Anayitullah Chesti[4]

[1] *Division of Fish Genetics & Biotechnology, Faculty of Fisheries, SKUAST-K, Rangil, J&K, India-06*
[2] *Division of Fisheries Resource Management, Faculty of Fisheries, SKUAST-K, Rangil, J&K, India-06*
[3] *Division of Fish Nutrition & Biochemistry, Faculty of Fisheries, SKUAST-K, Rangil, J&K, India-06*
[4] *Division of Aquaculture, Faculty of Fisheries, SKUAST-K, Rangil, J&K, India-06*
[5] *Division of Social Sciences, Faculty of Fisheries, SKUAST-K, Rangil, J&K, India-06*
*Corresponding author. E-mail: ahmadirfan@skuastkashmir.ac.in

Abstract. *Carassius carassius* (Linnaeus, 1758) is an exotic fish to Kashmir, locally known as "gang gad" and commonly called as "crucian carp". It belongs to family Cyprinidae. The present study aimed to identify the chromosome number of the *Carassius carassius* and to optimize the colchicine concentrations (0.01%, 0.025%, and 0.05%) and hypotonic treatment timings (25, 35, and 45 minutes) for the chromosome preparation in *Carassius carassius* in order to obtain the highest number of clear and identifiable metaphasic chromosomal spreads. Data collected was analyzed and the means of each treatment was compared. The findings of the present study indicated that there was a significant influence of colchicine concentration, hypotonic timings as well as colchicine concentration× hypotonic timings ($P<0.01$) on the number of metaphase chromosome spreads. Furthermore a significant ($P<0.01$) strong positive correlation obtained between colchicine concentrations, hypotonic timings and the number of metaphase chromosome spreads. The findings of the present study recommends further research into chromosomal modification techniques such as fish polyploid production, gynogenesis, androgenesis, and inter or intra-species hybridization is needed to generate unique and good inbred lines in aquaculture.

Keywords: *Carassius carassius,* Colchicine, optimization, metaphase chromosome, kidney, hypotonic solution.

INTRODUCTION

The Cyprinidae (Teleostei: Cypriniformes) is a globally widespread and one of the richest and most vital family of fish (Al-Sabti, 1991; Kalbassi,

2008). It is a large family of freshwater fishes commonly called the carp family comprising of vast majority of bony fishes (Abdoli, 1999). The Crucian Carp (*Carassius carassius* Linnaeus, 1758) is a medium-sized fish in the Cyprinidae family and is a widespread European species. *Carassius carassius* is locally known as "gang gad" and more specifically known as "crucian carp" and was introduced into Dal Lake in Kashmir, India between 1956 and 1958 (Shafi, 2012). It is one of the most abundant cyprinids in Dal Lake Kashmir and it has adapted to a wide range of habitats to cope with abiotic environmental challenges such as low oxygen levels and water temperature variations (Holopainen and Hyvarinain, 1985).

The study of fish chromosomes has long been a popular topic of study due to its usefulness in fish population conservation, cytotaxonomy, phylogeny research and evolutionary studies Luca *et al*. (2010); Bazaz *et al*. (2022). The development of techniques such as karyotyping has made it possible to visualize undetected chromosomal anomalies such as small portions of chromosomes and translocations of tiny parts of chromosomes to one another Bazaz *et al*. (2022). Fish cytology may be beneficial in interpreting the evolution of higher vertebrates and the interrelationships among the numerous divisions of fishes, because they are a primordial chordate group. In terms of species characterisation, evolution and systematics, chromosomal studies have acquired a lot of traction in recent years (Barat *et al*., 2002). One of the most critical parts of fish conservation is genetic characterisation. Using cytogenetic, biochemical-genetic and advanced molecular genetic approaches, this is conceivable. Cytogenetic characterisation is concerned with the study of chromosomes, which serve as genetic vehicles for a variety of genetic investigations, from the creation of gene maps and chromosome organisation models to the investigation of gene function and dysfunction. Various methods are now being used to study fish chromosomes, with improvements and modifications such as the pretreatment with colchicine and hypotonic solution, which causes the cells to enlarge and the chromosomes to separate (Luca *et al*., 2010; Bazaz *et al*., 2022).

There are a number of factors that may have contributed to the decline of fish species including habitat loss and degradation, displacement via competition with introduced species such as the polyploid biotype such as the goldfish (*Carassius auratus*) and the common carp (*Cyprinus carpio communis*). Moreover, all species of *Carassius*, including the crucian carp (*Carassius carassius*), Prussian carp (*Carassius gibelio*) and goldfish (*Carassius auratus*) are often confused due to their morphological similarity Knytl et al. (2021). Such confusion may lead to inappropriate stocking of wrong species instead of intended support of a population of crucian carp with negative consequences.

Genetic contamination seems to be a very important but a hidden threat. Hybridization occurs and has been reported in various carassius species between such as *Carassius carassius* and *Carassius gibelio* (Prokes and Barus 1996). This type of hybridization was also confirmed using molecular (Wouters et al. 2012) and cytogenetic techniques (Knytl et al. 2013).

Hybrids between *Carassius carassius* and *Carassius auratus* (Hanfling et al. 2005; Smartt 2007) and intergeneric hybrids between *Carassius carassius* and *Cyprinus carpio* (Hanfling et al. 2005) has been observed. Moreover, molecular data suggest that these hybrids are able to reproduce and form relative generations by backcrossing (Hanfling et al. 2005, Wouters et al. 2012).

The cytogenetics of *Carassius carassius* is still inadequately understood. Interestingly, different diploid chromosome numbers 2n = 50 Raicu et al. (1981), 2n = 98 Manna, (1983), 2n = 100 Knytl et al. (2021) and 2n = 104 Chiarelli et al. (1969) has been reported. Similarly Knytl et al. 2021 reported the number of chromosomes in three Carassius species (*C. auratus*, *C. carassius* and *C. gibelio*) was uniform (2=100). The authors reported no differences in chromosomal morphology between male and female individuals. This findings confirmed homomorphic sex chromosomes at least in diploid biotypes of the genus *Carassius*.

Such an unclear condition encourages to present cytogenetic analyses of *Carassius carassius* with respect to hybridization processes and the related threats to indigenous species in Kashmir waters. Furthermore, the considerable karyotypic study on *Carassius carassius* has not been published in the Kashmir valley from decades. The cyto-taxonomic status of *Carassius carassius* with respect to the species hybridization and diploid/tetraploid status has remained unclear. In respect to its unclear distribution of possible diploid and/or tetraploid forms as well as hybridization process, the present study is an important contribution to the cytogenetics and cytotaxonomy of *Carassius carassius*. The present study deals with chromosomal characteristics of crucian carp (*Carassius carassius*) from the cold waters of Kashmir Himalayas.

MATERIALS AND METHODS

The research work was carried in the Division of Fish Genetics and Biotechnology, Faculty of Fisheries, SKUAST Kashmir, Rangil, Ganderbal, J&K, India.

Sample collection

A total of 45 specimens of *Carassius carassius* were collected from Dal Lake Srinagar, Kashmir and were transported live in an insulated box containing ice packs and equipped with aerators to the Fish Genetics and Biotechnology laboratory, faculty of fisheries, SKUAST-Kashmir. Fish were kept in 50L tubs equipped with continuous aeration. Identification of *Carassius carassius* was done following the diagnostic characters described by Kullander *et al*. (1999).

Chromosome preparation

Chromosome preparation for *Carassius carassius* species was done by the methods described by Killgerman and Bloom (1977), and Shao *et al*. (2010) with some modifications. For each treatment, five samples were used. Three different concentrations of freshly prepared colchicine (0.01%, 0.025% and 0.05%), were injected intramuscularly at 1ml/100g of body weight for 90 minutes to depress the mitotic division at the metaphase stage (Table 1). The fish were anesthetized using clove oil and were dissected. The anterior kidney was removed, homogenized and hypotonised simultaneously in 0.56% KCl for 25, 35 and 45 minutes at room temperature. Thereafter, the cell suspension was centrifuged for 10 min at 1300 rpm. Supernetant was removed and cells were fixed by chilled carnoy's fixative solution (methanol: glacial acetic acid) and left overnight, fixation process was repeated two-three times until the clear suspension was obtained with the fresh chilled fixative solution replaced every time. The suspension was centrifuged at 1300 rpm for 10 minutes before to each subsequent procedure in the formal treatment; the supernatant was then removed, leaving one ml of the solution above the cell pellet in its place. The next solution was used to resuspend the cells. Slides were prepared by dropping method, three drops of the cell suspension on the pre-heated slide from about 40-50 cm height with slide slightly placed in an inclined position. The slides were stained using Giemsa stain (10%) distilled water and air-dried. Coverslips were placed on slides by mounting with D.P.X mountant to make them permanent and protect them from drying out.

Table 1. Experimental details.

Treatments	Colchicine concentration	Hypotonic treatments timings (mins)	No. of Samples/ treament	No. of Slides / treatment
T1	0.01%	25	5	15
T2	0.01%	35	5	15
T3	0.01%	45	5	15
T4	0.025%	25	5	15
T5	0.025%	35	5	15
T6	0.025%	45	5	15
T7	0.05%	25	5	15
T8	0.05%	35	5	15
T9	0.05%	45	5	15

Screening of slides

The slides were observed under the field illuminated trinocular microscope (Olympus CX-21) fitted with camera at 100X objective and screened for good metaphase chromosomal spreads.

Statistical analysis

The data obtained from the different treatments was tested statistically by applying TWO-WAY ANOVA (SPSS, version 20) to evaluate the significant differences between each treatment and their interactions. Differences among the means between the groups and within the groups were tested by "Duncan's multiple mean range test" $P<0.01$.

RESULTS

The highest (Mean±SE) number of chromosomal spreads among the treatment groups were recorded in group T9 at 64.46±2.50 and the lowest (Mean±SE) number of chromosomal spreads were recorded in group T1 at 1.93±1.83 (Table 2). A significant ($P<0.01$) positive correlation between colchicine concentration and the number of metaphasic chromosomal spreads at various hypotonic timings was observed as presented in Table 3 indicating that increase in colchicine concentration from 0.01% to 0.05%, the number of chromosomal spreads also increased (Table 3). Hypotonic treatment timings also estimated a significant ($P<0.01$) positive correlation with number of metaphasic chromosomal spreads (Table 4). The modal diploid chromosome number of *C. carassius* was found to be 2n = 100 (Figure 1). The chromosomes were classified into 20 metacentric, 36 sub- metacentric, 44 sub-telocentric and telocentric chromosomes 20 (M), 36 (SM), 44 (ST/T) (Figure 2).

Figure 3 depicts the frequency percentage of diploid chromosome number ranging from 94 to 102 per

Table 2. Average number of metaphase chromosome spreads among various treatments.

Treatments	Number of metaphasic chromosomal spreads (Mean±SE)
T_1	1.93±1.83
T_2	3.6±2.84
T_3	9.6±2.84
T_4	26.13±2.55
T_5	40.8±3.40
T_6	47.86±2.32
T_7	28.53±2.16
T_8	50.93±1.79
T_9	64.46±2.50

Table 3. Correlation between colchicine concentrations and number of metaphase chromosome spreads.

	Colchicine concentrations (25 minutes of hypotonic timings)	Colchicine concentrations (35 minutes of hypotonic timings)	Colchicine concentrations (45 minutes of hypotonic timings)
Metaphase Chromosome Spreads	0.890*	0.942*	0.969*

Table 4. Correlation between Colchicine concentrations and number of metaphase chromosome spreads.

	Hypotonic timings (0.01% Colchicine concentration)	Hypotonic timings (0.025% Colchicine concentration)	Hypotonic timings (0.05% Colchicine concentration)
Metaphase Chromosome Spreads	0.761*	0.939*	0.980*

* Significant at 0.01 level of significance.

metaphases. A total of 250.00 metaphasic chromosomal spreads studied from the cells of kidney tissues of *Carassius carassius* revealed that the modal diploid chromosome number of this species was found to be 2n = 100 which is valid over 70% of metaphasic cells. Figure 4 depicts the number of metaphase chromosome spreads at different colchicene concentrations (0.01%, 0.025%, 0.05%) and varied hypotonic treatment timing (25, 35, 45 minutes) indicating an increasing pattern of number of chromosome spreads with an increase in colchicene concentration and hypotonic treatment timings.

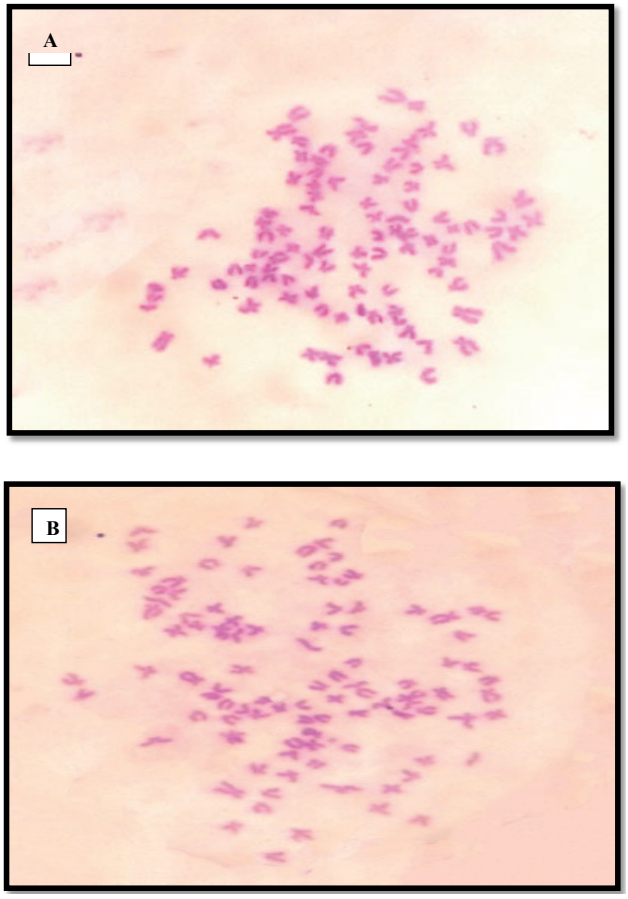

Figure 1. (A&B): Metaphase chromosome spreads of *Carassius carassius* (2n=100) at 100x oil emulsion.

DISSCUSSION

Chromosomes are best Karyotyped during somatic metaphase whereby one can study chromosomal number, size and morphology. To date, a variety of Karyotyping techniques have been developed to visualise chromosomes of fish at various developmental stages, including tissue cultures (Lomax *et al*., 2000), squashing techniques (Armstrong and Jones 2003) and cell suspensions of tissues undergoing mitosis (Fan and Fox 1990; Henegariu *et al*., 2001). Nonetheless, approaches aimed at the embryonic and larval stages of fish have struggled to achieve a consistent number of recognisable and widely distributed metaphase chromosomes, owing to differences in mitotic cell division rates among fish species (Shao *et al*., 2010). Pretreatment with colchicine combined with various kayotyping techniques has led to a revolution in fish chromosomal studies (Roberts, 1964; Denton and Howell, 1969). Cochicine is a spindle poison used in traditional chro-

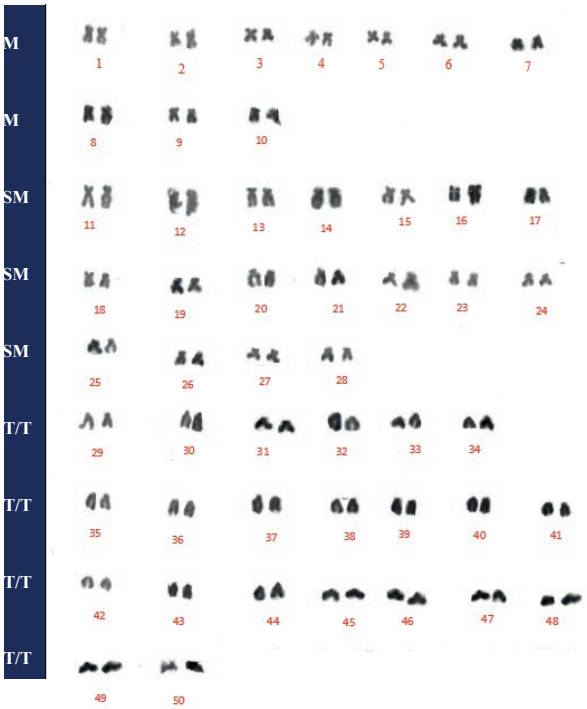

Figure 2. Chromosomal classification of diploid *Carassius carassius* 2n= 100. Metacentric (M)= 20, Sub-metacentric (SM)=36, Sub-telocentric/ Telocentric (ST/T)= 44.

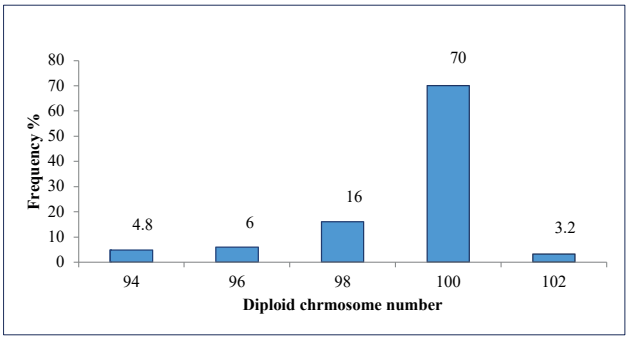

Figure 3. Frequency percentage of diploid Chromosome number of *Carassius carassius*.

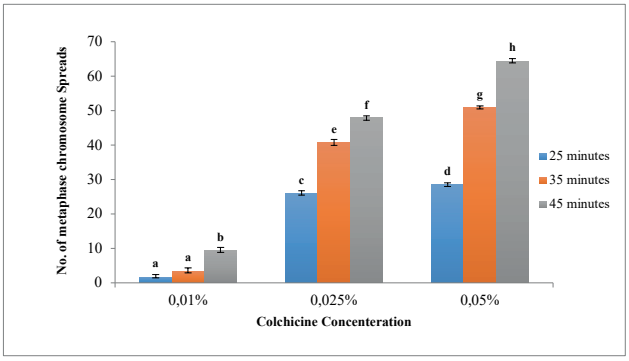

Figure 4. Graphical representation of number of metaphase chromosome spreads at different colchicene concentrations and varied hypotonic treatment timing. Data shown are mean ± SE with different letters are significantly different from each other (P≤ 0.01).

mosomal preparation techniques to stop the cells from entering metaphase (Kligerman and Bloom, 1977). It is a naturally occurring alkaloid found in the Colchicum autumnale plant which binds to tubulin, preventing it from polymerizing, affecting microtubule dynamics and causing mitosis to be disrupted, generating a shift in the tubulin dimer, which is largely irreversible. When a tubulin dimer bounds to colchicine the polymer becomes unstable and disassembles. (Schliwa 1986). Cells or larvae must be treated in a hypotonic solution after mitotic spindle inhibition to expand the nuclei and disperse the chromosomes over the slides (Moore and Best, 2001). Pretreatment with colchicine solution two hours before collection of the tissue in hypotonic sodium citrate or potassium chloride, followed by bringing the cells in suspension, fixation of cells in Cornoy's fixative solution, smear on slides. and staining in various stains is now widely used for Karyotypic preparation. The staining techniques (e.g., aceto-orcein, haematoxylin, Giemsa, Wright and Leishman stains) or banding techniques (e.g., Q-banding, G-banding, R-banding, C-banding and high-resolution banding) are used to stain chromosomes for various purposes (Calado *et al*., 2013; Moore and Best 2001).

The choice of a right concentration and duration of exposure of colchicine is very important. This is because in sufficient amount of could fail to arrest the target cells amount could fail to arrest the target cells at metaphase stage (Rieder & Palazzo, 1992; Caperta *et al*., 2006), however too high a concentrations or prolonged exposure, on the other hand, may lead to chromosomal condensation. As a result, the first stage in this technique was to optimize colchicine concentration to inhibit cell division in *Carassius carassius*. The optimum concentration of 0.05% for colchicine recorded in this study is similar to the findings of Karami *et al.* (2015), the authors reported that the optimum concentration of colchicine was observed at 0.05% among the 0.01%, 0.025% and 0.05% tested in African catfish (*Clarias gariepinus*) and the zebrafish (*Danio rerio*). Similarly, Okomoda *et al.* (2018) reported that juveniles of *Pangasianodon hypophthalmus* and *Clarias gariepinus* had better chromosome spreads at 0.05% colchicines concentration compared to 0.01% and 0.025%. This, however, contra-

dicts with the findings of Shao *et al.* (2010) and Pradeep *et al.* (2011) in chromosomal preparation of fish larvae and reported the best metaphase chromosomal spreads at colchicine concentrations of 0.02% and 0.01%, respectively. While, this may be a sufficient amount concentration to penetrate the vitelline membrane of the egg and the thin walls of the larvae, the present study shows this is not optimum for adult *Carassius carassius*.

It's vital to choose a suitable hypotonic solution to swell the mitotic cell nuclei to the point of bursting and spread out the chromosomes after mitotic spindle inhibition (Moore & Best, 2001). Choosing an improper hypotonic solution and incubation period may result in overlapping or significant loss of chromosomes (Baksi and Means, 1988). Hypotonic treatment allows the swelling of the cell, which facilitates cell disruption and the dispersion of chromosomes when the cell contents are spread on slides. Potassium chloride (KCl 0.075 M) is one of the most commonly used hypotonic solutions in chromosomal preparation protocols Bayat and Woznicki, (2006); Shao *et al.* (2010); Pradeep *et al.* (2011); Bazaz *et al.* (2022). The efficiency of potassium chloride (KCl 0.075M) over distilled water was demonstrated by Okomoda *et al.* (2018) reported that the number of clear metaphase chromosome spreads were significantly higher using the former than the latter. Smilarly, Ida *et al.* (1978) reported that the use of potassium chloride showed the best chromosome spreads as compared to other two hypotonic solutions of sodium citrate and distilled water. In order to improve chromosome spreads, hypotonic treatment is essential. Hypotonic treatment induces swelling when cell contents are distributed on slides, facilitating cell disintegration and chromosomal dispersion. To procure a desirable number of clear chromosome spreads, the hypotonic solution should be modified according to the species of fish and/or larval age (Karami *et al.,* 2015). The current study found that hypotonic treatment time of 45 minutes was more effective than 25 and 35 minutes, however majority of the chromosomes were overlapped at 25 minutes of hypotonic treatment. In rainbow trout, chromosomal spreading was insufficient at 0.56% KCl for hypotonic treatment at a lower temperature Chourrout and Happe (1986). Furthermore, it was shown that the same concentration of KCl yielded superior results when the experiments were carried out at ambient temperature. However, 0.56% KCl for hypotonic treatment with an adequate time at room temperature provided good results in the current investigation.

Chromosome counts have long been used to characterize an organism or lineages most basic genetic characteristics. Chromosome counts have been utilized as useful phylogenetic indicators (Guerra 2008) and their role in evolutionary processes has been discussed several times (Mayr 1982; Clark and Donoghue, 2018). Cyprinid fishes have long been the considerable cytogenetic research, with a focus on evolutionary issues (Taki *et al.*, 1977). The 2n number in the Cyprinidae family ranges from 44 to 100 (Arai, 1982). The most common diploid number in the Cyprinidae family is 50, which is regarded as the modal number in this family (Manna, 1984; Rishi, 1989). Cyprinid fishes have short chromosomes with centromere placements that range from median to nearly terminal, making it difficult to allocate some chromosomes to specific chromosomal groups as a result, making accurate identification of individual chromosomes nearly impossible (Rab and Collares-Pereira, 1995). The results of the current study revealed that *Carassius carassius* (crucian carp) possess 2n=100 chromosomes in its somatic cells. The results of the current study are in agreement with findings of Spoz *et al.* (2014); Knytl *et al.* (2013); Boron *et al.* (2010); Wang *et al.* (1995); Kasama and Kobayasi (1991); Mayr *et al.* (1986); Sofradzija *et al.* (1978); Hafez *et al.* (1978); and Kobayasi *et al.* (1970), as they all reported the same diploid chromosome count of 2n=100. However, Raicu *et al.* (1981) reported the diploid chromosome number 2n = 50 in Danube Delta of *Carassius carassius* individuals. In contrast to Raicu *et al.* (1981), Chiarelli *et al.* (1969) reported a diploid chromosomal number of 2n=104, which might most likely be attributed to preparation artifact.

CONCLUSION

The results obtained from the present study showed that 0.05% colchicine concentration resulted highest number of chromosomal spreads compared to other colchicine concentrations. KCl treatment for 45 minutes in *Carassius carassius* proved to be more effective than other treatment timings in terms of chromosome spread quality and highest number of metaphase chromosome spreads. A significant ($P<0.01$) positive correlation between colchicine concentration and the number of metaphasic chromosomal spreads at various hypotonic timings indicating an increase in colchicine concentration from 0.01% to 0.05%, the number of chromosomal spreads also increased. The modal chromosome number of *Carassius carassius* species was found to be 2n = 100.

ACKNOWLEDGEMENT

The authors are grateful to faculty of fisheries, SKUAST-Kashmir for their valuable support in completing this study.

REFRENCES

Abdoli, A, 1999. The Inland water fishes of Iran. *Natural and wildlife museum of Iran, Tehran* pp. 378.

Al-Sabti, K, 1991. Handbook of genotoxic effects and fish chromosomes. *Slovenia* pp. 221

Arai, R, 1982. A Chromosome study on two cyprinid fishes, *Acrossocheilus labiatus* and *Pseudorasbora pumila pumila*, with notes on Eurasian cyprinids and their karyotypes. *Bull. Natl. Sci. Mus.* Tokyo pp. 131-152.

Armstrong S J, Jones G H, 2003. Meiotic cytology and chromosome behaviour in wild-type *Arabidopsis thaliana*. *Journal of experimental botany*, **54**(380): 1-10.

Baksi S M, Means J C, 1988. Preparation of chromosomes from early stages of fish for cytogenetic analysis. *Journal of fish biology*, **32**(3): 321-325

Barat, A, Sahoo, P K and Ponniah, A G, 2002. Karyotype and Nucleolar Organizer Regions (NORs) in a few hill Stream fishes. *The Fifth Indian Fisheries Forum*.

Bayat, D F and Woznicki, P. 2006. Verification of ploidy level in sturgeon larvae. *Aquaculture Research* **37**: 1671-1675.

Bazaz, A I, Ahmad, I, Shah, T H, Arab, N U, (2022). Karyomorphometric analysis of fresh water fish species of India, with special reference to cold water fishes of Kashmir Himalayas. A Mini Review. Caryologia 75(1): 109-121. doi: 10.36253/caryologia-1362.

Boron, A, Kirtiklis, L, Porycka, K, Abe, S, Juchno, D, Grabowska, A, Duchnowska, K, Karolewska, M, Kuczewska, A, Miroslawska, U and Wierzibicki, P, 2010. Comparative cytogenetic analysis of two *Carassius* species (Pisces, Cyprinidae) using chromosome banding and FISH with rDNA. *Chromosome Research* **20(**10): 749.

Calado, L L, Bertollo, L A C, Costa, G W W Fd, Molina, W F, 2013. Cytogenetic studies of Atlantic mojarras (Perciformes–Gerreidae): chromosomal mapping of 5S and 18S ribosomal genes using double FISH. *Aquac Res,* **44**: 829–835

Caperta A, Delgado M, Ressurreic F, Meister A, Jones R, Viegas W, Houben A. 2006. Colchicine-induced polyploidization depends on tubulin polymerization in c-metaphase cells. Protoplasma, **227:147**–153

Chiarelli, B, Ferrantelli, O, Cucchi, C, 1969. The caryotype of some teleostean fish obtained by tissues culture in vitro. *Experientia* **25**(4): 426–427.

Chourrout, D. and Happe, A, 1986. Improved methods of direct chromosome preparation in rainbow trout, Salmo gairdneri. *Aquaculture* **52**: 255–261

Clark, J W and Donoghue, P C J, 2018. Whole-genome duplication and plant macroevolution. *Trends Plant Sci*. **2**(10): 933–945.

Denton, T E and Howell, W M, 1969. A technique for obtaining chromosomes from the scale epithelium of teleost fishes. *Copeia* **2**: 392-393.

Fan, Z and Fox, D P, 1990. A new method for fish chromosome preparation. *Journal of fish biology* **37**(4): 553-561.

Guerra, M. 2008. Chromosome numbers in plant cytotaxonomy: concepts and implications. *Cytogenet Genome Res*. **120**(3–4): 339–350

Hafez, R, Labat, R and Quiller, R, 1978. Etude cytogenetique chez quelques especes de cyprinides de la region Midi-Pyrenees. *Bulletin de la Societe d'Histoire Naturelle de Toulouse* **114**(1–2): 122–159.

Hanfling B, Bolton P, Harley M, Carvalho G.R. (2005). A molecular approach to detect hybridisation between crucian carp (Carassius carassius) and non-indigenous carp species (Carassius spp. and Cyprinus carpio). *Freshwater Biology* **50**(3): 403-417. doi: 10.1111/j.1365-2427.2004.01330.x

Henegariu O, Heerema N A, Wright L L, Brayward P, Ward D C, Vance G H, 2001. Improvements in cytogenetic slide preparation: Controlled chromosome spreading, chemical aging and gradual denaturing. Cytometry, **43**: 101-109.

Holopainen, K J and Hyvarinain, H, 1985. Ecology and physiology of crucian carp *Carassius carassius* (L) in small conditions in fin fish ponds with anoxic conditions in winter. *Verh. Internal. Verem. Limnol.* **22**(4): 2566-2570.

Ida H, Murofush I M, Fujiwara S, Fujino K, 1978. Preperation of Fish chromosomes by in vitro Cochicine treatment. *Japanese Journal of Ichthyology*, **24** (4): 281-284.

Kalbassi, M R, Hosseini, S V and Tahergorabi, R, 2008. Karyotype Analysis in Schizothorax zarudnyi from Hamoon Lake, Iran. *Turkish Journal of Fisheries and Aquatic Sciences* **8**: 335-340.

Karami, A, Araghi, P E, Syed, M A, Wilson, S P, 2015. Chromosome preparation in fish: effects of fish species and larval age. *International Aquatic Research*, **7**, 201-210

Kligerman A D, Bloom S E, 1977. Rapid chromosome preparations from solid tissues of fishes. *Journal of fisheries research board of Canada*, **34**: 249-261

Knytl, M, Kalous, L and Rab, P, 2013. Karyotype and chromosome banding of endangered crucian carp, *Carassius carassius* (Linnaeus, 1758)(Teleostei, Cyprinidae). *Comparative Cytogenetics* **7**(3): 205.

Knytl M, Fornaini NR, 2021. Measurement of Chromosomal Arms and FISH Reveal Complex Genome Architecture and Standardized Karyotype of Model Fish, Genus Carassius. *Cells,* **10**(9):2343. https://doi.org/10.3390/cells10092343.

Kobayasi, H, Kawashima, Y and Takeuchi, N, 1970. Comparative chromosome studies in the genus *Carassius*, especially with a finding of polyploidy in the ginbuna (*C. auratus langsdorfii*) (Teleostei: Cyprinidae). *Japanese Journal of Ichthyolog*y **17**: 153–160.

Kullander S O, Fang F, Delling B, Ahlander E, 1999.The fishes of the Kashmir Valley. River Jhelum, Kashmir Valley. Impacts on the Aquatic Environment: 99-168.

Lomax B, Tang S, Separovic E, Phillips D, Hillard E, Thomson T and Kalousek D K, 2000. Comparative genomic hybridization in combination with flow cytometry improves results of cytogenetic analysis of spontaneous abortions. *The American Journal of Human Genetics*, **66**(5): 1516-1521.

Luca, C., Suciu, R., Costache, M, 2010. Comparative karyotype in different lineages of cyprinid fish (Teleostei: Cypriniformes: Cyprinidae). *Studia Universitatis "Vasile Goldiş", Seria Ştiinţele Vieţii*; **20**: 37-41.

Manna GK. 1983. Cytogenetic studies on fishes and Amphibia. Genetical Research in India. Indian Council of Agricultural Research Publication, pp. 886-898.

Mayr, B, Rab, P. and Kalat, M, 1986. NORs and counterstain-enhanced fluorescence studies in Cyprinidae of different ploidy level. *Genetica* **69**(2): 111–118.

Mayr, E, 1982. Speciation and macroevolution. *Evolution* **36**(6): 1119–1132

Moore C M, Best R G. 2001. Chromosomal genetic disease: structural aberrations. *Encyclopedia of Life Sciences.*

Okomoda VT, Koh IC, Hassan A, Amornsakun T, Moh JH, Shahreza SM. 2018. Optimization of the cytogenetic protocol for *Pangasianodon hypophthalmus* (Sauvage, 1878) and *Clarias gariepinus* (Burchell, 1822). *Peer Journal*, 6: e5712.

Pradeep P J, Srijaya T C, Zain R B M, Papini, A, Chatterji, A K, 2011. A simple technique for chromosome preparation from embryonic tissues of teleosts for ploidy verification. *Caryologia*, **64**: 235–241.

Prokes M, Barus V. (1996). On the natural hybrid between common carp (Cyprinus carpio) and Prussian carp (Carassius auratus gibelio) in the Czech Republic. *Folia Zoologica,* 45: 277-282.

Rab, P and Collares-Pereira, M J, 1995. Chromosomes of european cyprinid fishes. *Folia Zool.* **44**: 193-214

Raicu, P, Taisescu, E and Banarescu, P, 1981. *Carassius carassius* and *C. auratus*, a pair of diploid and tetraploid representative species (Pisces, Cyprinidae). *Genetica* **46**: 233–240.

Rieder C L, Palazzo RE.1992. Colcemid and the mitotic cycle. J Cell Sci 102:387–392

Rishi, K K, 1989. Current status of fish cyto-genetics. *Fish Genetics in India* pp 728-756.

Roberts, F L, 1964. A chromosome study of twenty species of Centrachidae. *Journal of Morphology* **115** (3): 401-417.

Smartt, J. 2007. A possible genetic basis for species replacement: preliminary results of interspecific hybridisation between native crucian carp Carassius carassius (L.) and introduced goldfish Carassius auratus (L.). *Aquatic Invasions,* **2**: 59-62. doi: 10.3391/ai.2007.2.1.7

Shafi, S, 2012. Study on fecundity and GSI of *Carassius carassius* from Dal Lake Kashmir. *Journal of Biology, Agriculture and Healthcare* **2**(3): 68-75.

Shao C W, Wu, P F, Wang, X L, Tian, Y S, Chen, S L, 2010. Comparison of chromosome preparation methods for the different developmental stages of the half-smooth tongue sole, *Cynoglossus semilaevis*. *Micron,* **41**:47–50

Sofradzija, A, Berberovic, L and Hadziselimovic, R, 1978. Hromosomske garniture karaša (*Carassius carassius*) i babuške (*Carassius auratus gibelio*)] Chromosome sets of *Carassius carassius* and *Carassius auratus gibelio*. *Ichthyologia* **10**(1): 135–148.

Spoz, A, Boron, A, Porycka, K, Karolewska, M, Ito, D, Abe, S, Kirtiklis, L and Juchno, D, 2014. Molecular cytogenetic analysis of the crucian carp, *Carassius carassius* (Linnaeus, 1758) (Teleostei, Cyprinidae), using chromosome staining and fluorescence in situ hybridisation with rDNA probes. *Comp Cytogenet* **8**: 233-248.

Taki, Y., Urvushido, T., Suzuki, A. and Seriziawa, C, 1977. A Comparative study of Puntius (Cyprinidae: Pisces). *Proceedings of Japan Academy* **53**(B): 231-235.

Wouters J, Janson S, Lusková V, Olsén K.H. (2012). Molecular identification of hybrids of the invasive gibel carp Carassius auratus gibelio and crucian carp Carassius carassius in Swedish waters. *Journal of Fish Biology* **80**(7): 2595-2604. doi: 10.1111/j.1095-8649.2012.03312.x

Caryologia
International Journal of Cytology, Cytosystematics and Cytogenetics

Firenze University Press
www.fupress.com/caryologia

OPEN ACCESS

Citation: Biplab Kumar Bhowmick, Sayani Nag (2023). Unfolding chromosomal uniqueness of the Scilloid ornamental *Albuca virens* by application of EMA based Giemsa- DAPI staining. *Caryologia* 76(2): 31-39. doi: 10.36253/caryologia-2124

Received: April 25, 2023

Accepted: October 19, 2023

Published: December 31, 2023

Data Availability Statement: All relevant data are within the paper and its Supporting Information files.

Competing Interests: The Author(s) declare(s) no conflict of interest.

ORCID
BKB: 0000-0001-6029-1098
SN: 0009-0009-1353-892X

Unfolding chromosomal uniqueness of the Scilloid ornamental *Albuca virens* by application of EMA based Giemsa- DAPI staining

Biplab Kumar Bhowmick*, Sayani Nag

Department of Botany, Scottish Church College, 1&3, Urquhart Square, Kolkata- 700006, West Bengal, India
*Corresponding author. E-mail: biplab.bhowmick@scottishchurch.ac.in

Abstract. The cytogenetic features in the tribe Ornithogaleae of subfamily Scilloideae is a prerequisite for understanding genome evolution. Unfortunately, genomic or the foundational chromosomal features are neglected within majority of Ornithogaloids, incuding *Albuca*, one of the largest genus of the tribe. *Albuca virens* (Lindl.) J.C. Manning & Goldblatt is the only ornamental species of *Albuca* found to be exotic to India. Analysis of karyotype by EMA method followed by Giemsa and DAPI staining is the first step towards molecular cytogenetics attempted in this species and has currently brought significant resolution in chromosome morphology (especially NORs). The Indian population of *A. virens* with 2n=6 chromosomes, symmetric karyotype and heterophorphy of NORs provide excellent scope to navigate questions on dysploid origin of *Albuca*. The regular meiotic stages advocate genomic stability despite vegetative propagation and polysomaty in root cells. The comparative review of chromosomal evolution within *Albuca* has been discussed in relation to the Indian *A. virens* as a prototype.

Keywords: *Albuca virens*, EMA, DAPI, meiosis, dysploidy, NORs.

INTRODUCTION

The genus *Albuca* belongs to the tribe Ornithogaleae of Asparagaceae/Hyacinthaceae, subfamily Scilloideae, sensu APG III 2009; APG IV 2016) with more than 100 species distributed mainly in sub-Saharan Africa (Goldblatt and Manning 2011; Martinez- Azorin et al. 2011). Considering repeated taxonomic amendments and changes in species circumscription (Martinez-Azorin 2011, 2023; Manning 2020), chromosomal features are given special attention to resolve species boundaries within the tribes of Asparagaceae/Hyacinthaceae (Goldblatt and Manning 2011). It is evident from the recent compilation that cytogenetic investigation is so far confined to chromosome counts or karyotypes by conventional staining methods in less than 50% of accepted species belonging to tribes Hyacintheae, Urgineeae, Orni-

thogaleae and Oziroëeae (Nath et al. 2022). *Albuca virens* (Lindl.) J.C. Manning & Goldblatt of subgenus *Urophyllon* (Salisb.) J.C. Manning & Goldblatt (Manning et al. 2009a,b) has been found to occur as an ornamental exotic to India while some wild populations are reported from north eastern part (Bhattacharya et al. 2016). Within subgenus *Urophyllon* of *Albuca*, karyotype analysis by fluorochrome staining is reported in *Albuca bracteata* (Thunb.) J.C.Manning & Goldblatt (worked out as syn. *Ornithogalum longibracteatum* Jacq.), the sister species of *A. virens* (Pedrosa et al. 2001). Nomenclatural ambiguity in previous cytological reports is another reason for blurring analysis of chromosomal relationships in *Albuca*. *A. virens* has four subspecies of which *A. virens* ssp. *virens* is previously known and worked out as different species of *Ornithogalum* with varying chromosome counts *viz*. *Ornithogalum virens* Lindl. (2n=6*), O. flavovirens* Baker (2n=10), *O. ecklonii* Schldl. (2n=10), *O. tenuifolium* Delaroche (2n=12, 10, 8, 16, 6, 4), *O. pretoriense* Baker (2n=12) or *O. inconspicuum* Baker (2n=20) (Goldblatt and Manning 2011). In our country also, very few traditional cytological studies have been conducted on *A. virens*, in the name of the syn. *Ornithogalum virens* (Ravindran 1977; Bhattacharya et al. 2016). Owing to the backdrops of conventional cytological studies, lucid karyotype features of *A. virens* is still missing.

Hence the aim of the present work is to obtain better cytogenetic analysis with enzymatic maceration and air drying (EMA) method (Kurata and Omura 1978; Fukui 1996) in *A. virens* over the traditional orcein staining approach. In spite of being a well-known alternate method for chromosome analysis (Fukui and Iijima 1991; Yamamoto *et al*. 2010, 2015; Nath et al. 2015; Jha et al. 2020; Jha 2021; Bhowmick and Jha 2022), EMA based approach has not been yet attempted in *Albuca virens*. Our adoption of EMA method enabled lucid karyotype interpretation, fluorescence staining and understanding meiotic chromosome behavior in this plant. The outcome of the present paper upgraded existing knowledge about chromosome configuration in this species and provides foundational data for taxonomic revisions, genome research and hybridization breeding of *A. virens* as a potential ornamental plant.

MATERIALS AND METHODS

Plant materials

Bulbs of *Albuca virens* were collected from local nurseries of Darjeeling district of West Bengal, India as ornamentals and were duly identified by Dr. Manoj M. Lekhak, Shivaji University, Kolhapur, India. The bulbs are potted, grown and maintained in the medicinal plant garden of Scottish Church College, Kolkata (Figs. 1a, b). Actively growing underground roots were used for chromosome analysis. Young flower buds from inflorescence (Fig. 1b) were picked to study meiotic chromosomes.

Chromosome preparation

Pre-treatment of healthy underground secondary roots (0.5- 1 cm in length) was done in 0.002M hydroxyquinoline at 15 °C for 4 hours and then roots were fixed in freshly prepared 1:3 aceto-methanol solution. Mitotic frequency and chromosome morphology were firstly studied by conventional squashing method. Fixed roots were then subjected to enzymatic maceration and air drying method (Kurata and Omura 1978; Fukui 1996) after necessary standardization (Jha and Bhowmick 2021; Bhowmick and Jha 2022) for the present plant material. Roots were firstly digested in a cocktail of 1% cellulase (Onuzuka RS), 0.15% pectolyase (Y-23), 0.75% macerozyme (R-10) and 1mM EDTA (pH 4.2) for varying time durations (45-50 min) at 37 °C before maceration on clean glass slides in a drop of 1:3 aceto-methanol solution. Slides with macerated roots were air-dried and stained with 2% Giemsa solution (Giemsa azure eosine methylene blue solution Merck Germany: 1/15th phosphate buffer: distilled water :: 2:50:48) for 15 min. Metaphase plates were observed under 100X objectives of Zeiss Axioscope microscope with attached Axiocam 202 mono camera and Zen software for capturing photomicrographs.

Karyotype preparation and analysis

Minimally ten different metaphase plates from seven individual plants were selected for chromosome measurements [long arm length (l), short arm length (s), chromosome length (CL), total diploid chromatin length (TCL=$\sum_{i=1}^{2n} CL$)]. Chromosomes were categorized after Levan et al. (1964) on the basis of r value (l/s) and arranged in an order of decreasing length for constructing karyotypes and ideograms. Any trend of asymmetry in karyotype was determined after calculating values of twelve different indices. These include Stebbins asymmetry index (Stebbins 1971), total form percentage (TF%) (Huziwara 1962), intrachromosomal asymmetry index (A1) and interchromosomal asymmetry index (A2) (Zarco 1986), coefficients of variation of chromosome length (CV_{CL}) (Paszko 2006), index of karyotype symmetry (Syi) (Greilhuber and Speta 1976), asymme-

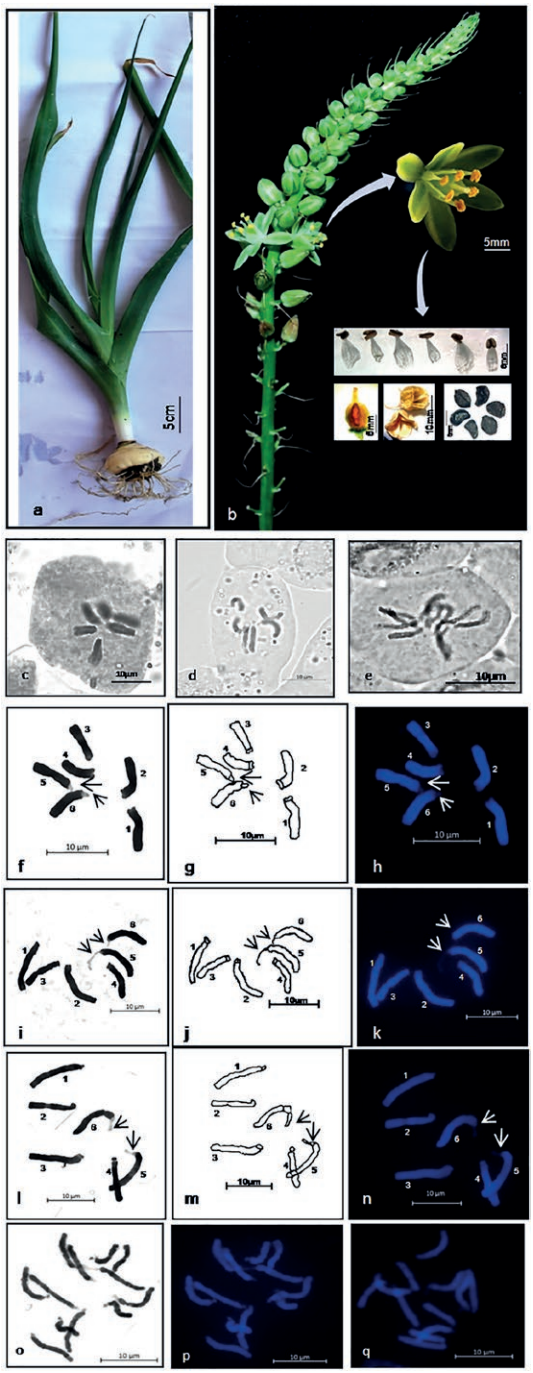

Figure 1. a. Whole plant. **b** Part of inflorescence with flowers, floral organs, fruit and seeds in insets. **c-e** Somatic metaphase chromosomes (2n=6) stained with orcein (**c, d**) and polysomatic cell photograph stained with Feulgen (2n=12) (**e**), note obscure chromosome morphology in conventional staining. **f-n** Somatic metaphase chromosomes (2n=6) represented from three individual plants: **f, i, l** Giemsa stained chromosomes with corresponding hand drawings (**g, j, m**) and subsequent DAPI stained plates (**h, k, n**). Arrows indicate satellite part of chromosomes in Giemsa plates that are correspondingly DAPI^{-ve}. **o-q** Somatic chromosomes showing polysomatic condition (2n= 12) stained with Giemsa (**o**), DAPI (**p-q**).

try index of karyotype (AsK%) (Arano 1963), degree of karyotype asymmetry (A) (Watanabe *et al*. 1999), mean centromeric index (X_{CI}) (Seijo and Fernández 2003), dispersion index (DI) (Lavania and Srivastava 1992), asymmetry index (AI) (Paszko 2006) and mean centromeric asymmetry (M_{CA}) (Peruzzi and Eroğlu 2013). Considering the absence of the allied *Albuca* species in India, chromosome morphometric data have been borrowed from a published report involving *Ornithogalum comosum* Sadler, *O. montanum* Cirillo, *O. pyrenaicum* L. and *O. sigmoideum* Freyn & Sint. (Öztürk et al. 2014) to compare the asymmetry indices and comment on trend of karyotype evolution in *Albuca virens*. Since only chromosome lengths and centromeric indices were provided in the published paper (Öztürk et al. 2014), only A2, CV_{CL}, X_{CI} and AI values could be estimated for the reference taxa.

Fluorochrome staining of somatic metaphase chromosomes

The Giemsa stained slides were marked under the fluorescent microscope Zeiss Axioscop5 followed by destaining in 70% methanol for 45min. Fluorochorme staining with DAPI (4',6-diamidino-2-phenylindole) was performed following Schweizer (1976) after required standardization and modifications (Bhowmick and Jha 2021; Jha and Bhowmick 2021). Slides were incubated in McIlvaine buffer (0.1M citric acid, 0.2M Na_2HPO_4, pH 7.0) for 30 min and stained with 0.1mg/ml DAPI solution for 25-30 min in dark. Excess stain from slides was washed off in McIlvaine buffer followed by blow drying and mounting in non-fluorescent glycerol. Observation of DAPI stained metaphase plates was carried out under the Zeiss Axioscop2 with UV filter cassette. Fluorescent chromosome images were captured with the attached Axiocam 202 mono camera and Zen software.

Meiotic chromosome preparation following DAPI staining

Young flower buds of approximately 0.5-0.8cm length were collected at around 10a.m. Initial screening of the meiotic stages were conducted by staining PMCs (pollen mother cells) in 2% acetocarmine solution. Due to dense cytoplasmic content in the PMCs, EMA- DAPI staining (Bhowmick and Jha 2015) was conducted with minor modifications. The anthers were isolated from flower buds and then digested in enzyme cocktail (same as mentioned for somatic chromosome preparation) for 2-4mins at 37°C. Macerated anthers were pipetted out in clean glass slides and P.M.C.s were spread in 1:3 v/v acetic acid- ethanol solution and air dried. The slides

were kept in McIlvaine buffer (0.1M citric acid, 0.2M Na_2HPO_4, pH 7.0) for 10min. Slides were then stained with 0.1mg/ml DAPI solution for 20min in dark. Excess stain was washed off in Mc Ilvaine's buffer and slides were mounted in non-fluorescent glycerol. Slides were observed and images of meiotic stages were captured under UV filter cassette of Zeiss Axioscope 5 fluorescence microscope with attached Axiocam 202 mono camera and Zen software.

RESULTS AND DISCUSSIONS

Somatic chromosome morphology and karyotype

In the conventional method, cytoplasmic density was difficult to overcome and visualization of chromosome morphology was problematic (Fig. 1c-e). Application of EMA method enabled elimination of cytoplasmic background and rendered chromosome spreading in one plane with clear morphology (Fig. 1f-q) which was not possible in previous reports due to limitations of conventional method (Ravindran 1977; Bhattacharya et al. 2016). There are six chromosomes in the diploid complement (2n=6) (Fig. 1c, d, f-n), with few records of 2n=12 chromosomes in some cells (4-8%), corresponding with previous reports (Bhattacharya et al. 2016) (Fig. 1e, o-q). Present study shows that the chromosomes are telocentric in nature with one satellited pair of chromosomes. The chromosomes range in size from 6.88 to 10.83µm (Table 1), with an average TCL (total length of diploid complement) of 53.20±14.58. The modal karyotype of *A. virens* is 4t+2T.sat (Fig. 2a-c), showing no signs of distinct difference of short or long chromosomes and hence Indian population of *A. virens* does not show bimodal nature of karyotype (Table 1). However, every pair has at least a little difference in chromosome length between the homologues (Table 1). The largest chromosomes are the ones with a terminal satellite (Table 1). Centromeric position in this pair cannot be determined as they are terminally located, only the satellite part is visible in metaphase plates (Fig. 1f-n, 2a-c). Again, the size of the satellited region varies between the homologues (Fig. 1f-n).

In the previous works, 2n=6 was consistently associated with *O. virens* and 2n=4, 6, 12, 16, 26 was reported in the African *A. virens* (worked out as *Ornithogalum tenuifolium*) (Goldblatt and Manning 2011). However, *Ornithogalum tenuifolium* was included later in *Stellarioides* (Castiglione and Cremonini 2012). Other counts (2n=8, 10 and 12) were reported in *O. setifolium*, *O. eck-*

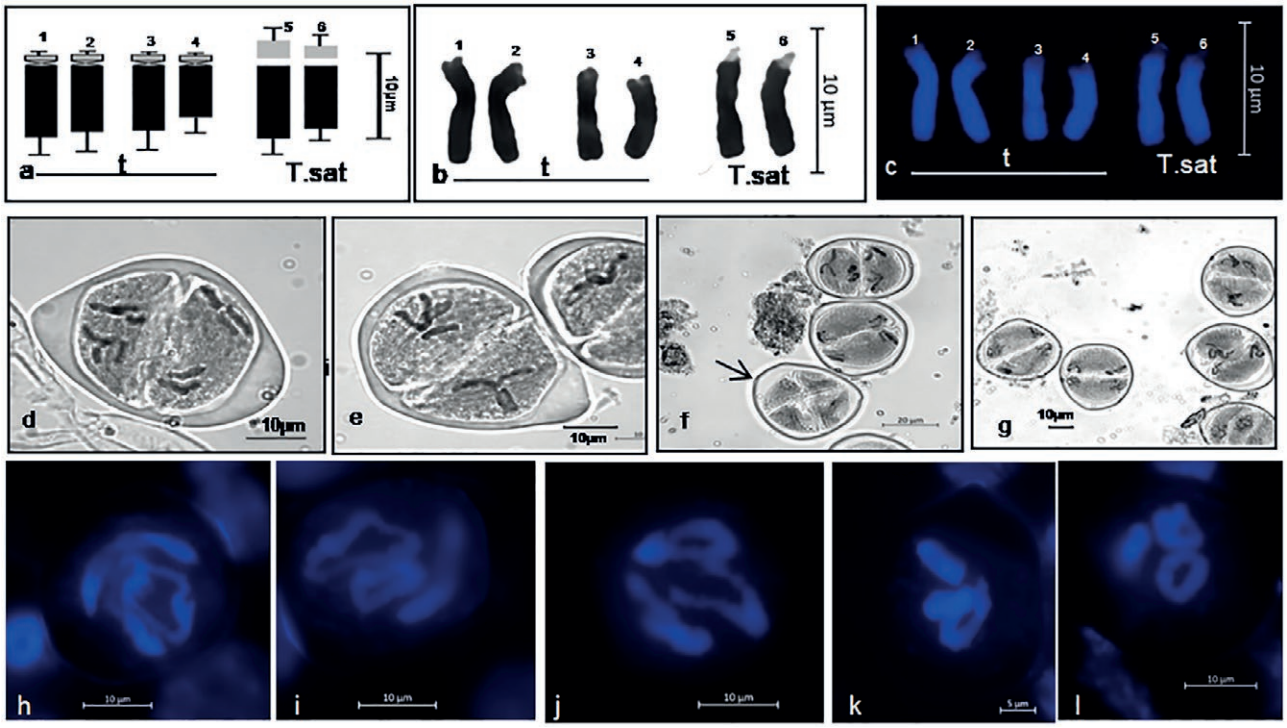

Figure 2. a-c Idiogram and Giemsa (**b**)- DAPI (**c**) karyotype. **d-g** Carmine stained meiotic chromosomes from PMCs at metaphase II (**e**) with three chromosomes in each cell of diad, anaphase II showing regular segregation (**d, f, g**), telophase II indicated with arrow (**f**), showing no signs of abnormality. **h-l** DAPI stained meiotic chromosomes from PMCs at diakinesis (**h-j**) and metaphase I (**k, l**) showing 3 bivalents.

Table 1. Chromosome morphometric features of *Albuca virens.*

Chromosome no.	Long arm (l) (μm)	Short arm (s) (μm)	Sat (μm)	Chromosome length (μm)	r=l/s	Type	RL
1	8.5 ± 2.18	0.68± 0.08	-	9.18±2.34	12.25 ± 2.51	t	17.37 ± 0.75
2	7.87± 2.66	0.788± 0.28	-	8.65± 2.80	10.52 ±4.36	t	15.99± 1.18
3	7.718± 2.66	0.75± 0.11	-	8.47± 2.63	10.57±4.44	t	15.91± 2.67
4	6.15± 1.90	0.73± 0.18	-	6.88± 1.98	8.67±2.98	t	12.92± 0.73
5	8.65±2.27	-	2.18± 1.14	10.83± 3.14	-	T. sat	20.35± 1.67
6	7.48±1.52	-	1.8±1.30	9.28± 2.61	-	T. sat	17.43± 0.45

The data are shown as average values± standard deviation from ten different metaphase plates chosen from seven individual plants. Sat: satellite part of chromosome, r: arm ration (Levan et al. 1964), RL: relative length calculated as: Chromosome length/ Total Chromatin Length*100.

lonii, *O. flavovirens* and *O. pretoriense*, respectively, all of these species being now identified as *Albuca virens* (Goldblatt and Manning 2011). Again, one population of *A. virens* from southern Mozambique shows 2n=4 (Stedje 1989), with one long metacentric pair and one medium sized sub telocentric pair. So far, the ancestral base number of x=10 is suggested for *Albuca*, with many evidences for derived base numbers x=9 (for subgenera *Albuca*, *Monarchos*, *Osmyne*) and x=6 (subgen. *Urophyllon*) (Goldblatt and Manning 2011). Later, 2n=6 was suggested to be a primitive cytotype that may have potentially led to origin of 2n=4 by chromosome translocation and fusion (Castiglione and Cremonini 2012). The other phylogenetically sister species with 2n= 18, 54 (*A. bracteata*, syn *O. caudatum*, *O. longibracteatum*), are suggested to have x=9 (Goldblatt and Manning 2011). Extensive cytological interpretations led Goldblatt and Manning (2011) conclude dysploidy to be a characteristic of subgenus *Urophyllon*, with particularly extreme intraspecific dysploidy notable in *Albuca virens*. Previously, bimodal karyotype has been reported in diploid populations of *A. virens*, like its sister species *Albuca volubilis* from Madagascar (Goldblatt and Manning 2011). The species of subgenus *Albuca* consistently show bimodal karyotypes (Knudtzon and Stedje 1986; Jong 1991; Stedje 1996; Johnson 1999). Although, the present population *of A. virens* in India does not have bimodal karyotype, differences in chromosome length between the homologues may be expressions of ongoing intraspecific rearrangements, as reported for cytotypes with 2n=6 (Castiglione and Cremonini 2012). Considering the difference in the size of satellites in the present study, heteromorphy in the size of the satellite NORs is reported in sections of subgenus *Albuca* (Jong 1991) and hence can be treated as a conserved phenomenon in *A. virens* of subgenus *Urophyllon*.

Knowledge about the symmetric/asymmetric nature of karyotype is a fundamental requirement to gain substantial concept of evolution in any group (Liang and Chen 2015). The inter-chromosomal asymmetry indices depict heterogeneity in chromosome sizes while intra-chromosomal asymmetry depends on relative centromere position (Paszko 2006). Unfortunately, detailed chromosome measurement data of *Albuca* species is missing in literature (Ravindran 1977; Knudtzon and Stedje 1986; Jong 1991; Stedje 1996; Johnson 1999; Pedrosa 2001). Therefore, the present karyomorphometric analysis has been conducted in comparison with some species of *Ornithogalum* by retrieving a few chromosome morphometric records from published data (Öztürk et al. 2014) (Table 2). According to the values determined, *A. virens* shows symmetric nature of karyotype, considering decreased values for A2, CV_{CL}, X_{CI} and AI (Table 3). Symmetric nature of karyotype is justified also according to Stebbins' index (2A) (Table 3). The chromosomes do not have discrete difference in size or centromeric position, in contrast to the bimodal karyotypes of other *Albuca* species and the *Ornithogalum* taxa referred in the present analysis (Table 3). The present detail of karyotype asymmetry parameters can be used as a reference to the allied species of *Albuca* in future studies.

Confirmation of nucleolar chromosomes following DAPI staining

The same Giemsa stained chromosome plates were subjected to DAPI staining. Chromosomes were brightly stained with DAPI except at the short arm which was relatively faintly stained (Fig. 1f-n). Comparing the same metaphase plate stained with Giemsa and then with DAPI, satellite part of the two chromosomes was found to be the $DAPI^{-ve}$ NORs (Fig. 1h, k, n). Thus, DAPI staining supported confirmation of NORs in the somatic metaphase chromosomes. $DAPI^{-ve}$ NORs are a common

Table 2. Chromosome morphometric data from *Ornithogalum* species retrieved from published work (Öztürk et al. 2014).

Ornithogalum comosum:			*Ornithogalum montanum:*			*Ornithogalum pyrenaicum :*			*Ornithogalum sigmoideum:*		
Chromosome Pair no.	ChL (A) (μm)	CI (A)	Chromosome Pair no.	ChL (A) (μm)	CI (A)	Chromosome Pair no.	ChL (A) (μm)	CI (A)	Chromosome Pair no.	ChL (A) (μm)	CI (A)
1	7.84	19.87	1	4.64	36.45	1	10.5	43.75	1	7.8	32.63
2	6.58	27.35	2	4.2	30.39	2	7.28	30.12	2	6.64	27.2
3	6.05	22.72	3	3.68	39.92	3	7.05	21.71	3	6.51	24.31
4	5.86	24.81	4	3.31	33.34	4	6.78	27.06	4	6.22	41.08
5	5.55	35.36	5	3	20.48	5	6.28	27.46	5	5.7	46.28
6	5.04	23.65	6	2.88	22.52	6	5.96	22.75	6	5.2	26.16
7	4.46	22.6	7	1.84	34.98	7	4.46	44.26	7	4.2	31.71
8	4.35	24.02				8	4.39	40.85			
9	4.12	27.12				9	3.48	28.16			
10	3.08	45.39				10	2.91	36.74			
						11	2.68	37.15			
						12	1.6	40.86			

ChL: chromosome length, CI: centromere index, A: average.

Table 3. Karyotype Symmetry/Asymmetry values in *Albuca virens* estimated with quantitative and qualitative indices in comparison with published data from *Ornithogalum* species (Öztürk et al. 2014).

	Quantitative parameters											Qualitaive parameter
	Inter-Chromosomal Symmetry/ Asymmetry		Intra-Chromosomal Symmetry/Asymmetry							Inter- & Intra-(Combined) Chromosomal Asymmetry		Stebbins asymmetry index
	A2	CV_{CL}	Syi	TF%	Ask%	A1	A	X_{CI}	M_{CA}	DI	AI	
Albuca virens	0.14	14.48	6.38	5.55	86.98	0.06	0.74	1.50	74.66	8.31	2.04	2A
*Ornithogalum comosum**	0.25	25.98	-	-	-	-	-	2.72	-	-	7.24	-
*O. montanum**	0.27	27.45	-	-	-	-	-	4.45	-	-	6.36	-
*O. pyrenaicum**	0.47	47.32	-	-	-	-	-	2.78	-	-	11.52	-
*O. sigmoideum**	0.19	19.02	-	-	-	-	-	4.98	-	-	4.73	-

A2: Interchromosomal asymmetry index (Romero-Zarco 1986); $CV_{CL:}$ Coefficient of variation of chromosome length (Paszko 2006); Syi: Index of karyotype symmetry (Greilhuber and Spelta 1976); TF%: Total form percentage (Huziwara 1962); AsK%: Asymmetry index of karyotype (Arano 1963); A1: Intrachromosomal asymmetry index (Romero-Zarco 1986) ; A: Degree of karyotype asymmetry (Watanabe et al 1999); X_{CI} : Mean centromeric index (Seijo et al. 2003) ; $M_{CA:}$ Mean centromeric asymmetry (Peruzzi and Eroglu 2013) ; DI: The dispersion index (Lavania and Srivastava 1992); AI: Asymmetry index (Paszko 2006); Stebbins asymmetry index A-C,1-4 (Stebbins 1971);* data derived from previously published average chromosome length and average centromeric index of four *Ornithogalum* species (Öztürk et al. 2014).

feature of plant chromosomes since nucleolar regions are usually enriched with GC- heterochromatin and thus take up dense stain after application of GC- specific fluorochrome namely chromomycin A3 (Schweizer 1976; Guerra et al. 2000). *Albuca virens* also conforms to the usual negative banding pattern of DAPI at NORs. Previously, $DAPI^{+ve}$ signals on centromeric and intercalary regions and $CMA^{+ve}/DAPI^{-ve}$ signals on nucleolar regions are reported in the phylogenetically close *A. bracteata* (Pedrosa et al. 2001). Therefore, distribution of non-nucleolar AT-rich heterochromatin (depicted by $DAPI^{+ve}$ bands, Bhowmick and Jha 2015, 2019, 2021) may follow differential distribution among the species of subgenus *Urophyllon*, to be confirmed after analysis of DAPI banding pattern in *A. volubilis* and related species in question (Goldblatt and Manning 2011). Till then, $DAPI^{-ve}$ NORs remain to be a conserved chromosomal landmark so far in the subgen. *Urophyllon* of *Albuca*. In future, chromo-

mycin A^{3+ve} banding or FISH with nucleolar rDNA probe in *A. virens* and related species is needed to complement our observation. Additionally, somatic paring is reported in *A. bracteata* around the AT rich intercalary heterochromatin which was also claimed long back in *A. virens* (Ravindran 1977). However, in the present population, neither AT rich intercalary $DAPI^{+ve}$ bands nor such association trend was noted.

Meiotic chromosome study

Different stages of meiosis were obtained following carmine staining, showing regular chromosome segregation patterns (Fig. 2d-g). After EMA method followed by DAPI staining, clearly visible bivalents were observed in diakinesis and metaphase I of PMCs (Fig. 2h-l). The haploid number was confirmed as n=3. The absence of any earlier gametic count reports, haploid number of *A. virens* was questionable, especially considering the occurrence of polysomaty (Bhattacharya et al. 2016, present study). Presently, regular chromosome paring (Fig. 2h-l) and segregation (Fig. 2d-g) is confirmed in *Albuca virens*, in line with successful fruit and seed set in spite of frequent vegetative propagation. This information is a pre-requisite for infra- or inter-specific crosses for floriculture purposes as in the *Ornithogalum* species (Griesbach et al. 1990, 1993).

CONCLUSION

The karyotype of *Albuca virens* shows distinguishable features like i) diploid number 2n=6, ii) variation in length of chromosomes between homologues and iii) variation in the size of NORs. With the knowledge of dysploid reduction and several rearrangements among the chromosomes, the Indian *A. virens* certainly stands as one unique population of *Albuca*, like the one found by Stedje (1989) from Mozambique with 2n=4. It is questionable whether occurrence of polysomatic numbers in the present plants represents evidences in support of an unstable chromosomal background or a usual feature associated with bulbous ornamentals enjoying abundant vegetative propagating (Sharma and Sharma 1956). Considering the literatures in support of dysploidy and chromosome evolution from 2n=6 (Castiglione and Cremonini 2012), present study adds to the significance of this species as a prototype to analyze chromosome evolution with the help of modern cytogenetic methods. In course of the conventional mitotic chromosome analysis, it was felt that the chromosomes remain in different planes, rendering analysis of morphology difficult, as we also encounter inadequate karyotype information in earlier report of *A. virens* (Bhattacharya et al. 2016). Successful preparation of EMA-based Giemsa- DAPI stained slides and DAPI staining of PMCs open the path for application of molecular cytogenetics like florescence *in situ* hybridization or Ag-NOR staining. Therefore the present dataset along with the technical standardization part, would be an asset for molecular cytogenetic assessment of evolution of the understudied *Albuca virens* in relation to its allied species.

ACKNOWLEDGEMENTS

BKB sincerely thanks Principal, Scottish Church College for providing the Scottish Church College Faculty Research Grant (SCCFRG) 2021-2023 for conducting the present research work. BKB thanks Prof. Sumita Jha, Department of Botany, University of Calcutta, India, for kindly gifting the bulbs of *Albuca virens*. BKB thanks Dr. Manoj M. Lekhak, Angiosperm Taxonomy Laboratory, Department of Botany, Shivaji University, Kolhapur, India, for identification of the plant specimen. BKB and SN acknowledges the support of BOOST grant from Department of Science & Technology and Biotechnology, Government of West Bengal (sanction no. 1096/BT(Estt)/1P-09/2018 dated 24.10.2019) for the instrumentation facility developed in Dept. of Botany, Scottish Church College. Authors express sincere gratitude to the Head, Department of Botany for providing the lab facilities to carry out this research.

REFERENCES

Angiosperm Phylogeny Group. 2009. An update of the Angiosperm Phylogeny Group classification for the orders and families of flowering plants: APG III. Bot J Linn Soc. 161: 105–121.

Angiosperm Phylogeny Group. 2016. An update of the Angiosperm Phylogeny Group classification for the orders and families of flowering plants: APG IV. Bot J Linn Soc. 181: 1-20.

Arano H. 1963. Cytological studies in subfamily Carduoideae (Compositae) of Japan IX. Bot Mag Tokyo. 76: 32.

Bhattacharya S, Ghosh B, Choudhury M. 2016. A Simple Reliable Protocol for Cytogentically Stable Mass Propagation of *Ornithogalum virens* Lindl. Plant Tissue Cult Biotech. 26: 1-14.

Bhowmick BK, Jha S. 2022. A critical review on cytogenetics of Cucurbitaceae with updates on Indian taxa. Comp Cytogenet. 16: 93-126.

Bhowmick BK, Jha S. 2015. Differential heterochromatin distribution, flow cytometric genome size and meiotic behavior of chromosomes in three Cucurbitaceae species. Sci Hortic. 193: 322-329.

Bhowmick BK, Jha S. 2019. Differences in karyotype and fluorochrome banding patterns among variations of *Trichosanthes cucumerina* with different fruit size. Cytologia. 84: 237-245.

Bhowmick BK, Jha S. 2021. A comparative account of fluorescent banding pattern in the karyotypes of two Indian *Luffa* species. Cytologia. 86: 35-39.

Castiglione MR, Cremonini R. 2012. A fascinating island: 2n= 4. Plant Biosyst. 146: 711-726.

Fukui K. 1996. Plant chromosomes at mitosis. In: Fukui K, Nakayama S, editors. Plant chromosomes. Laboratory methods. Boca Raton, Tokyo: CRC Press, p. 1-18.

Fukui K, Iijima K. 1991. Somatic chromosome map of rice by imaging methods. Theor Appl Genet. 81: 589-596.

Greilhuber J, Speta F. 1976. C-banded karyotypes in the Scilla hohenackeri group, S.persica and Puschkinia (Liliaceae). Plant Syst Evol. 126: 149–188.

Griesbach RJ, Meyer F, Koopowitz H. 1990. Interspecific hybridization of *Ornithogalum*. Hort Science. 25: 1142d-1142.

Griesbach RJ, Meyer F, Koopowitz H. 1993. Creation of new flower colors in *Ornithogalum* via interspecific hybridization. J Am Soc Hortic Sci. 118: 409-414.

Goldblatt P, Manning JC. 2011. A review of chromosome cytology in Hyacinthaceae subfamily Ornithogaloideae (*Albuca*, *Dipcadi*, *Ornithogalum* and *Pseudogaltonia*) in sub-Saharan Africa. South Afr J Bot. 77: 581-591.

Guerra M, Santos KGBD, E Silva AEB, Ehrendorfer F. 2000. Heterochromatin banding patterns in Rutaceae-Aurantioideae—a case of parallel chromosomal evolution. Am J Bot. 87(5): 735–747.

Huziwara Y. 1962. Karyotype analysis in some genera of Compositae. VIII. Further studies on the chromosomes of *Aster*. Am J Bot. 49: 116–119.

Jha TB. 2021. Karyotype diversity in cultivated and wild Indian rice through EMA-based chromosome analysis. J Genet. 100: 81.

Jha TB, Saha PS, Jha S. 2020. A comparative karyo-morphometric analysis of Indian landraces of *Sesamum indicum* using EMA-giemsa and fluorochrome banding. Caryologia. 73: 81-88.

Jha TB, Bhowmick BK. 2021. Conservation of floral, fruit and chromosomal diversity: a review on diploid and polyploid *Capsicum annuum* complex in India. Mol Biol. 48: 5587-5605.

Johnson MA. 1999. Two new chromosome numbers in an unusual *Albuca* (Hyacinthaceae) from Saudi Arabia. Kew Bulletin. 437-444.

Jong K. 1991. Cytological observations in *Albuca*, including a survey of polymorphic variation in thesat-chromosome pair. Edinb J Bot. 48: 107–128.

Knudtzon SH, Stedje B. 1986. Taxonomy and cytology of the genus *Albuca* (Hyacinthaceae) in East Africa. Nord J Bot. 6: 773-786.

Kurata N, Omura T. 1978. Karyotype analysis in rice. 1. A new method for identifying all chromosome pairs. Japan J Genet. 53:251–255.

Lavania UC, Srivastava S. 1992. A simple parameter of dispersion index that serves as an adjunct to karyotype asymmetry. J Biosci. 17: 179–182.

Liang G, Chen H. 2015. Scaling chromosomes for an evolutionary karyotype: a chromosomal trade off between size and number across woody species. PLoS One. 10: e0144669.

Manning JC. 2020. Systematics of *Ledebouria* sect. *Resnova* (Hyacinthaceae: Scilloideae: Massonieae), with a new subtribal classification of Massonieae. S Afr J Bot. 133: 98-110.

Manning JC, Goldblatt P, Williamson G. 2009a. Hyacinthaceae. *Pseudogaltonia liliiflora* (Ornithogaloideae), a new species from the Richtersveld, Northern Cape. Bothalia. 39: 229–231.

Manning JC, Forest F, Fay MF, Devey S, Goldblatt P. 2009b. A molecular phylogeny and a revised classification of Ornithogaloideae (Hyacinthaceae) based on an analysis of four plastid DNA regions. Taxon. 58: 77–107.

Martinez-Azorin M, Crespo MB, Juan A, Fay MF. 2011. Molecular phylogenetics of subfamily Ornithogaloideae (Hyacinthaceae) based on nuclear and plastid DNA regions, including a new taxonomic arrangement. Ann Bot. 107: 1-37.

Martínez-Azorín M, Crespo MB, Alonso-Vargas MÁ, et al. 2023. Molecular phylogenetics of subfamily Urgineoideae (Hyacinthaceae): Toward a coherent generic circumscription informed by molecular, morphological, and distributional data. J Syst Evol. 61: 42-63.

Nath S, Jha TB, Mallick SK, Jha S. 2015. Karyological relationships in Indian species of *Drimia* based on fluorescent chromosome banding and nuclear DNA amount. Protoplasma. 252: 283-299.

Nath S, Sarkar S, Patil SD, et al. 2022. Cytogenetic Diversity in Scilloideae (Asparagaceae): a comprehensive recollection and exploration of karyo-evolutionary trends. Bot Rev. 1-43.

Öztürk D, Koyuncu O, Koray Yaylacı Ö, Özgişi K, Sezer O, Tokur S. 2014. Karyological studies on the four

Ornithogalum L. (Asparagaceae) taxa from Eskişehir (Central Anatolia, Turkey). Caryologia. 67: 79-85.

Paszko B. 2006. A critical review and a new proposal of karyotype asymmetry indices. Plant Syst Evol. 258: 39-48.

Pedrosa A, Jantsch MF, Moscone EA, Ambros PF, Schweizer D. 2001. Characterisation of pericentromeric and sticky intercalary heterochromatin in *Ornithogalum longibracteatum* (Hyacinthaceae). Chromosoma. 110: 203–213.

Peruzzi L, Eroğlu HE. 2013. Karyotype asymmetry: again, how to measure and what to measure? Comp Cytogenet. 7: 1–9.

Ravindran PN. 1977. Homologous Association in Somatic Cells of *Ornithogalum virens*. Cytologia. 42: 1-4.

Schweizer D. 1976. Reverse fluorescent chromosome banding with chromomycin and DAPI. Chromosoma. 58: 307–324.

Seijo JG, Fernández A. 2003. Karyotype analysis and chromosome evolution in South American species of *Lathyrus* (Leguminosae). Am J Bot. 90: 980–987.

Sharma AK, Sharma A. 1956. Fixity in chromosome number of plants. Nature. 177: 335-336.

Stebbins GL. 1971. Chromosomal changes, genetic recombination and speciation. In: Barrington EJW, Willis AJ, editors. Chromosomal Evolution in Higher Plants. Edward Arnold Publishers Pvt. Ltd., London. p. 72–123.

Stedje B. 1989. Chromosome evolution within the *Ornithogalum tenuifolium* complex (Hyacinthaceae), with species emphasis on the evolution of bimodal karyotypes. Plant Syst Evol. 166: 79–89.

Stedje B. 1996. Karyotypes of some species of Hyacinthaceae from Ethiopia and Kenya. Nord J Bot. 16: 121–126.

Watanabe K, Yahara T, Denda T, Kosuge K. 1999. Chromosomal evolution in the genus Brachyscome (Asteraceae, Astereae): statistical tests regarding correlation between

changes in karyotype and habit using phylogenetic information. J Plant Res. 112: 145–161.

Yamamoto M, Takada N, Hirabayashi T, Kubo T, Tominaga S. 2010. Fluorescent staining analysis of chromosomes in pear (*Pyrus* spp.). J Jpn Soc Hortic Sci. 79: 23-26.

Yamamoto M, Terakami S, Yamamoto T. 2015. Enzymatic maceration/air-drying method for chromosome observations in the young leaf of pear (*Pyrus* spp.). Chromosome Sci. 18: 29-32.

Zarco CR. 1986. A new method for estimating karyotype asymmetry. Taxon. 35: 526–530.

Caryologia
International Journal of Cytology, Cytosystematics and Cytogenetics

Firenze University Press
www.fupress.com/caryologia

OPEN ACCESS

Citation: Denise Felicetti, Chrystian Aparecido Grillo Haerter, Lucas Baumgärtner, Leonardo Marcel Paiz, Daniel Rodrigues Blanco, Eliana Feldberg, Vladimir Pavan Margarido, Maelin da Silva, Roberto Laridondo Lui (2023). Cytogenetic analysis of sympatric *Trachelyopterus* Valenciennes 1840 (Siluriformes, Auchenipteridae) species reveals highly conserved karyotypes despite the geographic distance. *Caryologia* 76(2): 41-50. doi: 10.36253/caryologia-2284

Received: August 16, 2023

Accepted: October 24, 2023

Published: December 31, 2023

Data Availability Statement: All relevant data are within the paper and its Supporting Information files.

Competing Interests: The Author(s) declare(s) no conflict of interest.

Cytogenetic analysis of sympatric *Trachelyopterus* Valenciennes 1840 (Siluriformes, Auchenipteridae) species reveals highly conserved karyotypes despite the geographic distance

Denise Felicetti[1], Chrystian Aparecido Grillo Haerter[2], Lucas Baumgärtner[1], Leonardo Marcel Paiz[1], Daniel Rodrigues Blanco[3], Eliana Feldberg[2], Vladimir Pavan Margarido[1], Maelin da Silva[4], Roberto Laridondo Lui[1,*]

[1] *Centro de Ciências Biológicas e da Saúde, Universidade Estadual do Oeste do Paraná, Cascavel, Paraná, Brazil*
[2] *Coordenação da Biodiversidade, Instituto Nacional de Pesquisas da Amazônia, Manaus, Brasil*
[3] *Universidade Tecnológica Federal do Paraná, Santa Helena, Brasil*
[4] *Universidade Estadual de Ponta Grossa, Ponta Grossa, Brasil*
*Corresponding author. E-mail: roberto.lui@unioeste.br

Abstract. *Trachelyopterus* Valenciennes 1840 species exhibit striking morphological and cytogenetic similarities, leading to persistent taxonomic challenges. This research focuses on *Trachelyopterus galeatus* Linnaeus 1766 and *Trachelyopterus porosus* Eigenmann & Eigenmann 1888, both widely distributed throughout South America and often sympatric, facilitating cytogenetic comparisons. These taxonomic entities are noteworthy for their extensive geographical ranges within the genus. We examined two populations of *T. galeatus* and *T. porosus* collected from sympatric sites in the Amazon and Pantanal regions. Both species had the same diploid number and simple AgNORs. The 18S rDNA sites were found in only one subtelocentric chromosome pair. Meanwhile, the 5S rDNA sites were found on two distinct chromosomal pairs, with differences in the chromosomal morphology and site position among the species, constituting the most efficient chromosomal marker to distinguish them. The 5S rDNA pattern differed between species but remained consistent between populations of the same species. Minor differences were observed between the *T. galeatus* populations, probably related to chromosomal rearrangements. In contrast, despite the considerable geographical distance, no cytogenetic differences were detected among the *T. porosus* populations. Overall, the congruence between cytogenetic and morphological characteristics, combined with our findings from sympatric samples and existing data from geographically separated populations of *Trachelyopterus*, indicates that the cytogenetic is a promising tool for species differentiation and for delving into the cytotaxonomic and evolutionary aspects of Auchenipteridae.

Keywords: "*Parauchenipterus*", sympatric species, neotropical fish species, cytotaxonomy, chromosomal markers, taxonomic challenges, biogeography.

INTRODUCTION

Siluriformes comprises 39 families and 499 genera, representing a significant component of the world's freshwater fish diversity, with over 4,000 valid species (Fricke et al. 2023). Within the neotropical region, it stands as the second-largest group of fish, accounting for approximately 40% of the total Brazilian fish species (de Pinna 1998; Ferraris 2007). Among the families of Siluriformes, Auchenipteridae, commonly referred to as the driftwood catfishes, is an endemic group to the Neotropical region, encompassing 25 genera and 128 species. Auchenipteridae is subdivided into two subfamilies: Centromochlinae with seven valid genera, and Auchenipterinae, comprosing 18 valid genera (Fricke et al. 2023), including *Trachelyopterus* Valenciennes 1840, the focus of this paper. *Trachelyopterus* species are widely distributed throughout South America, occurring in the Paraná-Paraguay, Amazon, Orinoco, Guiana and São Francisco River basins, trans-Andean and Brazilian coast basins. Among *Trachelyopterus* species, *Trachelyopterus galeatus* Linnaeus 1766 and *Trachelyopterus porosus* Eigenmann & Eigenmann 1888 exhibit the most extensive geographical distribution within the genus. *Trachelyopterus galeatus* can be found across most hydrographic basins of South America, whereas *T. porosus* inhabit the Paraná-Paraguay, Amazon and French Guiana basins.

The genus *Trachelyopterus* has been a subject of controversy for over two centuries, characterized by ongoing discussions and taxonomic reviews, largely driven by the morphological similarities among its species (Akama 2004). While some authors have affirmed its validity as a distinct genus (Mees 1974; Curran 1989; Royero 1999; Akama 2004; Birindelli 2010), others have treated it as synonymous with other genera, such as *Parauchenipterus* (Ferraris 1988, 2003), *Auchenipterus* Valenciennes, 1840 (Günther 1864) and *Trachycorystes* Bleeker 1858 (Eigenmann and Eigenmann 1888, 1890; Regan 1911; Miranda-Ribeiro 1911; Britski 1972). In this context, cytogenetic studies can provide new information that can contribute to the taxonomy and enhance discussions concerning the evolutionary and biogeographic aspects of *Trachelyopterus* species.

Currently, seven genera of Auchenipteridae catfishes have been cytogenetically analyzed (see Santos et al. 2021). The diploid number of 58 chromosomes is constant for this family, except for *Ageneiosus* Lacépède 1803, *Centromochlus* Kner 1858 and *Tympanopleura* Eigenmann 1912, in which some species exhibited a diploid number reduction (e.g., Fenocchio and Bertollo 1992; Lui et al. 2013b; Kowalski et al. 2020). In *Trachelyopterus*, cytogenetic analyses include four valid species and two suggested new ones (*Trachelyopterus* aff. *galeatus* and *Trachelyopterus* aff. *coriaceus*). All of them had the same diploid number (58), with small karyotypic and fundamental number differences (Tab. 1). *Trachelyopterus galeatus* is the most studied species of the genus, and recently, a cytogenetic study suggested that a population of *T. galeatus* from the Araguaia River basin may constitute a new species (Santos et al. 2021). In contrast to *T. galeatus*, *T. porosus* has three cytogenetic studies related to only one population, which focused on the evolution of B chromosomes and chromosomal markers through fluorescence in situ hybridization (Felicetti et al. 2021; Haerter et al. 2022, 2023).

Interestingly, *T. galeatus* and *T. porosus* have few morphological differences and are often found in sympatry, creating a propitious scenario to compare cytogenetic data with morphological identification as well as trace evolutionary patterns among geographically isolated populations. Thus, using classic and molecular cytogenetic tools, we aimed to compare two sympatric populations of *T. galeatus* and *T. porosus* from the Amazon River and Paraguay River basins, seeking cytogenetic differences that can contribute to better identification of them and also discussing chromosomal evolutionary patterns.

MATERIAL AND METHODS

The sympatric populations of *Trachelyopterus porosus* and *Trachelyopterus galeatus* were collected from two hydrographic basins of South America: (1) in the Catalão Lake, Amazonas River basin, near Manaus 03°09'47"S and 59°54'29"W, northern South America; (2) and in the Miranda River, municipality of Corumbá 19°34'37.80"S and 57°01'07.08"W, Paraguay River basin (Permanent license SISBIO 49379-1). In the Catalão Lake, we collected 14 specimens of *T. porosus* (4 males and 10 females) and 13 specimens of *T. galeatus* (6 males and 7 females). In the Paraguay River Basin, we collected 13 specimens of *T. porosus* (6 males and 7 females) and 12 specimens of *T. galeatus* (6 males 6 females). They were deposited in the Zoology Museum at the Universidade Estadual de Londrina (MZUEL 18212 for *T. porosus* and MZUEL 18213 for *T. galeatus*) and in the Zoological Collection at the Instituto Nacional de Pesquisas da Amazônia (INPA 57939 for *T. galeatus* and INPA 57940 for *T. porosus*).

Classic and molecular cytogenetic

Anterior kidney cells were used to obtain the mitotic chromosome suspension (Bertollo et al. 1978). The

Table 1. Cytogenetic data available for *Trachelyopterus*. FN: Fundamental number; 2n: diploid number; Res.: Reservoir; AM: Amazonas; GO: Goiás; PR: Paraná; MS: Mato Grosso do Sul; MG: Minas Gerais; RN: Rio Grande do Norte; MT: Mato Grosso; Ref.: References; m: metacentric; sm: submetacentric; st: subtelocentric; a: acrocentric; p: short arm; q: long arm; i interstitial; t: terminal; References: 1- Santos et al. (2021); 2- Felicetti et al. (2021); 3- Ravedutti and Júlio (2001); 4- Lui et al. (2010); 5- Araujo and Molina (2013); 6- Lui et al. (2021); 7- Haerter et al. (2022 ; 8- Haerter et al. (2023); 9- Lui et al. (2009). *The citation of the species name has changed over the years, and can be found in the two formats mentioned.

Species	Locality	FN	2n	Karyotype formula	AgNORs/18S rDNA	5S rDNA	Histone H3	Histone H4	U2 snRNA	SSR $(GATA)_n$	Ref
Trachelyopterus coriaceus	Araguaia River, Araguaia-Tocantins river basin - GO	108	58	20m+18sm+12st+8a	pair 23, p, st	pair 3, p, m / pair 16, q, sm	pair 23, p, st	pair 23, p, st	pair 28, p ,a	scattered	1, 7, 8
Trachelyopterus aff. *galeatus* (*cited as *Parauchenipterus galeatus*)	Araguaia River, Araguaia-Tocantins river basin - GO	108	58	20m+18sm+12st+8a	pair 24, p, st	pair 3, p, m	pair 24, p, st/ pair 25, p, st	pair 24, p, st/ pair 25, p, st	pair 26, q/p, a	scattered	1*, 7, 8
Trachelyopterus galeatus (*cited as *Parauchenipterus galeatus*)	Catalão Lake, Amazonas River basin - AM	106	58	20m+12sm+18st+8a	pair 20, p, st	pair 14, p, sm/ pair 17, q, sm	pair 20, p, st/ pair 21, p, st	pair 20, p, st/ pair 21, p, st	pair 28, p, a	scattered	2, 7, 8
	Miranda River, Paraguay River basin - PY	108	58	24m+12sm+14st+8a	pair 24, p, st	pair 14, p, sm/ pair 17, q, sm	-	-	-	-	2
	Paraná River, Paraná River basin - PR	98	58	22m+12sm+6st+18a	pair 23, p, a	-	-	-	-	-	3*
	Paraná River, Paraná River basin - MS	108	58	24m+18sm+8st+8a	pair 25, p, st	pair 16, p, sm / pair 17, q, sm	-	-	-	-	4*
	Piumhi River, Paraná River basin - MG	108	58	20m+16sm+14st+8a	pair 24, p, st	pair 15, p, sm / pair 16, q, sm	-	-	-	-	4*
	Lagoa da Prata – São Francisco River basin - MG	108	58	22m+16sm+12st+8a	pair 23, p, st	pair 16, p, sm / pair 17, q, sm	-	-	-	-	4*, 6, 9
	Pium River, Parnamirim - RN	108	58	24m+16sm+10st+8a	p, sm	-	-	-	-	-	5*
Trachelyopterus porosus	Catalão Lake, Amazonas River basin - AM	106	58	22m+16sm+10st+10a	pair 23, p, st	pair 3, p, m/ pair 4, p, m	pair 23, p, st/ pair 24, p, st	pair 23, p, st/ pair 24, p, st	pair 26, p, a	scattered	2, 7, 8
	Miranda River, Paraguay River basin - PY	106	58	22m+16sm+10st+10a	pair 23, p, st	pair 3, p, m/ pair 4, p, m	-	-	-	-	2
Trachelyopterus aff. *coriaceus* (*cited as *Trachelyopterus* sp.)	Arrombado lagoon, Bento Gomes River basin- MT	108	58	22m+20sm+8st+8a	pair 22, p, st	pair 16, p, sm/ pair 18, q, sm	pair 23, p, st	pair 23, p, st	pair 27, p, a	scattered	6*, 7, 8
Trachelyopterus striatulus (*cited as *Parauchenipterus striatulus*)	Verde lagoon, Doce River basin - MG	106	58	18m+20sm+10st+10a	par 23, p, st	pair 10, p, sm/ pair 13, p, sm/ pair 15, q, sm	pair 18, p, sm/ pair 23, p, st	pair 18, p, sm/ pair 23, p, st	pair 28, p, a	scattered	1*, 7, 8

samples were treated with a 0.02% colchicine solution (1 mL/100g of body weight) for 30-40 minutes before euthanizing the animal by clove oil overdose (Griffiths 2000) (according to the ethics committee on animal experimentation and practical classes at Unioeste: 09/13 - CEEAAP / Unioeste) to remove tissues for cytogenetic and molecular analyses. The chromosome morphology was classified according to Levan et al. (1964). The heterochromatin distribution pattern was determined according to Sumner (1972), with changes in the staining process proposed by Lui et al. (2012). The nucleolar organizer regions (Ag-NOR) were detected by silver nitrate impregnation (Howell and Black 1980).

Fluorescent *in situ* hybridization (FISH) was carried out according to Pinkel et al. (1986) with modifications suggested by Margarido and Moreira-Filho (2008). The 5S rDNA probes were obtained from Mini-prep of *Megaleporinus elongatus* Valenciennes 1850 (Martins et al. 2000) and the 18S rDNA probes were obtained from Mini-prep of *Prochilodus argenteus* Spix and Agassiz 1829 (Hatanaka and Galetti Jr, 2004). The 5S probes were labeled by nick translation with digoxigenin-11-dUTP (Dig 11 Nick Translation Mix - Roche), according to the manufacturer's instructions, and detected with anti-digoxigenin rhodamine (Roche Diagnostics). The 18S rDNA probes were labeled with biotin-16-dUTP (Biotin 16 Nick Translation Mix - Roche), according to the manufacturer's instructions, and detected using anti-biotin-avidin (Roche Diagnostics). The FISH stringency was 77% for both the 5S and 18S rDNA probes (200 ng of each probe, 50% formamide, 10% dextran sulfate, 2xSSC, pH 7.0-7.2, at 37°C overnight). All images were captured by the DP Controller 3.2.1.276 software using the Olympus DP71 digital camera connected to the BX61 epifluorescence microscope (Olympus America Inc., Center Valley, PA, United States of America).

RESULTS

Trachelyopterus porosus from the Amazon River basin had 2n=58 chromosomes for both sexes (4 males and 10 females), with 22 metacentric, 16 submetacentric, 10 subtelocentric, 10 acrocentric and a fundamental number (NF) of 106 (Fig. 1a). Among the 14 specimens, eight individuals (3 males and 5 females) had 1-3 small and metacentric B chromosomes (Bs). The Bs had intraindividual and interindividual numerical variation. The C-banding revealed heterochromatin in the terminal position of almost all complement A chromosomes (Fig. 1b). The silver nitrate impregnation showed simple NOR in the terminal position of the short arm of the pair 23 (Fig. 1b), which was confirmed by FISH with the 18S rDNA probes (Fig. 2). FISH with the 5S rDNA probes revealed sites on the short arm of the pair 3 and 4, both metacentric (Fig. 2).

Trachelyopterus porosus from the Paraguay River basin had 2n=58 chromosomes for both sexes (6 males and 7 females), with 22 metacentric, 16 submetacentric, 10 subtelocentric, 10 acrocentric, and NF=108 (Fig. 1c). The C-banding revealed heterochromatin in the terminal position of almost all complement A chromosomes (Fig. 1d). The silver nitrate impregnation showed simple NOR in the terminal position of the short arm of the pair 23 (Fig. 1d), which was confirmed by FISH with the 18S rDNA probes (Fig. 2). FISH with the 5S rDNA probes revealed sites on the short arm of the pair 3 and 4, both metacentric (Fig. 2).

Trachelyopterus galeatus from the Amazon River basin had 2n=58 chromosomes for both sexes (6 males and 7 females), with 20 metacentric, 12 submetacentric, 18 subtelocentric, 8 acrocentric, and NF=106 (Fig. 1e). Among the 13 specimens, six (1 male and 5 females) had 1-3 small and metacentric Bs. The Bs had intraindividual and interindividual numerical variation. The C-banding revealed heterochromatin in the terminal position of almost all complement A chromosomes (Fig. 1f). The silver nitrate impregnation showed simple NOR in the terminal position of the short arm of the pair 20 (Fig. 1f), which was confirmed by FISH with rDNA 18S probes (Fig. 2). FISH with the 5S rDNA probes revealed sites on the short arm of the pair 14 and on the long arm of the pair 16, both submetacentric Fig. 2).

Trachelyopterus galeatus from the Paraguay River basin had 2n=58 chromosomes for both sexes (6 males and 6 females), with 24 metacentric, 12 submetacentric, 14 subtelocentric, 8 acrocentric, and NF=108 (Fig. 1g). Among the 12 specimens, one female had 1-2 small and metacentric Bs. The Bs had intraindividual and interindividual numerical variation. The C-banding revealed heterochromatin in the terminal position of almost all complement A chromosomes (Fig. 1h). The silver nitrate impregnation showed simple NOR in the terminal position of the short arm of the pair 24 (Fig. 1h), which was confirmed by FISH with the 18S rDNA probes (Fig. 2). FISH with the 5S rDNA probes revealed sites on the short arm of the pair 14 and on the long arm of the pair 17, both submetacentric (Fig. 2).

DISCUSSION

The diploid number of 58 chromosomes is a recurrent pattern in Auchenipteridae species (Ravedutti and

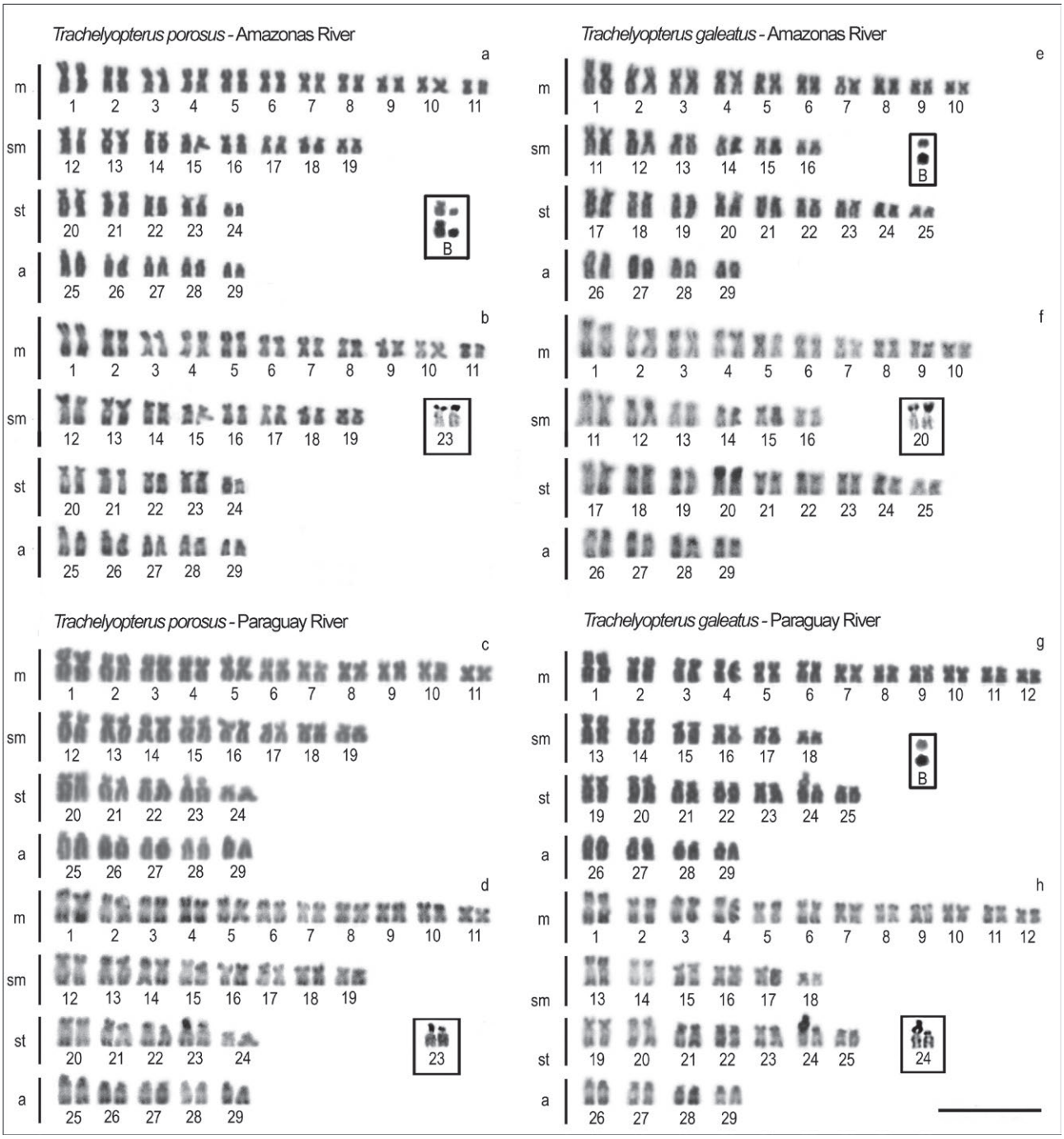

Figure 1. Karyotypes of *Trachelyopterus porosus* (a, c) and *Trachelyopterus galeatus* (e, g) stained with Giemsa and sequentially C-banded (b, d, f and h, respectively). The boxes correspond to the Ag-NORs and the B chromosomes of their respective populations. Bar = 10μm.

Júlio Jr 2001; Fenocchio et al. 2008; Lui et al. 2009, 2010, 2013a, 2013b, 2015, 2021; Santos et al. 2021), indicating that it is a conserved aspect of the family. Historically, deviations from this pattern were only reported for *Ageneiosus inermis* Linnaeus 1766 and *Tympanopleura atronasus* Eigenmann and Eigenmann 1888 with a 2n = 56 (Fenocchio and Bertollo 1992; Lui et al. 2013b), a potential consequence of chromosomal fusions that appear to be a basal event in the diversification of the genus *Ageneiosus* (Lui et al. 2013b). However, Kowalski

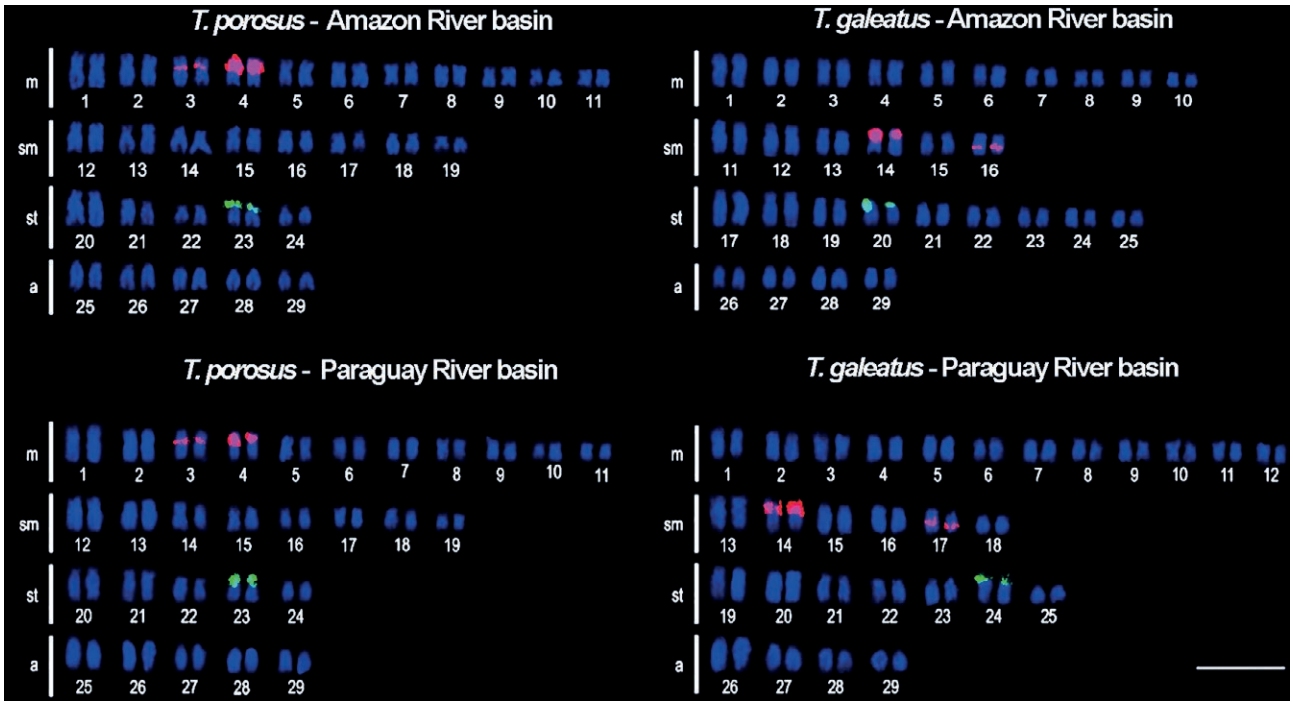

Figure 2. Karyotypes hybridized with 5S rDNA (Rhodamine, red) and 18S rDNA probes (FITC, green) in *Trachelyopterus porosus* from the Amazon River and Paraguay River and *Trachelyopterus galeatus* from the Amazon River and Paraguay River. Bar = 10 µm.

et al. (2020) recently introduced a new exception to this prevailing diploid number pattern in Auchenipteridae, *Centromochlus heckelii* De Filippi 1853 with 46 chromosomes, further emphasizing the role of chromosome rearrangements in the family diversification.

In the closest group, Doradidae, a variable diploid number can be observed (2n=56, 2n=58 and 2n=66). For a considerable period, 2n=58 was regarded as the plesiomorphic state for the family, given its prevalence among most analyzed species (Eler et al. 2007; Milhomem et al. 2008; Baumgärtner et al. 2016; Takagui et al. 2017, 2019). However, seeking to ascertain the ancestral diploid number within the nodes of the Doradidae family, Takagui et al. (2021) concluded that the determination of the plesiomorphic condition remains elusive, as both 56 and 58 chromosomes are equally parsimonious states. In Auchenipteridae, there are still too few species cytogenetically studied to reconstruct the ancestral diploid number. Therefore, even though 58 chromosomes are the most recurrent diploid number, it is also premature to determine whether it is a plesiomorphic trait or not.

Karyotypic formula variations are frequently reported among *Trachelyopterus galeatus* populations (Tab. 1), and our study corroborates this trend. However, similar to most studies, *T. galeatus* from the Amazon basin also showed only four pairs of acrocentric chromosomes—a recurrent characteristic of this species. Thus far, the only exceptions are *T. galeatus* from Puerto Rico in the Paraná River, which had nine acrocentric pairs (e.g., Ravedutti and Júlio Jr 2001) and *T. galeatus* from the Araguaia River, a suggested new species with five pairs of acrocentric chromosomes (Santos et al. 2021). The karyotypic differences between these species populations may be the result of geographic isolation. It is important to highlight that *T. galeatus* is widely distributed throughout South America (Akama 2004). Similar cytogenetic differences have been reported in other groups of neotropical fish, such as *Astyanax* Baird and Girard 1854 (Peres et al. 2009; Tenório et al. 2013; Piscor et al. 2017) and *Rhamdia* Bleeker 1858 (Stivari and Martins-Santos 2004; Martinez et al. 2011). On the other hand, both *T. porosus* populations presented the same karyotype formula, C-band pattern, Ag-NORs, 18S and 5S rDNA sites. Compared to *T. galeatus*, only small differences could be observed, primarily related to the karyotype formula and 5S rDNA sites.

In both species, *T. galeatus* and *T. porosus*, the heterochromatin was found in the terminal regions of most chromosomes. The C-band pattern aligns with findings from other cytogenetic studies in Auchenipteridae, such as in *A. inermis*, *Tympanopleura atronasus* (cited as *Ageneiosus atronases*), *Glanidium ribeiroi* Haseman 1911 and *T. galeatus* (Fenocchio and Bertollo 1992; Ravedutti and Júlio Jr 2001; Fenocchio et al. 2008; Lui et al. 2009,

2010, 2013b, 2015), which suggests that it is a shared feature within the family. Only small differences in the heterochromatin pattern can be seen in Auchenipteridae catfishes: *A. inermis* exhibited strongly marked heterochromatic blocks (Lui et al. 2013b); some chromosomes of *Tatia jaracatia* Pavanelli and Bifi 2009 showed centromeric heterochromatic blocks, and *Tatia neivai* Ihering 1930, which had an interstitial heterochromatic block in a submetacentric pair (Lui et al. 2013a). Similar to most studied Auchenipteridae species, no differences in the heterochromatin distribution patterns for both species were found; therefore, it does not seem to be a reliable marker for distinguishing *Trachelyopterus* species.

Simple NORs (silver nitrate staining and FISH with 18S rDNA probes) were found in the terminal position of a subtelocentric chromosome pair in both species. Currently, only *C. heckelii* was reported with multiple NORs (Kowalski et al. 2020), whereas all other cytogenetically analyzed Auchenipteridae species had simple NORs, with differences only in the position (terminal and interstitial), which may be a consequence of non-Robertsonian rearrangements, such as paracentric and/or pericentric inversions. In both species, *T. galeatus* and *T. porosus*, the 18S rDNA pattern is similar to other *Trachelyopterus* species. It can be found in subtelocentric chromosomes, acrocentric chromosomes (Ravedutti and Júlio Jr. 2001) or even in submetacentric pairs (Araújo and Molina 2013). However, it is worth noting that variations in chromosome measurement employed by different researchers could introduce a minor margin of error. These variations may stem from considerations such as the inclusion or exclusion of secondary constrictions as part of chromosomal arms, as well as discrepancies in chromosome condensation levels, which could contribute to subtle differences in karyotype organization.

In both species, *T. galeatus* and *T. porosus*, the 5S rDNA sites were detected on two chromosome pairs. Although this 5S rDNA pattern is prevalent in most Auchenipteridae species (see Lui *et al.* 2021), it should not be unequivocally viewed as a plesiomorphic or a conserved trait. In fact, it is the most variable chromosomal marker within the family (Santos et al. 2021), ranging from only one chromosome pair with the ribosomal sequence, as found in *Glanidium ribeiroi*, *Ageneiosus inermis* (Lui et al. 2013b, 2015), *T. galeatus* from the Araguaia River basin (Santos *et al.* 2021) and in *Auchenipterus nuchalis* Spix 1829 (Machado et al. 2021) to three chromosome sites in *T. striatulus* Steindachner 1876 (Lui et al. 2021) and *T. neivai* (Lui et al. 2013a), four chromosome sites in *T. jaracatia* (Lui et al. 2013a) or even seven chromosome carriers in *Entomocorus radiosus* Reis and Borges 2006 (Machado et al. 2021). This substantial variation positions the 5S rDNA marker as one of the most promising tools for species differentiation and for delving into the cytotaxonomic and evolutionary aspects of Auchenipteridae thus far.

ACKNOWLEDMENTS

We thank to Instituto Chico Mendes de Conservação da Biodiversidade (ICMBio) for the authorization to collect the animals (Permit 49379-1), Instituto Nacional de Pesquisas da Amazônia (INPA) for logistical support and for providing laboratory technicians who helped with the sample collections in the Amazon rainforest, and the Universidade Estadual de Londrina (UEL) researchers and students for their support in the sample collection in the Pantanal.

DATA AVAILABILITY

The chromosomal data that support the findings of this study are fully available within the article and additional information are available from the corresponding author, Roberto Laridondo Lui.

DATA DEPOSITION

They specimens used in this study were deposited in the Zoology Museum at Universidade Estadual de Londrina (MZUEL 18212 for *T. porosus* and MZUEL 18213 for *T. galeatus*) and in the Zoological Collection at the Instituto Nacional de Pesquisas da Amazônia (INPA 57939 for *T. galeatus* and INPA 57940 for *T. porosus*).

GEOLOCATION INFORMATION

The sympatric populations of *Trachelyopterus porosus* and *Trachelyopterus galeatus* were collected from two hydrographic basins of South America: (1) in the Catalão Lake, Amazonas River basin, near Manaus 03°09'47"S and 59°54'29"W, northern South America; (2) and in the Miranda River, municipality of Corumbá 19°34'37.80"S and 57°01'07.08"W, Paraguay River basin.

STATEMENT OF ETHICS

Fish collections were authorized by Instituto Chico Mendes de Conservação da Biodiversidade (ICMBio, Permit number 49379- 1), and the experimental proce-

dures were approved by the Ethics Committee on Animal Experimentation and Practical Classes at Unioeste (09/13-CEEAAP/Unioeste).

FUNDING

This work was supported by the Fundação Araucária de Apoio ao Desenvolvimento Científico e Tecnológico do Paraná (Public Call 09/2016); Conselho Nacional de Desenvolvimento Científico e Tecnológico (CNPq Universal, Proc. 446660/2014-4); Coordenação de Aperfeiçoamento de Pessoal de Nível Superior (CAPES); Universidade Estadual do Oeste do Paraná (Unioeste); Postgraduate Program in Conservação e Manejo de Recursos Naturais (Unioeste-PPRN); and Instituto Nacional de Pesquisas da Amazônia (INPA).

REFERENCES

Akama A. 2004. Sistemática dos gêneros *Parauchenipterus* Bleeker 1862 e *Trachelyopterus* Valenciennes, 1840 (Siluriformes, Auchenipteridae) [dissertation]. São Paulo (SP): Universidade de São Paulo.

April J, Mayden RL, Hanner RH, Bernatchez L. 2011. Genetic calibration of species diversity among North America's freshwater fishes. Proc Natl Acad Sci USA. 108(26):10602–10607. doi: 10.1073/pnas.1016437108.

Araújo WC, Molina WF. 2013. Citótipo exclusivo para *Parauchenipterus galeatus* (Siluriformes, Auchenipteridae) na Bacia do Atlântico NE Oriental do Brasil: Indicações de um complexo de espécies. Biota Amazôn. 3(2):33–39. doi: 10.18561/2179-5746/biotaamazonia.v3n2p33-39.

Baumgärtner L, Paiz LM, Margarido VP, Portela-Castro ALB. 2016. Cytogenetics of the thorny catfish *Trachydoras paraguayensis* (Eigenmann e Ward, 1907), (Siluriformes, Doradidae): Evidence of pericentric inversions and chromosomal fusion. Cytogenet Genome Res. 149(3):201–206. doi: 10.1159/000448126 .

Bertollo LAC, Takahashi CS, Moreira-Filho O. 1978. Cytotaxonomic considerations on *Hoplias lacerdae* (Pisces, Erythrinidae). Revista Brasileira de Genética. 1:103–120.

Birindelli, JLO. 2010. Relações filogenéticas da superfamília Doradoidea (Ostariophysi, Siluriformes) [dissertation]. São Paulo (SP): Universidade de São Paulo.

Britski HÁ 1972. Sistemática e evolução dos Auchenipteridae e Ageneiosidae (Teleostei, Siluriformes) [dissertation]. São Paulo (SP): Universidade de São Paulo.

Castro Paz FP, da Silva Batista JB, Porto JIR. 2014. DNA barcodes of rosy tetras and allied species (Characiformes: Characidae: Hyphessobrycon) from the Brazilian Amazon Basin. PloS One. 9(5): e98603. doi: 10.1371/journal.pone.0098603.

Curran DJ. 1989. Phylogenetic relationships among the Catfish Genera of the Family Auchenipteridae (Teleostei: Siluroidea). Copeia. 1989(2):408–419. https://doi.org/doi:10.2307/1445438.

de Pinna M. 1998. Phylogenetic relationships of Neotropical Siluriformes (Teleostei: Ostariophysi): historical overview and synthesis of hypotheses. In: Malabarba LR, Reis RE, Vari RP, Lucena ZM, Lucena CAS, editors. Phylogeny and Classification of Neotropical Fishes. Porto Alegre: Edipucrs; pp. 279–330.

Eigenmann CH, Eigenmann RS. 1888. Preliminary notes on South American Nematognathi. Proc Calif Aca. Sci. 1:119–172.

Eigenmann CH, Eigenmann RS. 1890. A revision of the South American Nematognathi, or catfishes. Occas pap Calif Acad Sci. 1:1–508.

Eler ES, Dergam JA, Vênere PC, Paiva LC, Miranda GA, Oliveira AA. 2007. The karyotypes of the thorny catfishes *Wertheimeria maculata* Steindachner, 1877 and *Hassar wilderi* Kindle, 1895 (Siluriformes, Doradidae) and their relevance in doradids chromosomal evolution. Genetica. 130(1):99–103. doi: 10.1007/s10709-006-0023-4.

Felicetti D, Haerter CAG, Baumgärtner L, Paiz L, Takagui FH, Margarido VP, Blanco DR, Feldberg E, Silva M, Lui RL. 2021. A new variant B chromosome in Auchenipteridae: The role of $(GATA)_n$ and $(TTAGGG)_n$ sequences in understanding the evolution of supernumeraries in *Trachelyopterus*. Cytogenet Genome Res. 161:70–81. doi: 10.1159/000513107.

Fenocchio A, Bertollo LAC. 1992. Karyotype, C-bands and NORs of the neotropical Siluriform fish *Ageneiosus brevifilis* and *Ageneiosus atronases* (Ageneiosidae). Cytobios. 72(288):19–22.

Fenocchio AS, Dias AL, Margarido VP, Swarça AC. 2008. Molecular cytogenetic characterization of *Glanidium ribeiroi* (Siluriformes) endemic to the Iguaçu River, Brazil. Chromosome Sci. 11:61–66.

Ferraris Jr CJ. 1988. The Auchenipteridae: putative monophyly and systematics, with a classification of the neotropical Doradoid catfishes (Ostariophysi: Siluriformes) [unpublished dissertation]. New York(NY): City University of New York.

Ferraris Jr CJ. 2003. Family Auchenipteridae. In: Reis RE, Kullander SO, Ferraris Jr CJ, editors. Check List of Freshwater Fishes of South and Central America. Porto Alegre: Edipucrs; pp. 742.

Ferraris Jr CJ. 2007. Checklist of catfishes, recent and fossil (Osteichthyes: Siluriformes), and catalogue of Siluriform primary types. Zootaxa. 1418:1–628. doi: 10.11646/zootaxa.1418.1.1.

Frézal L, Leblois R. 2008. Four years of DNA barcoding: current advances and prospects. *Infec Genet Evol.* 8(5):727–736. doi: 10.1016/j.meegid.2008.05.005.

Fricke R, Eschmeyer WN, Van Der Laan R. 2021. Eschmeyer's Catalog of Fishes: Genera, Species, References. San Francisco(SF): The California Academy of Sciences; [accessed 2023 sep 23]. http://researcharchive.calacademy.org/research/ichthyology/catalog/fishcatmain.asp

Griffiths SP. 2000. The use of clove oil as an anaesthetic and method or sampling intertidal rockpool fishes. J Fish Biol. 57(6):1453–1464. doi: 10.1111/j.1095-8649.2000.tb02224.x.

Günther A. 1864. Catalogue of the fishes in the British Museum. Catalogue of the Physostomi, containing the families Siluridae, Characinidae, Haplochitonidae, Sternoptychidae, Scopelidae, Stomiatidae in the collection of the British Museum. 5nd ed. Londres (LND): Printed by order of the trustees.

Haerter CAG, Blanco DR, Traldi JB, Feldberg E, Margarido VP, Lui RL, 2023. Are scattered microsatellites weak chromosomal markers? Guided mapping reveals new insights into *Trachelyopterus* (Siluriformes: Auchenipteridae) diversity. PLoS ONE. 18(6):e0285388. doi: 10.1371/journal.pone.0285388

Haerter CAG, Margarido VP, Blanco DR, Traldi JB, Feldberg E, Lui RL. (2022). Contributions to *Trachelyopterus* (Siluriformes: Auchenipteridae) species diagnosis by cytotaxonomic autapomorphies: from U2 snRNA chromosome polymorphism to rDNA and histone gene synteny. Org Div Evol. 22: 1021-1036. doi: 10.1007/s13127-022-00560-0

Hatanaka T, Galetti Jr, PM. 2004. Mapping of the 18S and 5S ribosomal RNA genes in the fish *Prochilodus argenteus* Agassiz, 1829 (Characiformes, Prochilodontidae). Genetica. 122(3):239244. doi: 10.1007/s10709-004-2039-y.

Howell WM, Black DA. 1980. Controlled silver staining of nucleolus organizer regions with a protective colloidal developer: a 1-step method. Experientia. 36(8):1014–1015. doi: 10.1007/BF01953855.

Kowalski S, Paiz LM, Silva M, Machado AS, Feldberg E, Traldi JB, Margarido VP, Lui RL. 2020. Chromosomal analysis of *Centromochlus heckelii* (Siluriformes: Auchenipteridae), with a contribution to *Centromochlus* definition. Neotrop Ichthyol. 18: e200009. doi: 10.1590/1982-0224-2020-0009.

Levan A, Fredga K, Sandberg AA. 1964. Nomenclature for centromeric position on chromosomes. Hereditas. 52:201–220. doi: 10.1111/j.1601-5223.1964.tb01953.x.

Lui RL, Blanco DR, Margarido VP, Moreira-Filho O. 2009. First description of B chromosomes in the family Auchenipteridae, *Parauchenipterus galeatus* (Siluriformes) of the São Francisco River Basin (MG, Brazil). Micron. 40:552–559. doi: 10.1016/j.micron.2009.03.004.

Lui RL, Blanco DR, Margarido VP, Moreira-Filho O. 2010. Chromosome characterization and biogeographic relations among three populations of the driftwood catfish *Parauchenipterus galaetus* (Linnaeus, 1766) (Siluriformes: Auchenipteridae) in Brazil. Biol J Linn Soc. 99:648–656. doi: 10.1111/j.1095-8312.2009.01389.x.

Lui RL, Blanco DR, Moreira-Filho O, Margarido VP. 2012. Propidium iodide for making heterochromatin more evident in the C-banding technique. *Biotech Histochem.* 87(7):433–438. doi: 10.3109/10520295.2012.696700.

Lui RL, Blanco DR, Margarido VP, Troy WP, Moreira-Filho O. 2013a. Comparative chromosomal analysis and evolutionary considerations concerning two species of genus *Tatia* (Siluriformes, Auchenipteridae). Comp Cytogenet. 7(1):63–71. doi: 10.3897/CompCytogen.v7i1.4368.

Lui RL, Blanco DR, Martinez JF, Margarido VP, Venere PC, Moreira-Filho O. 2013b. The role of chromosomal fusion in the karyotypic evolution of the genus *Ageneiosus* (Siluriformes, Auchenipteridae). Neotrop Ichthyol. 11:327–334. doi: 10.1590/S1679-62252013005000004.

Lui RL, Blanco DR, Traldi JB, Margarido VP, Moreira-Filho O. 2015. Karyotypic variation of *Glanidium ribeiroi* Haseman, 1911 (Siluriformes, Auchenipteridae) along the Iguazu River basin. Braz J Biol: 75(4):215–221. doi: 10.1590/1519-6984.10714.

Lui RL, Traldi JB, Blanco DR, Margarido VP, Mariotto S, Centofante L, Artoni RF, Moreira-Filho O. 2021. Possible common origin of B chromosomes in Neotropical Fish (Siluriformes, Auchenipteridae) reinforced by repetitive DNA mapping**.** Braz Arch Biol Technol. 64:e21190494. doi: 10.1590/1678-4324-2021190494.

Machado AS, Kowalski S, Paiz LM, Margarido VP, Blanco DR, Venere PC, Mariotto S, Centofante L, Moreira-Filho O, Lui RL. 2021. Comparative cytogenetic analysis between species of *Auchenipterus* and *Entomocorus* (Siluriformes, Auchenipteridae). Caryologia. 74(2):89–101. doi: 10.36253/caryologia-1058.

Margarido VP, Moreira-Filho O. 2008. Karyotypic differentiation through chromosome fusion and number reduction in *Imparfinis hollandi* (Ostariophysi, Heptapteridae). Genetic Mol Biol. 31:235–238. doi: 10.1590/S1415-47572008000200012.

Martinez JF, Lui RL, Blanco DR, Traldi JB, Silva LF, Venere PC, Souza IL, Moreira-Filho O. 2011. Comparative cytogenetics of three populations from the *Rhamdia quelen* species complex (Siluriformes, Heptapteridae) in two Brazilian hydrographic Basins. Caryologia. 64:121–128. doi: 10.1080/00087114.2011.10589772.

Martins C, Wasko AP, Oliveira C, Wright JM. 2000. Nucleotide sequence of 5S rDNA and localization of the ribosomal RNA genes to metaphase chromosomes of the Tilapiine cichlid fish, *Oreochromis niloticus*. Hereditas. 133:39–46. doi: 10.1111/j.1601-5223.2000.00039.x.

Mees GF. 1974. The Auchenipteridae and Pimelodidae of Suriname (Pisces, Nematognathi). Zool Verh. 132: 12–256.

Milhomem SSR, Souza ACP, Nascimento AL, Carvalho Jr JR, Feldberg E, Pieczarka JC, Nagamachi CY. 2008. Cytogenetic studies in fishes of the genera *Hassar*, *Platydoras* and *Opsodoras* (Doradidae, Siluriformes) from Jarí and Xingú Rivers, Brazil. Genet Mol Biol. 31:256–260. doi: 10.1590/S1415-47572008000200017.

Miranda-Ribeiro A. 1911. Fauna brasiliensis. Peixes IV(a). Eleutherobranchios Aspirophoros. Arch Mus Nac Rio de J. 16:1–504.

Nelson JS, Grande TR, Wilson MVH. 2006. Fishes of the World. 5nd ed. New Jersey(NJ): John Wiley and Sons.

Peres WAM, Buckup PA, Kantek DLZ, Bertollo LAC, Moreira-Filho O. 2009. Chromosomal evidence of downstream dispersal of *Astyanax fasciatus* (Characiformes, Characidae) associated with River shed interconnection. Genetica. 137(3):305–311. doi: 10.1007/s10709-009-9389-4.

Pinkel D, Straume T, Gray J. 1986. Cytogenetic analysis using quantitative, high-sensitivity, fluorescence hybridization. Proc Natl Acad Sci USA. 83(9):2934–2938. doi: 10.1073/pnas.83.9.2934.

Piscor D, Centofante L. Parise-Maltempi PP. 2017. Distinct classical and molecular cytogenetics of *Astyanax marionae* and *A. fasciatus* (Characiformes: Characidae): a comparative study of the organization of heterochromatin and repetitive genes. J Genet. 96(4):665–671. doi: 10.1007/s12041-017-0813-8.

Ravedutti CG, Júlio Jr H.F. 2001. Cytogenetic analysis of three species of the neotropical family Auchenipteridae (Pisces, Siluriformes) from the Paraná River Basin, Brazil. Cytologia. 66:65–70. doi: 10.1508/cytologia.66.65.

Regan CT. 1911. The classification of the teleostean fishes of the order Ostaripophysi. 2. Siluroidea. Ann Mag Nat. 8(8):552–577.

Reis RE, Albert JS, Di Dario F, Mincarone MM, Petry P, Rocha LA. 2016. Fish biodiversity and conservation in South America. J Fish Biol. 89:12–47. doi: 10.1111/jfb.13016.

Royero RL. 1999. Studies on the systematics and phylogeny of the catfish family Auchenipteridae (Teleostei: Siluriformes) [unpublished dissertation]. Bristol (BS): University of Bristol.

Santos DP, Felicetti D, Baumgärtner L, Margarido VP, Blanco DR, Moreira-Filho O, Lui RL. 2021. Contributions to the taxonomy of *Trachelyopterus* (Siluriformes): comparative cytogenetic analysis in three species of Auchenipteridae. Neotrop Ichthyol. 19:e200115. doi: 10.1590/1982-0224-2020-0115.

Stivari MK, Martins-Santos IC. 2004. Karyotype diversity in two populations of *Rhamdia quelen* (Pisces, Heptapteridae). Cytologia. 69(1):25–34. doi: 10.1016/0014-4827(72)90558-710.1508/cytologia.69.25.

Sumner AMT. 1972. A simple technique for demonstrating centromeric heterochromatin. Exp Cell Res. 75:304–306. doi: 10.1016/0014-4827(72)90558-7.

Takagui FH, Dias AL, Birindelli JLO, Swarca AC, Rosa R, Lui RL, Fenocchio AS, Giuliano-Caetano L. 2017. First report of B chromosomes in three Neotropical thorny catfishes (Siluriformes, Doradidae). Comp Cytogenet. 11:55–64. doi: 10.3897/CompCytogen.v11i1.10496.

Takagui FH, Baumgärtner L, Baldissera JN, Lui RL, Margarido VP, Fonteles SBA, Garcia G, Birindelli JO, Moreira-Filho O, Almeida FS, Giuliano-Caetano L. 2019. Chromosomal diversity of thorny catfishes (Siluriformes-Doradidae): a case of allopatric speciation among Wertheimerinae species of São Francisco and Brazilian Eastern coastal drainages. Zebrafish. 16:477–485. doi: 10.1089/zeb.2019.1769.

Takagui FG, Viana P, Baumgartner L, Bitencourt JA, Margarido VP, Lui RL, Feldberg E, Birindelli JLO, Almeida FS, Giuliano-Caetano L. 2021. Reconstruction of the Doradinae (Siluriformes-Doradidae) ancestral diploid number and NOR pattern, reveals new insights about the karyotypic diversification of the Neotropical thorny catfishes. Genet Mol Biol. 44:e20200068. doi: 10.1590/1678-4685-GMB-2020-0068.

Tenório RCCO, Vitorino CA, Souza IL, Oliveira C, Venere PC. 2013. Comparative cytogenetics in *Astyanax* (Characiformes, Characidae) with focus on the cytotaxonomy of the group. Neotrop Ichthyol. 11(3):553–564. doi: 10.1590/S1679-62252013000300008.

Toussaint A, Charpin N, Brosse S, Villéger S. 2016. Global functional diversity of freshwater fish is concentrated in the Neotropics while functional vulnerability is widespread. Sci Rep. 6:22125. doi: 10.1038/srep22125.

Caryologia
International Journal of Cytology, Cytosystematics and Cytogenetics

Firenze University Press
www.fupress.com/caryologia

OPEN ACCESS

Citation: Fernando Tapia-Pastrana (2023). Cytogenetics of *Diphysa americana* (Mill.) M.Sousa (Leguminosae-Papilionoideae-dalbergioid clade), a rare species from the coast of Oaxaca, Mexico. *Caryologia* 76(2): 51-57. doi: 10.36253/caryologia-2300

Received: September 6, 2023

Accepted: October 27, 2023

Published: December 31, 2023

Data Availability Statement: All relevant data are within the paper and its Supporting Information files.

Competing Interests: The Author(s) declare(s) no conflict of interest.

ORCID
FT-P: 0000-0003-0232-2110

Cytogenetics of *Diphysa americana* (Mill.) M.Sousa (Leguminosae-Papilionoideae-dalbergioid clade), a rare species from the coast of Oaxaca, Mexico

Fernando Tapia-Pastrana

Facultad de Estudios Superiores Zaragoza, Universidad Nacional Autónoma de México, Laboratorio de Genecología, Batalla 5 de mayo s/n esquina Fuerte de Loreto, Col. Ejército de Oriente, Iztapalapa, C.P. 09230, Ciudad de México, Mexico
E-mail: pasfer@unam.mx

Abstract. *Diphysa* Jacq. is an essentially Mexican and Central American genus that includes 21 species and only one cytogenetic report. In this work, a surface spread and air-drying method was used to obtain the karyotype of *Diphysa americana* (Mill) M.Sousa, a rare native tree that grows in a coastal town in the State of Oaxaca, Mexico. Metaphase cells showed a $2n = 20$, consistent with the predominant diploid number in the dalbergioid clade. This number contrasts with a previously reported $2n = 16$. The karyotypic formula 5m + 5sm, first proposed for a species of the genus, denotes a slightly asymmetric karyotype. The presence of secondary constrictions associated with satellites on the short arms of a pair of sm chromosomes and other cytogenetic parameters require studies in other species of the genus to verify their taxonomic utility. In addition, cells in prometaphase exhibited a circular fragment of unknown origin like that observed in a species of the genus *Aeschynomene*, also dalbergioid. This fragment could be related to extrachromosomal circular DNA (eccDNA) observed in other plants. *Diphysa* is a small, cytogenetically favorable genus, and further studies will exhibit the karyotypic diversity that underlies its diversification.

Keywords: basic number, dalbergioid clade, karyotype, SAT-chromosomes.

INTRODUCTION

Leguminosae is the third largest family within angiosperms and exhibits enormous ecological, genomic, cytological, chemical, and morphological diversity (Doyle and Luckow 2003; Lewis et al. 2005). The Papilionoideae subfamily is the largest and most widespread of the three traditional Leguminosae subfamilies, with an estimated 478 genera and 13,860 species (Lewis et al. 2005; Cardoso et al. 2013). Phylogenetic reconstructions point to it as a monophyletic group with highly specialized papilionate flowers that have a clearly distinctive standard petal, wings, and keel as well as partially fused stamens that wrap around the ovary, although there are unusual lineages with

marked radial floral symmetry (Pennington et al. 2001; Wojciechowski et al. 2004; Lavin et al. 2005; McMahon and Sanderson 2006; Cardoso et al. 2012, 2013; LPWG 2013). By using molecular data Lavin et al. (2001) detected a pantropical monophyletic group of papilionate legumes called "dalbergioid" legumes, which is another example of a typical cryptic clade with an estimated age of 55.3 ± 0.5 million years (Lavin et al., 2005). All dalbergioids belong to one of three well-supported subclades, the Adesmia, Dalbergia, and Pterocarpus clades.

Circumscribed as up to now, the dalbergioids comprise 54 genera and more than 1300 species of perennial and annual trees, shrubs, and herbs (Lavin et al. 2001; Wojciechowski et al. 2004; Cardoso et al. 2012; Moraes et al. 2020). Economically important species are included as hardwood species (*Dalbergia* spp. and *Pterocarpus* spp.), forage legumes (*Stylosanthes* spp. and *Aeschynomene* spp.), but also weeds of rice crops (Martins et al. 2021), grown for consumption human (*Arachis hypogaea*, an allopolyploid) and some endangered taxa (*Centrolobium paraense*) and several *Dalbergia species* (Cervantes et al. 2019).

Diphysa Jacq. (subclade Dalbergia) is an essentially Mexican and Central American genus with extensions to the southwestern United States and northern South America (Lavin et al. 2000; Lewis et al. 2012; Rzedowski et al. 2016) and includes 21 usually unarmed tree or shrub species (WFO 2023). *Diphysa americana* (Mill.) M.Sousa is a 4-15 m tall tree that grows mainly in the seasonally dry tropical biome (Sousa 1990; WFO 2023). It is characterized by a fissured bark and leaves 8-14 cm long, imparipinnate. Its leaflets (5-21) are alternate or sub-opposite, generally 1.5-3.5 cm long and 0.5-1 cm broad, oval, or obovate with entire margin, dark green above, paler below, and glabrous rachis. The inflorescences with 6-7 yellow papilionate flowers (Fig. 1A), a standard with a macula with reddish edges (Fig. 1 B-C) and the turbinate calyx 6-9 mm (Fig. 1 D). Fruits 5.3-8.4 cm long and 1-1.8 cm wide, stipitate, reticulate, glabrous, veined margins and light brown seeds 6 x 3 mm (Fig. 1 E) (Martín et al. 2000; Rzedowski et al. 2016; Rojas-Rodríguez and Torres-Córdoba 2018).

In Mexico, *D. americana* is an uncommon native species of tropical deciduous, seasonally dry, and evergreen forests. Its distribution encompasses both coastlines as well as the center of the country at altitudes of 100 to 1000 m a.s.l. (Rzedowski et al. 2016; Villaseñor 2016). It is one of the first elements to colonize coastal dunes and is commonly found solitary in abandoned sites that were once used for agriculture (Acosta 1993; Ramírez-Pinero 2012). The trees have a high use value in agroforestry systems where the flowers are used as food

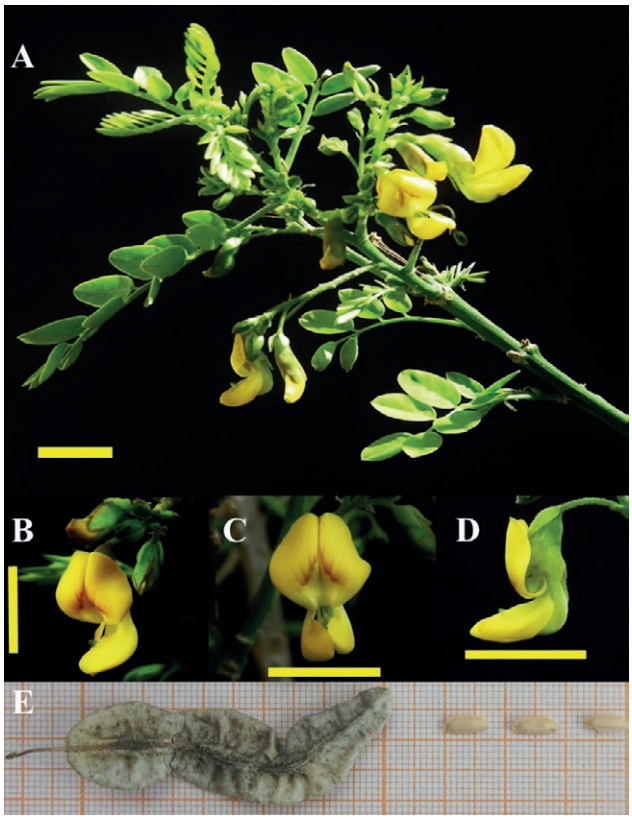

Figure 1. Morphological aspects in *Diphysa americana*. **A**. Inflorescences. **B-D**, Three-quarter, frontal, and lateral views of individual flowers. **E**, Fruit, and seeds. Scale bars = 1 cm.

cooked in salt or fried with egg (Manzanero-Medina et al. 2020), they can also be used as live fences to delimit cultivation areas and provide shade for coffee plantations. In addition, the stem is used as firewood or for the construction of houses (Pascual-Mendoza et al. 2020). It is also used in traditional medicine and is highly prized for the uses of its wood (Rzedowski et al. 2016; WFO 2023). Additionally, its influence on the structure and ecological dynamics of the dune vegetation describes it as a nucleating species (Ramírez-Pinero et al. 2018). It is known by the common names of Amarillo, Chilillo, Chipil, Chipilín, Flor de gallito, Cochipili, Cuachepil Guachipelín, Guachipilín, Macano, Palo amarillo, Quebracho, Quiebracha (CONABIO 2023; Rzedowski et al. 2016). It is not considered a frequent plant, however, the IUCN (2021) places it in the category of least concern.

The genus *Diphysa* records a $2n = 16$ chromosome count for *Diphysa robinioides* Benth., a synonymy of *D. americana* (Atchison 1951; Sousa 1990; WFO 2023). However, this number is far from the basic number $x = 10$ and the diploid number $2n = 20$ that predominate in genera belonging to the dalbergiod clade of Papilionoide-

ae (Goldblatt 1981; Lavin et al. 2001; Tapia-Pastrana et al. 2020) and therefore requires a cytogenetic reevaluation where, in addition to verifying its chromosome number, a detailed description of its karyotype is obtained.

The objective of this work is to carry out a detailed analysis of the chromosomal characteristics of a Mexican population of *D. americana*, establish its karyotype and compare it with previous cytogenetic descriptions carried out in the genus and in other species belonging to the dalbergioid clade of the Papilionoideae subfamily.

MATERIALS AND METHODS

During June 2016, ripe fruits of *Diphysa americana* were collected from two individuals separated by at least two kilometers in the vicinity of the municipality of Santiago Pinotepa Nacional in the coastal region of the state of Oaxaca, Mexico at 16°20'N, 98°03'W and 210 m a.s.l. The area is characterized by a warm sub-humid climate, with an average annual temperature of 26.2 °C and a rainfall of 1,237.5 mm. The vouchers of the studied specimens were deposited in the National Herbarium (MEXU) of the Instituto de Biología, UNAM.

The mitotic cells were obtained from meristems of seeds germinated in Petri dishes lined with cotton moistened in distilled water. Chromosome preparations were made by surface spreading and air-drying (Tapia-Pastrana and Mercado-Ruaro 2001). All meristems were collected from 3-5 mm long roots pretreated with 2 mM 8-hydroxyquinolin for 5 h at room temperature and fixed in the fixative (ethanol: acetic acid=3:1). They were then treated with a mixture of 20% pectinase (Sigma) and 2% cellulase (Sigma) in 75 mM KCl for 60 min at 37 °C. After centrifugation at 1500 rpm for 10 min, the cell pellet was transferred to 75 mM KCl solution for 13 min at 37 °C. After two successive rinses with the KCl solution, they were again fixed in the fixative and subsequently rinsed twice more. One or two drops of the suspension of pellet were placed on clean slides, air-dried, and stained in 10% Giemsa solution for 13 min for conventional karyotyping. At least ten metaphase and prometaphase plates with well-distributed chromosomes were photographed using a Carl Zeiss A1 axioscope. Five photographs of metaphases in which the chromosomes showed comparable degrees of contraction were used to determine: the diploid number (2*n*), the length difference between the longest chromosome and the shortest chromosome (range), total haploid chromosome length (THC), average chromosome size (AC) and the longest chromosome/shortest chromosome ratio (Ratio, L/S). The asymmetry index (TF %) was obtained following Huziwara (1962). Chromosomes were classified as metacentric (m), submetacentric (sm) according to their morphology and arm proportions (Levan et al. 1964). Chromosome size was estimated using a Mitutoyo Digimatic Caliper CD-G´´ BS digital caliper. Karyotypes were prepared from photomicrographs by cutting individual chromosomes, organizing them in descending order of length and matching according to their morphology.

RESULTS

A total of 184 cells in typical metaphase and well-distributed chromosomes were analyzed (Fig. 2 A-D), from which the *Diphysa americana* karyotype was prepared (Fig. 2 E). All of them exhibited a 2*n* = 20 and complements constituted by chromosomes m and sm, with a size that oscillated between 1.22 µm and 2.33 µm (Table 1). In some complements, the presence of one or two sm chromosomes carrying secondary constrictions and microsatellites on short arms was clearly visible (Fig. 2B-D). The observation of prometaphase cells revealed, on the one hand, the association between secondary constrictions and a single nucleolus (Fig. 3A) and, on

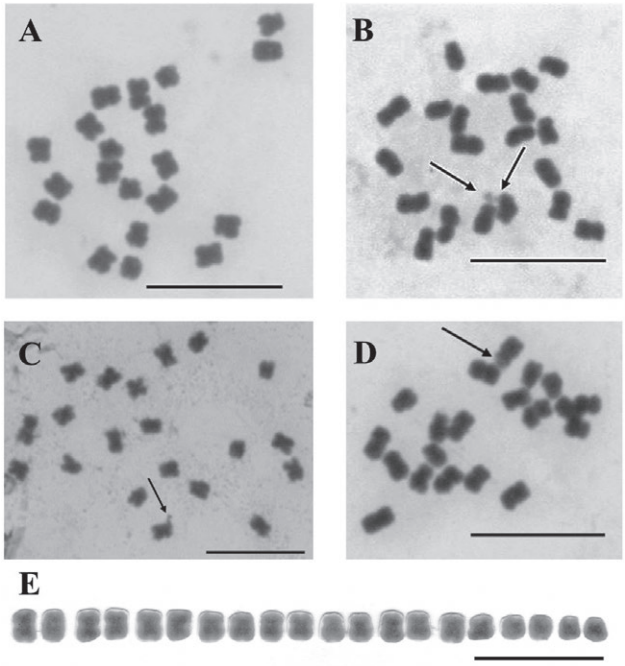

Figure 2. Mitotic cells in metaphase 2*n* = 20 and karyotype of *Diphysa americana*. **A-D**, Metaphase chromosome plates with optimal distribution. Arrows point to secondary constrictions and satellites on short arms of submetacentric chromosomes. **E**, Karyotype 5m + 5sm. Chromosomes are aligned by the centromere and arranged in decreasing order. Scale bars = 10 µm.

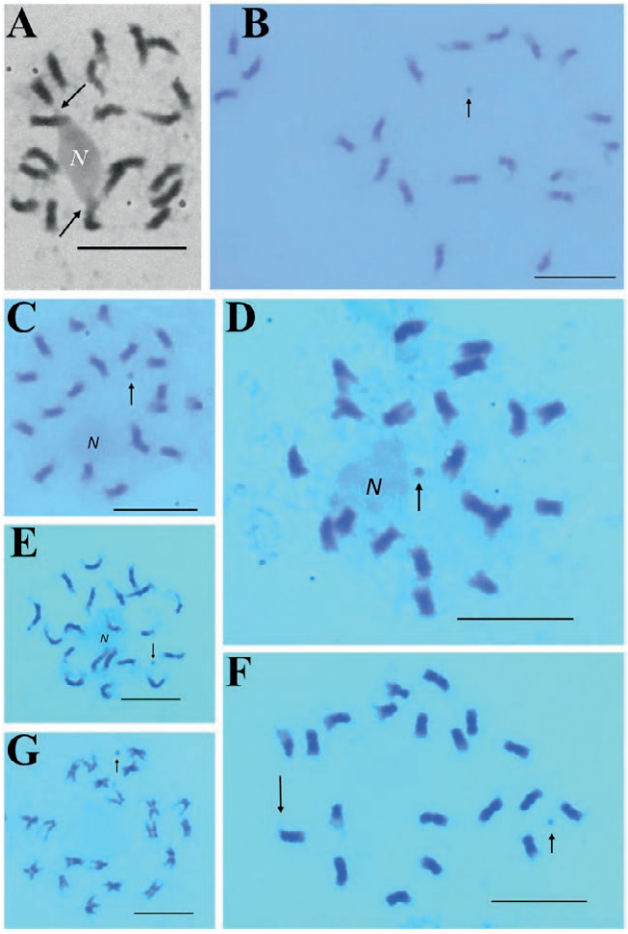

Figure 3. Prometaphase plates $2n = 20$ of *Diphysa americana*. **A**. Arrows indicate satellites of NOR chromosomes associated with the nucleolus. **B-G**. Presence of circular fragments (arrows) of unknown origin not associated with the nucleolus or aligned with the chromosomes. In **F** is shown for comparison, one of these fragments and a secondary constriction indicated by an arrow. *N* = nucleolus. Scale bars = 10 µm.

the other hand, the presence of a small circular-looking fragment that is not associated with the nucleolus or with any chromosome (Fig. 3B-G). This fragment cannot be confused with a secondary constriction or microsatellite, and it stains with the same color and intensity as the rest of the chromosomes (Fig. 3F). The proposed karyotypic formula for *D. americana*, the position of the SAT chromosomes, and other characteristics of its karyotype are summarized in Tables 1 and 2.

Table 1. Mean chromosome measures in *D. americana*.

CP	TCL (µm)	LLA (µm)	LSA (µm)	r	S
01	2.61±0.35	1.43±0.15	1.17±0.20	1.22	m
02	2.38±0.33	1.31±0.16	1.06±0.18	1.23	m
03	2.32±0.33	1.32±0.18	0.98±0.16	1.34	m
04	2.23±0.32	1.47±0.20	0.74±0.12	1.98	sm
05	2.19±0.32	1.23±0.17	0.95±0.15	1.29	m
06	2.15±0.36	1.48±0.29	0.66±0.07	2.24	sm*
07	2.08±0.29	1.17±0.18	0.90±0.11	1.30	m
08	2.05±0.30	1.44±0.21	0.60±0.09	2.40	sm
09	1.98±0.29	1.37±0.21	0.60±0.09	2.28	sm
10	1.82±0.23	1.26±0.17	0.54±0.06	2.33	sm

CP=Chromosome pair; TCL=total chromosome length; LLA=length long arm; LSA=length short arm; ±=SD; r=arms ratio; S=shape after Levan et al. (1964). *Chromosomes with secondary constrictions on short arm.

DISCUSSION

Diphysa americana is a species with a wide distribution in the New World and the results of its cytogenetic analysis could be of importance in the understanding of chromosome evolution in the dalbergioid clade of Papilionoideae. It represents the only species of its genus so far studied karyologically. This is the first report of both diploid number and karyotype of *Diphysa americana* obtained in a Mexican population. The $2n = 20$ confirms on the one hand the predominance of $x = 10$ as the basic chromosome number of the dalbergioids and on the other hand *Diphysa* as a cytogenetically favorable taxon. The number of metaphases analyzed (184) and the absence of nuclei with a different set of chromosomes allow us to state with certainty that the chromosome number recorded here for *D. americana* is correct and consistent with what is expected for a genus included in the dalbergioid clade. A $2n = 20$ (x= 10) recorded

Table 2. Karyotype analysis of the taxon under study.

Species	NA	$2n$	Karyotype formula	Sat	THC ± S.E (µm)	AC ± S.E (µm)	Range ± S.E (µm)	L/S ± S.E	TF%
D. americana	184	20	5m + 5sm	2	21.81 ± 3.14	2.18 ± 0.21	0.79 ± 0.12	1.43 ± 0.02	37.59

NA = Nuclei analyzed; Sat = Number of satellites; THC = Total haploid chromosome length; AC = Average chromosome size; TF% = Asymmetry index.

here differs from the $2n = 16$ (x=8) shown by Atchison (1951) for a Central American population. In this regard, it is worth mentioning that Lewke Bandara et al. (2013) highlight the existence of variations in the number of chromosomes and the level of ploidy in some species of the genera *Onobrychis*, *Hedysarum* and *Sulla* (Hedysareae: Papilioniodeae) and even information available in the IPCN database (tropicos.org, Missouri Botanical Garden) shows basic numbers far from x=10 in *Acosmium*, *Dalea* and *Ormocarpum* (dalbergioid clade: Papilionoideae). Without overlooking the possible existence of cryptospecies with similar morphology and different chromosome numbers, the predominance of $x = 10$ recognized in dalbergioids allows us to assume that numbers as low as $2n = 16$ in a diploid species can hardly be explained by decreasing aneuploidy. Clarifying this disagreement requires broader population sampling.

The karyotypic formula proposed here (5m + 5sm) shows that in the dalbergioid chromosome complements obtained so far, chromosomes with a medium (m) or slightly displaced (sm) centromere predominate (Table 1), and therefore they are symmetric or slightly asymmetric karyotypes (Tapia-Pastrana et al. 2020). Likewise, the presence of secondary constrictions associated with microsatellites in short arms of sm chromosomes (SAT chromosomes) corroborates a trend in plant species where secondary constrictions are located preferentially in short arms (Lima de Faria 1976; Lim et al. 2001), particularly in legumes (Biondo et al. 2006; Tapia-Pastrana 2012; Tapia-Pastrana and Tapia-Aguirre 2018; Tapia-Pastrana et al. 2020). Likewise, their role in the organization of the nucleolus is evident since they were observed associated with it in prometaphase cells (Fig. 3A) and considered nucleolar organizing regions (NOR) or at least part of them. In addition, its shape and behavior resemble those exhibited by species belonging to the genus *Aeschynomene*, Serie Americanae (Tapia-Pastrana et al. 2020).

On the other hand, the values of THC, AC, Range, L/S and TF% (Table 2) are parameters obtained for the first time in the genus *Diphysa* and to demonstrate their taxonomic value, a greater number of species must be studied. However, with respect to THC (21.81 ± 3.14 **µ**m) and AC (2.18 ± 0.21 **µ**m), it can be stated that they differ little from the values obtained for species of the recently reestablished genus *Ctenodon* (Tapia-Pastrana et al. 2020; Cardoso et al. 2020) and *Dalbergia spinosa* (Jena et al. 2004) also in the dalbergioid clade. Regarding the presence of small circular fragments, for the moment there is no information on their origin and function. It is noteworthy that similar structures in shape and size were also recorded in *Aeschynomene americana* var. *glandulosa*, another dalbergioid (Tapia-Pastrana et al. 2020). It remains to mention that this material is like extrachromosomal circular DNA (eccDNA) detected by electron microscopy in plants, which mainly contains repeated sequences derived from chromosomal DNA involved in the evolution of B chromosomes and rDNA mobility (Cohen et al. 2008). They also resemble the satellite-like structures recorded in the chromosomes of Giemsa-stained prometaphase cells of *Nicotiana kawakamii* Y. Ohashi (Nakamura et al. 2001). Deciphering this enigma will require molecular cytogenetic techniques and the analysis of a greater number of species.

Circumscribed as so far, the dalbergioid clade is composed of more than 1300 species (Lavin et al. 2001; Wojciechowski et al. 2004; Cardoso et al. 2012; Moraes et al. 2020) and only about 300 (≈ 28%) are known cytogenetically. As shown here, the genus *Diphysa*, which includes few species, is cytogenetically favorable and represents an opportunity to corroborate not only the constancy of the basic chromosome number ($x = 10$) exhibited in dalbergioid taxa, but also to verify the karyotypic diversity that surely underlies their evolutionary and speciation processes.

Characterizing the genome architecture of higher plants is an important scientific task. Its first approach is to visualize chromosomal domains by obtaining detailed karyotypes that reveal the physical organization of DNA in chromosomes. Comparative cytogenetic studies can be taxonomically relevant and complement phylogenies based on molecular data (Tapia-Pastrana et al. 2020; Cordeiro et al. 2020), so this task should continue.

ACKNOWLEDGEMENTS

The author is grateful for the support of the Division of Postgraduate Studies and Research, Faculty of Higher Studies Zaragoza.

REFERENCES

Acosta I. 1993. Lluvia de semillas en matorrales de dunas costeras en el Morro de La Mancha Veracruz. Bachelor of Science Thesis. Facultad de Ciencias. Universidad Nacional Autónoma de México, México, DF.

Atchison E. 1951. Studies in the Leguminosae. VI. Chromosome numbers among tropical woody species. Am J Bot. 38:538-546. https://doi.org/10.1002/j.1537-2197.1951.tb14855.x

Biondo E, Miotto STS, Schifino-Wittmann MT. 2006. Cytogenetics of species of *Chamaecrista* (Leguminosae-Caesalpinioideae) native to southern Brazil. Bot

J Linn Soc. 150(4):429-439. https://doi.org/10.1111/j.1095-8339.2006.00480.x

Cardoso D, de Queiroz LP, Pennington RT, de Lima HC, Fonty E, Wojciechowski MF, Lavin M. 2012. Revisiting the phylogeny of papilionoid legumes: new insights from comprehensively sampled early-branching lineages. Am J Bot. 99:1991-2013. http://www.jstor.org/stable/23321299.

Cardoso D, Pennington RT, de Queiroz LP, Boatwright JS, Van Wyk B-E, Wojciechowski MF, Lavin M. 2013. Reconstructing the deep-branching relationships of the papilionoid legumes. S Afr J Bot. 89:58-75. https://doi.org/10.1016/j.sajb.2013.05.001

Cardoso D, Mattos CMJ, Filardi F, Delgado-Salinas A, Lavin M, de Moraes PLR, Tapia-Pastrana F, de Lima HC. 2020. A molecular phylogeny of the pantropical papilionoid legume *Aeschynomene* supports reinstating the ecologically and morphologically coherent genus *Ctenodon*. Neodiversity, 13:1-38. https://doi.org/10.13102/neod/131.1

Cervantes A, Linares J, Quintero E. 2019. An updated checklist of the Mexican species of *Dalbergia* (Leguminosae) to aid in its conservation efforts. Rev Mex Biodivers. 90: e902528. https://doi.org/10.22201/ib.20078706e.2019.90.2528

CONABIO (Comisión Nacional para el Conocimiento y uso de la Biodiversidad). [accessed 2023 March 23]. https://enciclovida.mx/especies/185459

Cohen S, Houben A, Segal D. 2008. Extrachromosomal circular DNA derived from tandemly repeated genomic sequences in plants. Plant J. 53:1027-1034. https://doi.org/10.1111/j.1365-313X.2007.03394.x

Cordeiro JMP, Kaehler M, Souza LG, Felix LP. 2020. Heterochromatin and numeric chromosome evolution in Bignoniaceae, with emphasis on the Neotropical clade Tabebuia alliance. Genet Mol Biol. 43: e20180171. https://doi.org/10.1590%2F1678-4685-GMB-2018-0171

Doyle JJ, Luckow MA. 2003. The rest of the iceberg. Legume diversity and evolution in a phylogenetic context. Plant Physiol. 131:900-911. https://doi.org/10.1104%2Fpp.102.018150

Goldblatt P. 1981. Cytology and the phylogeny of Leguminosae. In: Polhill RM, Raven PH, editors. Advances in legume systematics. part 2. Royal Botanic Garden, London: Kew Publishing; p. 427-463.

Huziwara Y. 1962. Karyotype analysis in some genera of Compositae. VIII. Further studies on the chromosomes of *Aster*. Am J Bot. 49:116-119. https://doi.org/10.2307/2439026

IUCN (Red List of Threatened Species). Version 3.1. [accessed 2023 March 27]. https://www.iucnredlist.org/species/144264286/149030506

Jena S, Sahoo P, Mohanty S, Das AB. 2004. Identification of RAPD markers, *in situ* DNA content and structural chromosomal diversity in some legumes of the mangrove flora of Orissa. Genetica. 122:217-226. http://dx.doi.org/10.1007/s10709-004-2040-5

Lavin M, Pennington RT, Klitgaard BB, Sprent JI, de Lima HC, Gasson PE. 2001. The Dalbergioid legumes (Fabaceae): Delimitation of a pantropical monophyletic clade. Am J Bot. 88:503-533. https://doi.org/10.2307/2657116

Lavin M, Herendeen PS, Wojciechowski MF. 2005. Evolutionary rates analysis of Leguminosae implicates a rapid diversification of lineages during the Tertiary. Syst Biol. 54:575-594. https://doi.org/10.1080/10635150590947131

Lavin M, Thulin M, Labat J-N, Pennington RT. 2000. Africa, the odd man out: molecular biogeography of dalbergioid legumes (Fabaceae) suggests otherwise. Syst Bot. 25(3):449-467. https://doi.org/10.2307/2666689

Levan A, Fredga K, Sandberg AA. 1964. Nomenclature for centromeric position on chromosomes. Hereditas 52:201-219. https://doi.org/10.1111/j.1601-5223.1964.tb01953.x

Lewis G, Schrire B, Mackinder B, Lock M, editors. 2005. Legumes of the world. Richmond, U. K.: Royal Botanic Gardens, Kew.

Lewis GP, Wood JRI, Lavin M. 2012. *Steinbachiella* (Leguminosae: Papilionoideae: Dalbergieae), endemic to Bolivia, is reinstated as an accepted genus. Kew Bull. 67:789-796. https://doi.org/10.1007/s12225-012-9415-z

Lewke Bandara N, Papini A, Mosti S, Brown T, Smith LMJ. 2013. A phylogenetic analysis of genus *Onobrychis* and its relationships within the tribe Hedysareae (Fabaceae). Turk J Bot. 37:981-992. https://doi.org/10.3906/bot-1210-32

Lim KB, Wennekes J, de Jong JH, Jacobsen E, van Tuyl JM. 2001. Karyotype analysis of *Lilium longiflorum* and *Lilium rubellum* by chromosome banding and fluorescence in situ hybridisation. Genome, 44(5):911-918. https://doi.org/10.1139/g01-066

Lima de Faria A. 1976. The chromosome field. I. Prediction of the location of ribosomal cistrons. Hereditas, 83(1):1-22. https://doi.org/10.1111/j.1601-5223.1976.tb01565 .

LPWG (Legume PhylogenyWorking Group 2013). Legume phylogeny and classification in the 21st century: progress, prospects, and lessons for other species-rich clades. Taxon, 62:217-248. http://dx.doi.org/10.12705/622.8

Manzanero-Medina GI, Vásquez-Dávila MA, Lustre-Sánchez H, Pérez-Herrera A. 2020. Ethnobotany of

food plants (quelites) sold in two traditional markets of Oaxaca, Mexico. S Afr J Bot. 130:215-233. https://doi.org/10.1016/j.sajb.2020.01.002

Martín G, Milera M, Iglesias J, Simón L, Hernández H. 2000. Sistemas silvopastoriles para la producción ganadera en Cuba. Intensificación de la ganadería en Centroamérica, beneficios económicos y ambientales. CATIE-FAO. Costa Rica 247 p.

Martins MB, Agostinetto D, Fogliatto S, Vidotto F, Andres A. 2021. *Aeschynomene* spp. Identification and weed management in rice fields in Southern Brazil. Agronomy, 11:453. https://doi.org/10.3390/agronomy11030453

McMahon MM, Sanderson MJ. 2006. Phylogenetic supermatrix analysis of GenBank sequences from 2228 papilionoid legumes. Syst. Biol. 55:818-836. https://doi.org/10.1080/10635150600999150

Moraes AP, Vatanparast M, Polido C, Marques A, Souza G, Fortuna-Perez AP, Forni-Martins ER. 2020. Chromosome number evolution in dalbergioid legumes (Papilionoideae, Leguminosae). Braz J Bot. 43:575-587. https://doi.org/10.1007/s40415-020-00631-6

Nakamura R, Kitamura S, Inoue M, Ohmido N, Fukui K. 2001. Karyotype analysis of *Nicotiana kawakamii* Y. Ohashi using DAPI banding and rDNA FISH. Theor Appl Genet. 102(6-7):810-814. https://doi.org/10.1007/s001220100577

Pascual-Mendoza S, Manzanero-Medina GI, Saynes-Vásquez A, Vásquez-Dávila MA. 2020. Agroforestry systems of a Zapotec community in the Northern Sierra of Oaxaca, Mexico. Bot Sci. 98(1):128-144. https://doi.org/10.17129/botsci.2423

Pennington RT, Lavin M, Ireland H, Klitgaard B, Preston J, Hu JM. 2001. Phylogenetic relationships of basal papilionoid legumes based upon sequences of the chloroplast *trnL* intron. Syst. Bot. 26:537-556. http://dx.doi.org/10.1043/0363-6445-26.3.537

Ramírez-Pinero M. 2012. Técnicas para la restauración de la selva baja caducifolia en el centro de Veracruz [master's thesis]. Xalapa, Veracruz: Instituto de Ecología, A.C. México.

Ramírez-Pinero M, Lira-Noriega A, Guevara S. 2018. Canopy asymmetry in solitary *Diphysa americana* trees: wind and landscape on the Mexican coast. J Coast Conserv. 23:163-172. https://doi.org/10.1007/s11852-018-0648-3

Rojas-Rodríguez F, Torres-Córdoba G. 2018. Árboles del Valle Central de Costa Rica: reproducción guachipelín (*Diphysa americana* (Mill.) M. Sousa). RFMK. 16(38): 69-71. https://doi.org/10.18845/rfmk.v16i38.3998

Rzedowski J, Calderón de Rzedowski G, Torres Colín L, Grether R. 2016. Familia Leguminosae. Subfamilia Papilionoideae (*Aeschynomene - Diphysa*). In: Rzedowski J, Calderón de Rzedowski G, editors. Flora del Bajío y regiones adyacentes**.** Fascículo 192. Instituto de Ecología A.C., Michoacán, México; p.1-326.

Sousa MS. 1990. Adiciones a las papilionadas de la Flora de Nicaragua y una nueva combinación para Oaxaca, México. Ann Mo Bot Gard. 77: 573-577. https://doi.org/10.2307/2399521

Tapia-Pastrana F. 2012. Karyological characterisation of four American species of *Crotalaria* (Leguminosae: Papilionoideae) by splash method. Kew Bull. 67(3):427-433. https://doi.org/10.1007/s12225-012-9385-1

Tapia-Pastrana F, Delgado-Salinas A, Caballero J. 2020. Patterns of chromosomal variation in Mexican species of *Aeschynomene* (Fabaceae, Papilionoideae) and their evolutionary and taxonomic implications. Comp Cytogenet. 14(1):157-182. https://doi.org/10.3897%2FCompCytogen.v14i1.47264

Tapia-Pastrana F, Mercado-Ruaro P. 2001. A combination of the "squash" and "splash" techniques to obtain the karyotype and asses meiotic behavior of *Prosopis laevigata* L. (Fabaceae: Mimosoideae). Cytologia, 66:11-17. http://dx.doi.org/10.1508/cytologia.66.11

Tapia-Pastrana F, Tapia-Aguirre F. 2018. Localización de satélites y cromosomas NOR para la interpretación del cariotipo de *Sesbania virgata* (Papilionoideae, Sesbanieae) de dos poblaciones americanas. Bot Sci. 96(4):619-627. https://doi.org/10.17129/botsci.1972

Villaseñor JL. 2016. Checklist of the native vascular plants of Mexico. Rev Mex Biodivers. 87(3):559-902. https://doi.org/10.1016/j.rmb.2016.06.017

WFO (The World Flora Online). [accessed 2023 March 23]. http://www.worldfloraonline.org/taxon/wfo-0000210419

Wojciechowski MF, Lavin M, Sanderson MJ. 2004. A phylogeny of legumes (Leguminosae) based on analysis of the plastid *MatK* gene resolves many well-supported subclades within the family. Am J Bot. 91:1846-1862. https://doi.org/10.3732/ajb.91.11.1846

Caryologia
International Journal of Cytology, Cytosystematics and Cytogenetics

Firenze University Press
www.fupress.com/caryologia

OPEN ACCESS

Citation: R.N. Chougule, P.V. Deshmukh, P.E. Shelke, V.J. Patil, M.M. Lekhak (2023). Cytogenetical studies of some Convolvulaceae members from the Western Ghats, India reveal uniformity in karyotypes. *Caryologia* 76(2): 59-65. doi: 10.36253/caryologia-2304

Received: September 8, 2023

Accepted: October 29, 2023

Published: December 31, 2023

Data Availability Statement: All relevant data are within the paper and its Supporting Information files.

Competing Interests: The Author(s) declare(s) no conflict of interest.

Cytogenetical studies of some Convolvulaceae members from the Western Ghats, India reveal uniformity in karyotypes

R.N. Chougule, P.V. Deshmukh, P.E. Shelke, V.J. Patil, M.M. Lekhak*

Angiosperm Taxonomy Laboratory, Department of Botany, Shivaji University, Kolhapur, Maharashtra 416004, India
*Corresponding author. E-mail: mml_botany@unishivaji.ac.in

Abstract. Karyotypes of six *Ipomoea* and one *Merremia* species were studied. Chromosome counts of $2n = 30$ for *I. corymbosa, I. kotschyana, I. marginata* f. *candida* and *M. rhyncorhiza)* and $2n = 60$ for *I. ochracea* were observed for the first time. Meiotic course of five *Ipomoea* species was also examined for the first time and two counts, i.e. $n = 15$ and $n = 30$ were recorded. Meiosis was found normal. Karyotypes of the studied species exhibited uniformity. All the species had chromosomes with median region centromeres and karyotypes were symmetrical (Stebbins' 4A category). *I. marginata* f. *candida* had the shortest chromosomes with mean length of 0.99 ± 0.02 µm. *I. ochracea* and *I. corymbosa* had the longest chromosomes with mean length of 1.22 ± 0.05 µm and 1.22 ± 0.01 µm, respectively. As chromosomes were small and exhibited uniform morphology, fluorescent banding or fluorescent in-situ hybridization can be useful to differentiate the karyotypes and understand species interrelationships.

Keywords: chromosomes, morning glory, karyotype symmetry, Western Ghats.

INTRODUCTION

Convolvulaceae, called as *bindweeds* or *morning glories* are a family of about 58 genera and more than 1977 species worldwide (POWO 2023). In India, there are about 24 genera that include about 164 species of which 27 are endemic (Dash and Mao 2020; Singh et al. 2015). These species are mostly herbaceous to woody vines, rarely herbs, shrubs, or trees. India is home to a rich diversity of Convolvulaceae due to the presence of diverse habitats and exposure to introduced species. *Ipomoea* L. is a large genus that comprises more than 800 species distributed over tropical and subtropical regions of the world (Wood et al. 2020). In India, the genus is represented by (64 taxa) 55 species and 9 infraspecific taxa, of which only three species, *I. clarkei* Hook.f, *I. laxiflora* H.J.Chowdhery & Debta and *I. salsettensis* Santapau & Patel are endemic (Dash and Mao 2020; Singh et al. 2015). Some taxa such as *I. cairica* var. *semine-glabro* (Blatt. & Hallb.) Bhandari, *I. marginata* f. *candida* (Naik & Zate) Das Das & Lakshmin., *I. deccana* var. *lobata* (C.B.Clarke)

S.C.Johri, *I. nil* var. *himalaica* (C.B.Clarke) S.C.Johri, *I. obscura* f. *concolor* Naik & Zate, *I. pes-caprae* var. *perunkulamensis* P.Umam. & P.Daniel have also been reported as endemic to India (Kattee 2019). The Western Ghats consists of 42 taxa (37 species, 03 subspecies and 02 varieties) (Lekhak et al. 2018). *Merremia* Dennst. ex Endl., on the other hand includes 49 species distributed over tropical and subtropical regions of the world (POWO 2023). In India, *Merremia* comprises 17 species, of which two species, *M. rajasthanensis* Bhandari and *M. rhyncorhiza* (Dalzell) Hallier f. are endemic to the country (Dash and Mao 2020; Singh et al. 2015).

Convolvulaceae members are economically very important. For instance, *I. batatas* (L.) Lam., popularly known as sweet potato, is a rich source of energy for humans as well as animals. The plant parts of *I. pes-caprae* (L.) R.Br. have been traditionally used to treat gastrointestinal-related disorders and symptoms, such as dysentery, ulcer, abdominal pain, cramps and stomach aches (Emendörfer et al. 2005; Pereda-Miranda et al. 2005). Many members such as *Convolvulus* L., *Ipomoea*, *Stictocardia* Hallier f., etc. are used as ornamentals. Moreover, the members of the family serve as an important source of ergoline alkaloids (Fig. 1) that have been used to treat nervous system disorders like convulsions, epilepsy, migraine, Parkinson's disease or are used in childbirth and weaning (Groeger and Floss 1998; Mutschler et al. 2001; Schardl et al. 2006; Chen et al. 2018).

On account of its tremendous utility in medicinal and ornamental fields, the family is cytogenetically well explored. In India, somatic chromosomes of these members have been the focal point for the majority of studies (Vij et al. 1974, 1977; Bir and Sidhu 1975; Bir et al. 1978; Roy 1979; Sampathkumar 1979; Rao and Mwasumbi 1981; Sinha and Sharma 1992; Rane et al. 2012; Lekhak et al. 2018; Lawand et al. 2019; Ramanpreet and Gupta 2018). Most of these studies recorded chromosome counts for species of *Ipomoea*, *Argyreia* Lour., *Merremia* and *Operculina* Silva Manso. The most common diploid chromosome number reported in these genera is $2n = 30$. Although, $2n$ with 18, 22, 28, 32, 38, 58 and 60 chromosomes have also been reported in some species (Yeh and Tsai 1995; Lekhak et al. 2018; Lawand et al. 2019). Instances of polyploidy are usually rare. Nevertheless, polyploidy has been reported in *Ipomoea batatas* which is a hexaploid ($2n = 6x = 90$) (Sinha and Sharma 1992; Vij et al. 1977).

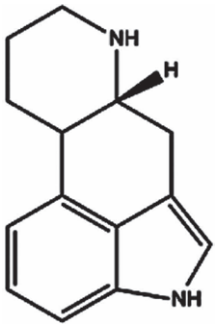

Figure 1. Structure of Ergoline alkaloid.

The present investigation aims at generating new cytogenetical data for the flowering plants (wild or introduced) of the Western Ghats, India. Since Convolvulaceae members are of horticultural and medicinal importance, chromosomal information would be useful in understanding their genetic potential, phylogenetic relationships and breeding strategies. Accordingly, here we provide comparative karyotypes of seven species. Meiotic chromosomes were studied for five *Ipomoea* species. Karyological analysis of taxa was based on karyological parameters such as diploid chromosome number ($2n$), mean chromosome length (MCL), total haploid chromosome length (THL), mean centromeric asymmetry (M_{CA}) and coefficient of variation of chromosome length (CV_{CL}).

MATERIAL AND METHODS

The plant materials for the present study were collected from different localities in Gujarat and Maharashtra state. Plants were cultivated in Lead Botanical Garden, Department of Botany, Shivaji University, Kolhapur and the voucher specimens deposited in the Herbarium of Shivaji University, Kolhapur (SUK) (Table 1). For mitotic preparations, seeds were nicked near the hilum with the help of a sharp razor, and then placed in the petri dish on a wet blotting paper. Well-grown root tips (1.5-3 cm long) were harvested from the germinating seeds and pre-treated with a saturated solution of *para*-Dicholorobenzene (*p*DB) for 4-5 h at 9±3°C. Further, the root tips were hydrolysed in 1N HCl and squashed in 2% propionic orcein. For meiotic studies, appropriately sized flower buds were fixed in Carnoy's solution and smears of anthers from floral buds were stained using 2% propionic orcein. Suitable somatic and meiotic plates from freshly prepared slides were photographed with Leica DM 750 microscope with attached camera at 1000X magnification. Five cells with well-spread metaphase chromosomes were selected for karyotype analysis. Nomenclature of chromosomes follows Levan et al. (1964). Karyotype asymmetry was ascertained using CV_{CL} (coefficient of variation of chromosome length)

Table 1. Collection localities and voucher details of studied species.

Sr. No.	Taxa	Collection locality	Voucher specimen
1.	*Ipomoea corymbosa* (L.) Roth	Shivaji University Campus, Kolhapur, Maharashtra	RNC 127
2.	*I. horsfalliae* Hook.	Uajalaiwadi, Kolhapur district, Maharashtra	RNC 121
3.	*I. kotschyana* Hochst. ex Choisy	Dinodhar hill, Nakhatrana taluka, Kutch district, Gujarat	RNC 206
4.	**I. laxiflora* H.J.Chowdhery & Debta	Gujarat	RNC 277
5.	**I. marginata* f. *candida* (Naik & Zate) Das Das & Lakshmin.	Shivaji University Campus, Kolhapur, Maharashtra	RNC 207
6.	*I. ochracea* (Lindl.) Sweet	Shivaji University Campus, Kolhapur, Maharashtra	RNC 120
7.	**I. salsettensis* Santapau & Patel	Rajapur, Ratnagiri district, Maharashtra	RNC 278
8.	**Merremia rhyncorhiza* (Dalzell) Hallier f.	Chaukul, Sawantwadi taluka, Sindhudurg district, Maharashtra	RNC 217

*Indicates endemic species.

Table 2. Comparative karyotypes.

Sr. No.	Taxa	2*n*	Range of chromosome length ± SE (μm)	Arm ratio (r) ± SE	THL (μm)	MCL ± SE (μm)	M_{CA}	CV_{CL}	R	St	Haploid karyotype formulae
1.	*I. corymbosa*	30	1.56 ± 0.02 - 0.90 ± 0.03	1.16 ± 0.01	18.35	1.22 ± 0.05	7.42	14.70	1.74	4A	15m
2.	*I. kotschyana*	30	1.21 ± 0.01 - 0.74 ± 0.01	1.22 ± 0.01	14.65	0.98 ± 0.03	14.65	13.16	1.65	4A	15m
3.	*I. laxiflora*	30	1.35 ± 0.04 - 0.86 ± 0.02	1.15 ± 0.04	15.76	1.05 ± 0.02	7.05	12.66	1.58	4A	15m
4.	*I. marginata* f. *candida*	30	1.20 ± 0.01 - 0.74 ± 0.02	1.22 ± 0.02	14.80	0.99 ± 0.02	8.84	12.28	1.65	4A	15m
5.	*I. ochracea*	60	1.57 ± 0.02 - 0.94 ± 0.01	1.21 ± 0.03	36.61	1.22 ± 0.01	9.26	12.85	1.66	4A	30m
6.	*I. salsettensis*	30	1.51 ± 0.07 - 0.95 ± 0.04	1.16 ± 0.04	17.85	1.19 ± 0.04	7.39	12.68	1.59	4A	15m + (0–4B)
7.	*M. rhyncorhiza*	30	1.38 ± 0.04 - 0.85 ± 0.02	1.15 ± 0.01	16.31	1.09 ± 0.04	6.85	12.83	1.61	4A	15m

THL = Total haploid length, MCL = Mean chromosome length, M_{CA} = Mean centromeric asymmetry, CV_{CL} = Coefficient of variation of chromosome length, R = ratio of the longest to shortest chromosome of a complement, St = karyotype asymmetry.

and M_{CA} (mean centromeric asymmetry) as suggested by Peruzzi and Eroğlu (2013).

RESULTS

In the present investigation mitotic metaphase chromosomes of seven species were studied. Meiotic study was performed on five species. *Ipomoea ochracea* (Lindl.) Sweet exhibited 2*n* = 60 chromosomes while the rest of the species had 2*n* = 30 chromosomes. Comparative karyotypes of all the species investigated are summarized in Table 2. Fig. 2 illustrates the mitotic metaphases while Fig. 3 depicts ideogram. Chromosomes were with median region centromeres, and hence the karyotype formula 15m (*I. corymbosa, I. kotshyana, I. laxiflora, I. marginata* f. *candida* and *M. rhyncorhiza*) or 30m (*I. ochracea*). Four B-chromosomes were observed in *I. salsettensis* (Fig. 2f) and the karyotype formula was 15m+4B. The highest mean chromosome length (MCL) (1.22 ± 0.05 and 1.22 ± 0.01 μm) was recorded in the case of *I. corymbosa* and *I. ochracea* whereas the lowest (0.98 ± 0.03 μm) in *I. kotschyana* (Table 2). Total haploid chromosome length (THL) ranged from 14.65 μm (*I. kotschyana*) to 36.61 μm (*I. ochracea*). *I. corymbosa* showed maximum value (1.74) for R (ratio of largest and the smallest chromosome of the complement) while the minimum (1.58) was recorded for *I. laxiflora*. M_{CA} was found to be the lowest (6.85) for *M. rhyncorhiza* and the highest (14.65) for *I. kotshyana*. The lowest CV_{CL} was recorded for *I. marginata* f. *candida* (12.28) and the highest for *I. corymbosa* (14.70) (Table 2).

Meiotic studies were carried out in five species (*I. horsfalliae*, *I. laxiflora*, *I. marginata* f. *candida*, *I. ochracea*, *I. salsettensis*). Meiosis was found to be normal. Pollen mother cells (PMCs) of *I. ochracea* showed 30 bivalents (*n* = 30) at diakinesis (Fig. 2k) whereas rest of the species (*I. horsfalliae*, *I. laxiflora*, *I. marginata* f. *candida* and *I. salsettensis*) showed 15 bivalents (*n* = 15) (Fig. 2h, i, j, l).

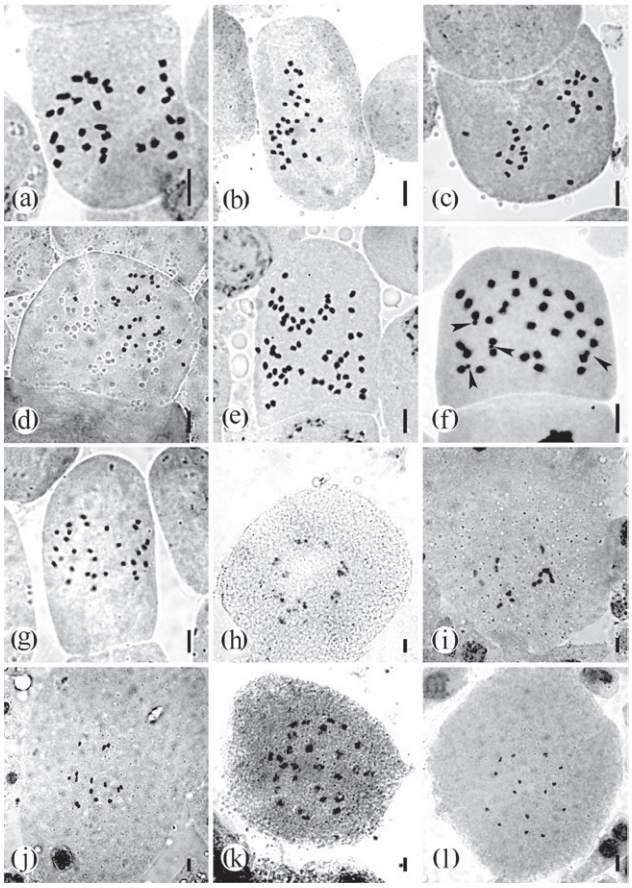

Figure 2. Mitotic metaphase and meiotic chromosomes: (a) *Ipomoea corymbosa* (2*n* = 30); (b) *I. kotschyana* (2*n* = 30); (c) *I. laxiflora* (2*n* = 30); (d) *I. marginata* f. *candida* (2*n* = 30); (e) *I. ochracea* (2*n* = 60); (f) *I. salsettensis* (2*n* = 30+4B) Arrowheads show B-chromosomes; (g) *Merremia rhyncorhiza* (2*n* = 30). (h-l) PMCs at diakinesis: (h) *I. horsefalliae* (*n* = 15); (i) *I. laxiflora* (*n* =15); (j) *I. marginata* f. *candida* (*n* = 15); (k) *I. ochracea* (*n* = 30); (l) *I. salsettensis* (*n* = 15). Scale bars = 5 µm.

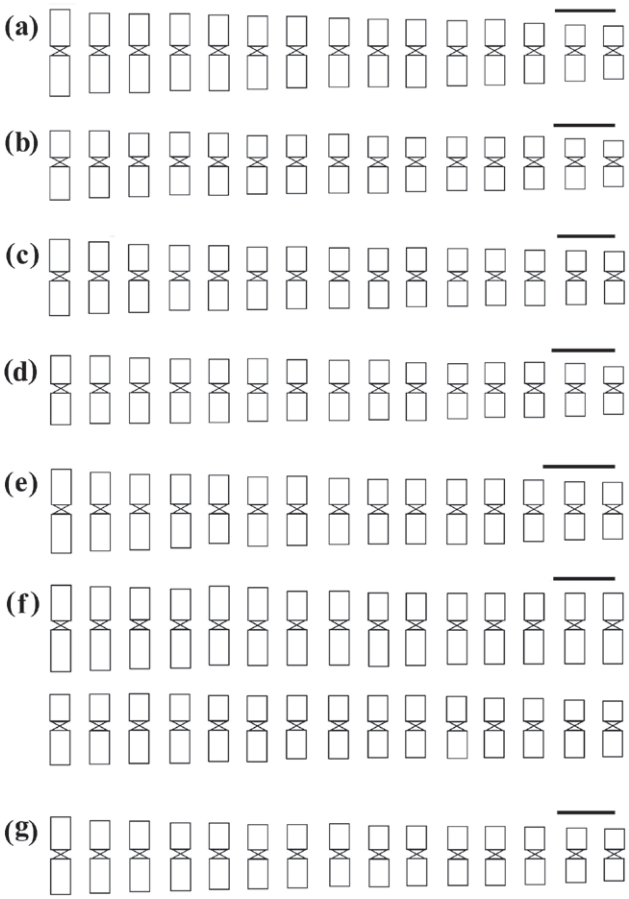

Figure 3. Ideograms of *Ipomoea* and *Merremia* species: (a) *I. corymbosa*; (b) *I. kotschyana*; (c) *I. laxiflora*; (d) *I. marginata* f. *candida*; (e) *I. salsettensis*; (f) *I. ochracea*; (g) *M. rhyncorhiza.* Scale bars = 1 µm.

DISCUSSION

According to Löve and Löve (in Sinha and Sharma 1992) $x = 5$ is the primary basic chromosome number for the family Convolvulaceae while $x = 14$ and $x = 15$ are secondarily derived basic numbers. Darlington and Wylie (1955) and Vij et al. (1977) considered $x = 14$ and $x = 15$ as the basic chromosome numbers for the genus *Ipomoea* and *Merremia*. Most of the Indian species exhibit a diploid chromosome number of $2n = 30$. In the present studies we observed $2n = 30$ chromosomes in six species whereas $2n = 60$ was found in *I. ochracea*. Earlier, the count of $2n = 60$ has been observed as an instance of tetraploidy in *I. wightii* (Wall.) Choisy, *I. plebeia* R.Br., *I. lonchophylla* J.M.Black, *I. racemigera* F.Muell. & Tate, *I. ramonii* Choisy, *I. tiliacea* (Willd.) Choisy and *I. arborescens* (Humb. & Bonpl. ex Willd.) G.Don (Jones 1964; Yen et al. 1992; Kattee 2019) whereas, *I. batatas* shows hexaploidy, i.e. $2n = 90$ chromosomes (Sinha and Sharma 1992; Pitrez et al. 2008). Some species such as *I. staphylina* Roem. & Schult., *I. purpurea* (L.) Roth possess $2n = 32$ chromosomes (Roy 1979; Sampathkumar 1979; Dhar 2015) whereas *I. coptica* Verdc., *I. diversifolia* R.Br., *I. pes-tigridis* L. show $2n = 28$ chromosomes (Sampathkumar 1979; Lekhak et al. 2018; Bir and Sidhu 1975). *I. triloba* L. is reported to have $2n = 38$ chromosomes (Wang et al. 1998). These chromosome numbers not confirming to base numbers $x = 14$ and $x = 15$ can be attributed to polyploidy, aneuploidy or dysploidy or to the occurrence of polysomaty (Vij et al. 1977; Sampathkumar 1979; Lekhak et al. 2018).

Sampathkumar (1979) studied the karyomorphology of eighteen *Ipomoea* species whereas Rane et al. (2012) studied ten species. In both the studies chromosomes

with median and submedian centromeres were observed. Nakajima (1963) also reported median, submedian and terminal centromere in *I. lacunosa* L. and *I. violacea* L. and hence, the karyotype was considered asymmetrical. In the present study we observed all the chromosomes with median region centromere and karyotype was highly symmetrical (Table 2). Similar observations have been made for *I. clarkei* and *I. diversifolia* (Lekhak et al. 2018) and in some NE Brazilian *Ipomoea* species (Pitrez et al. 2008). Kattee (2019) reported two counts, i.e. $2n$ = 30 (*I. laxiflora*, *I. salsettensis* and *I. tenuipes* Verdc.) and $2n$ = 60 (*I. wightii*). She observed chromosomes with median region centromere. In the present study, the chromosome number for *I. laxiflora* and *I. salsettensis* have been confirmed, although four B-chromosomes were observed in *I. salsettensis* for the first time (Fig. 2f). B-chromosomes (0-1) have also been reported in other *Ipomoea* species such as *I. mutabilis* Lindl. and *I. palmata* Forssk. (white flowered type) by Vij et al. (1977) whereas Yen and Tsai (1995) observed B-chromosomes (0-3) in some *Ipomoea* species from Taiwan. Sampathkumar (1979) recorded the presence of a satellite chromosome pair and secondarily constricted chromosomes in *Ipomoea* species. Similarly, Pitrez et al. (2008) observed satellite chromosomes in some *Ipomoea* species from NE Brazil inselbergs. In the present investigation, we could not find satellite chromosomes or secondarily constricted chromosomes.

Chromosome length ranged from 2.13 to 4.79 µm in *I. carnea* Jacq. and 1.25 to 2.67 µm in *I. aquatica* Forssk. (Rane et al. 2012). Lekhak et al. (2018) reported the shortest chromosome in *I. diversifolia* (1.62 µm) and the longest in *I. clarkei* (2.15 µm). In the present investigation, the longest chromosomes were observed in *I. ochracea* (0.94 to 1.57 µm) whereas the smallest (0.74 to 1.20 µm) in *I. marginata* f. *candida*. All the studied species fell under Stebbins's karyotype asymmetry class 4A. M_{CA} value was maximum in *I. kotschyana* (14.65) which indicated greater differences in the centromeric position across the chromosome complement whereas the highest CV_{CL} in *I. corymbosa* (14.70 µm) was on account of higher heterogeneity in the length of the chromosome complement.

Amongst the Indian *Merremia* species, cytogenetical data are available for 60% species (after Rice et al., 2015). Lewis et al. (1967) recorded $2n$ = 28 chromosomes for *M. aegyptia* (L.) Urb. whereas $2n$ = 30 chromosomes were reported by Jones (1968) and Pitrez et al. (2008). Vij et al. (1977) observed $2n$ = 30 chromosomes in *M. dissecta* (Jacq.) Hallier f. and *M. aegyptia*. Meiosis revealed n = 15 bivalents for both *M. dissecta* and *M. aegyptia*. Aberrant meiosis was reported in *M. aegyptia*. The presence of $2n$ = 28 and 30 chromosomes need to be further investigated. Secondly, this could also be possible due to the existence of two cytotypes in *M. aegyptia*. Ramanpreet and Gupta (2018) recorded n = 7 bivalents in *M. umbellata* (L.) Hallier f. Sampathkumar (1979) reported $2n$ = 32 and $2n$ =30 chromosomes in *M. dissecta* and *M. hederacea* (Burm.f.) Hallier f., respectively with median and submedian centromeres. R value was 2.5 and 3.3 and the chromosome length ranged from 1.2 µm to 3.0 µm and 1.0 µm to 3.3 µm for *M. dissecta* and *M. hederacea*, respectively. We observed $2n$ = 30 chromosomes in *M. rhyncorhiza*. Accordingly, the R value, i.e. 1.61 was smaller than *M. dissecta* and *M. hederacea*. The chromosomes were smaller in size (0.85 µm to 1.38 µm) and had median region centromeres and symmetrical karyotype. Pitrez et al. (2008) also reported symmetrical karyotype in *M. aegyptia* but the chromosomes were with metacentric and submetacentric region centromere with terminal secondary constriction on one of submetacentric pairs. Sampathkumar (1979) also found satellite chromosomes and secondary constrictions in both species *M. dissecta* and *M. hederacea*. We could not observe any satellite chromosomes and secondary constrictions in *M. rhyncorhiza*.

Recently, Ramanpreet and Gupta (2018) carried out meiotic studies on 19 species of Convolvulaceae from Indian hot desert Rajasthan. They studied nine *Ipomoea* species and reported normal meiosis and high pollen fertility in all studied *Ipomoea* species. For *I. cordatotriloba* Dennst., *I. triloba* and *I. sagittifolia* Burm.f. a meiotic count of n = 15 bivalents was recorded for the first time (Ramanpreet and Gupta 2018). They found n = 15 bivalents for eight *Ipomoea* species and n = 14 bivalents for *I. pes-tigridis*. This study also confirmed earlier reports on chromosome numbers of *Ipomoea*. In present investigation, meiotic counts of n = 15 in *I. horsfalliae, I. laxiflora*, *I. marginata* f. *candida* and *I. salsettensis* and n = 30 in *I. ochracea* were made for the first time. Meiotic course was normal. Lekhak et al. (2018) also found normal meiosis in *I. clarkei* and *I. diversifolia*. Vij et al. (1977) also studied meiosis in *Ipomoea* and some allied genera. They studied meiosis in 22 *Ipomoea* species and found normal bivalent formation. Most of the *Ipomoea* species exhibited n = 15 bivalents. *I. coccinea* L. and *I. batatas* were reported to have the counts of n = 14 and n = 45, respectively. Irregular anaphases were also observed some species. One B-chromosome was observed in *I. mutabilis* and *I. palmata* (white flowered type). We did not find B-chromosomes in the meiotic phases. Chromosome data are now lacking only in fourteen *Ipomoea* and six *Merremia* species in India (Table 3).

Table 3. Indian species of *Ipomoea* and *Merremia* awaiting karyological investigation and their geographical distribution. #Indicates introduced species and *endemic species.

Sr. No.	Taxa	Geographical distribution
1.	*Ipomoea acanthocarpa* (Choisy) Hochst. ex Schweinf. & Asch.	Gujarat
2.	*I. aitonii* Lindl.	Telangana
3.	*I. barlerioides* (Choisy) Benth. ex C.B.Clarke	Andhra Pradesh, Bihar, Daman & Diu, Goa, Himachal Pradesh, Karnataka, Kerala, Madhya Pradesh, Maharashtra, Odisha, Punjab, Sikkim, Tamil Nadu, Uttar Pradesh, West Bengal
4.	*I. cairica* var. *semine-glabro* (Blatt. & Hallb.) Bhandari	Rajasthan
5.	*I. marginata* f. *marginata*	Throughout India
6.	*I. nil* var. *himalaica* (C.B.Clarke) S.C. Johri	Sikkim, Jammu and Kashmir to Rajasthan
7.	*I. obscura* f. *concolor* Naik & Zate	Maharashtra
8.	*I. pes-caprae* var. *perunkulamensis* P.Umam & P. Daniel	Tamil Nadu
9.	#*I. heptaphylla* Sweet	Native range Tropical & Subtropical America
10.	*I. rubens* Choisy	Assam, Maharashtra, West Bengal
11.	*I. rumicifolia* Choisy	Rajasthan, Gujarat, Kerala, Tamil Nadu
12.	*I. tuberculata* Ker Gawl.	Gujarat, Himachal Pradesh, Kerala, Maharashtra, Tamil Nadu, Uttar Pradesh, West Bengal
13.	*I. vagans* Baker	Gujarat
14.	*I. velutina* R.Br.	West Bengal
15.	*M. cissoides* (Lam.) Hallier f.	Kerala
16.	*M. kentrocaulos* (C.B.Clarke) Hallier f.	Andhra Pradesh, Kerala, Tamil Nadu
17.	*M. mammosa* (Lour.) Hallier f.	Andaman & Nicobar Islands, Arunachal Pradesh, Assam
18.	*M. quinata* (R.Br.) Ooststr.	Bihar, Odisha, Tamil Nadu
19.	*M. rajasthanensis* Bhandari	Rajasthan
20.	*M. sibirica* (L.) Hallier f.	Himachal Pradesh, Uttar Pradesh

CONCLUSION

Comprehensive data on cytogenetics of *Ipomoea* and *Merremia* are important to understand the chromosomal evolution and harness the economic potential. As molecular phylogeny for the Indian taxa is not available, karyological data, particularly chromosome number and information from fluorescent banding or fluorescent in-situ hybridization can help to reveal species interrelationships. Based on the data of chromosome number for *Ipomoea* and *Merremia* presented here and previous reports it is clear that there are two basic chromosome numbers, i.e. $x = 14$ and $x = 15$. Nevertheless, more information on the hitherto studied taxa and confirmation of chromosome number in taxa where the count does not confirm to these numbers is needed to understand mechanisms underlying evolution in these genera.

ACKNOWLEDGEMENTS

Authors are grateful to the Head, Department of Botany, Shivaji University, Kolhapur (SUK) for providing research facilities. RNC thanks DBT for financial support under 'Network Programme for Enrichment and Update of Plant Chromosome Database for Spermatophytes and Archegoniate Phase - II' vide sanction letter BT/PR34491/NDB/39/678/2020 dated 11 November 2021.

REFERENCES

Bir SS, Kumari S, Shoree SP, Sagoo MS. 1978. Cytological studies in certain bicarpellatae from north and central India. J Cytol Genet. 13:99–106.

Bir SS, Sidhu M. 1975. Weed flora of cultivable lands in Punjab maize fields in Patiala district. Acta Bot Indica. 3:136–141.

Chen G-T, Lu Y, Yang M, Li J-L, Fan B-Y. 2018. Medicinal uses, pharmacology, and phytochemistry of Convolvulaceae plants with central nervous system efficacies: A systematic review. Phytother Res. 32(5):823–864.

Darlington CD, Wylie AP. 1955. Chromosome atlas of flowering plants. London: George Allen & Unwin.

Dash SS, Mao AA. 2020. Flowering Plants of India. An annotated checklist (Dicotyledons). Volume II. Botanical Survey of India; p. 176–194.

Dhar PT. 2015. Mitotic studies of selected *Ipomoea* species Linn. Int J Adv Res Biol Sci. 2 (9):81–83.

Emendörfer F, Emendörfer F, Bellato F, Noldin VF, Niero R, Cechinel-Filho V, Cardozo AM. 2005. Evaluation of the Relaxant Action of Some Brazilian Medicinal Plants in Isolated Guinea-Pig Ileum and Rat Duodenum. J Pharm Pharm Sci. 8(1): 63–68.

Groeger D, Floss HG. 1998. Biochemistry of ergot alkaloids-achievements and challenges, in Cordell, G.A., (Eds.), The Alkaloids-Chemistry and Biology, Vol 50. Academic Press, New York; p. 171–218.

Jones A. 1964. Chromosome numbers in the genus *Ipomoea*. J Heredity. 55(5):216–219.

Jones A. 1968. Chromosome number in *Ipomoea* and related genera. J Heredity. 59(2):99–102.

Kattee AV. 2019. Revision of the genus *Ipomoea* L. (Convolvulaceae) for India. Ph.D. Thesis, Shivaji University, Kolhapur.

Lawand PR, Gaikwad SV, Gurav RV, Shimpale VB. 2019. Karyomorphological studies in three species of *Argyreia* Lour. (Convolvulaceae) from India. Nucleus. 62:71–75.

Lekhak MM, Patil SD, Kattee AV, Yadav PB, Ghane SG, Gavade SK, Shimpale VB, Yadav SR, 2018. Cytopalynological studies in some Convolvulaceae members from northern Western Ghats, India. Caryologia. 71(3):263-271.

Levan A, Fredga K, Sandberg AA. 1964. Nomenclature for centromeric position on chromosomes. Hereditas. 52:201-220.

Lewis WH, Suda Y, Oliver RL. 1967. In Chromosome numbers of phanerogams. 2. Ann Missouri Bot Gard. 54:178-180.

Mutschler E, Geisslinger G, Kroemer HK, Schaefer-Korting M. 2001. Arzneimittelwirkungen- Lehrbuch der Pharmakologie und Toxikologie, (Ed) 8. Wissenschaftliche Verlagsgesellschaft mbH, Stuttgart.

Nakajima G. 1963. Karyotype of genus *Ipomoea*. Cytologia. 28(4):351-359.

Pereda-Miranda R, Escalante-Sánchez E, Escobedo-Martínez C. 2005. Characterization of lipophilic pentasaccharides from Beach Morning Glory (*Ipomoea pes-caprae*). J Nat Prod. 68(2):226–230.

Peruzzi L, Eroğlu HE. 2013. Karyotype asymmetry: again, how to measure and what to measure? Comp Cytogenet. 7(1):1–9.

Pitrez SR, de Andrade LA, Alves LIF, Felix LP. 2008. Karyology of some Convolvulaceae species occurring in NE Brazil inselbergs. Plant Syst Evol. 276(3):235–241.

POWO, 2023. Plants of the World Online. Facilitated by the Royal Botanic Gardens, Kew. Published on the Internet; Retrieved 2023 June 10. http://www.plantsoftheworldonline.org

Rice A, Glick L, Abadi S, Einhorn M, Kopelman NM, Salman-Minkov A, Mayzel J, Chay O, Mayrose I. 2015. The Chromosome Counts Database (CCDB) – a community resource of plant chromosome numbers. New Phytol. 206(1):19–26.

Ramanpreet, Gupta RC. 2018. Meiotic studies of the Convolvulaceae Juss. from Indian Hot Desert. Chromosom Bot. 12(4):77-85.

Rane VA, Patel BB, George J. 2012. Karyomorphological analysis of ten species of *Ipomoea* Jacq. Cytologia. 77(2):239-249.

Rao PN, Mwasumbi LB. 1981. In Chromosome number reports LXXII. Taxon. 30:701.

Roy R. 1979. Karyotype of *Ipomoea purpurea*. Proc Indian Sci Congr Assoc. (III, C). 66:84–85.

Sampathkumar R. 1979. Karyomorphological studies in some south Indian Convolvulaceae. Cytologia. 44:275-286.

Schardl CF, Pannacione DG, Tudzynski P. 2006. Ergot alkaloids-biology and molecular biology. In GA Cordell, ed, The Alkaloids: Chemistry and Biology, Vol 63. Academic Press, New York; p. 45–86.

Singh P, karthigeyan k, Lakshminarasimha P, Dash SS 2015. *Endemic Vascular Plants of India*, Botanical Survey of India; p. 144–145.

Sinha S, Sharma SN. 1992. Taxonomic significance of karyomorphology in *Ipomoea* spp. Cytologia. 57:289–293.

Vij SP, Singh S, Sachdeva VP. 1974. In IOPB chromosome number reports XLV. Taxon. 23:619–624.

Vij SP, Singh S, Sachdeva VP. 1977. Cytomorphological studies in Convolvulaceae II. *Ipomoea* and allied genera. Cytologia. 42:451–464.

Wang JX, Lu SY, Zhou HY, Liu QC. 1998. The second report of studies on overcoming the interspecific incompatibility and hybrid abortion between series A and B in the section Batatas of the genus *Ipomoea*. Acta Agron Sin. 24(2):139–146.

Wood JRI, Muñoz-Rodríguez P, Williams BRM, Scotland RW. 2020. A foundation monograph of *Ipomoea* (Convolvulaceae) in the New World. Phytokeys. 143(67):1–823.

Yeh HC, Tsai JI. 1995. Karyotype analysis of Convolvulaceae in Taiwan. Annual Taiwan Mus. 38:58–61.

Yen DE, Gaffey PM, Coates DJ. 1992. Chromosome number of Australian species of *Ipomoea* L. (Convolvulaceae). Austrabaileya. 3(4):749–755.

Caryologia
International Journal of Cytology, Cytosystematics and Cytogenetics

Firenze University Press
www.fupress.com/caryologia

OPEN ACCESS

Citation: Nicoleta Anca Şuţan, Diana Ionela Popescu (Stegarus), Oana Alexandra Drăghiceanu, Carmen Topală, Claudiu Şuţan, Aurelian Denis Negrea, Denisa Ştefania Vîlcoci, Georgiana Cîrstea, Sorin Georgian Moga, Liliana Cristina Soare (2023). *In vitro* cytotoxic activity of phytosynthesized silver nanoparticles using *Clematis vitalba* L. (Ranunculaceae) aqueous decoction. *Caryologia* 76(2): 67-81. doi: 10.36253/caryologia-2330

Received: May 10, 2023

Accepted: October 29, 2023

Published: December 31, 2023

Data Availability Statement: All relevant data are within the paper and its Supporting Information files.

Competing Interests: The Author(s) declare(s) no conflict of interest.

ORCID
NAŞ: 0000-0001-7459-628X
OAD: 0000-0001-8351-0919
LCS: 0000-0002-2874-3135
DIP: 0000-0002-3442-3760
CT: 0000-0002-9117-4983
CŞ: 0000-0002-1719-1814
ADN: 0000-0001-7525-1056
DŞV: 0000-0002-9777-6782
GC: 0000-0002-7442-7109
SGM: 0000-0001-9620-4283

In vitro cytotoxic activity of phytosynthesized silver nanoparticles using *Clematis vitalba* L. (Ranunculaceae) aqueous decoction

Nicoleta Anca Şuţan[1], Diana Ionela Popescu (Stegarus)[2], Oana Alexandra Drăghiceanu[1], Carmen Topală[3], Claudiu Şuţan[3,*], Aurelian Denis Negrea[4], Denisa Ştefania Vîlcoci[4], Georgiana Cîrstea[4], Sorin Georgian Moga[4], Liliana Cristina Soare[1]

[1] *Department of Natural Sciences, National University of Science and Technology POLITEHNICA Bucharest, Pitesti University Centre, Romania*
[2] *National Research and Development Institute for Cryogenics and Isotopic Technologies–ICSI Ramnicu Valcea, 4th Uzinei Street, 240050 Ramnicu Valcea, Romania*
[3] *Department of Environmental Engineering and Applied Sciences, National University of Science and Technology POLITEHNICA Bucharest, Pitesti University Centre, Romania*
[4] *Regional Center of Research and Development for Materials, Processes and Innovative Products Dedicated to the Automotive Industry, National University of Science and Technology POLITEHNICA Bucharest, Pitesti University Centre, Romania*
*Corresponding author. E-mail: claudiu.sutan@upb.ro

Abstract. In this study, we report a bottom-up approach for silver nanoparticles (AgNPs) synthesis using aqueous decoction of aerial parts of *Clematis vitalba* L. The phytosynthesized AgNPs were characterized by X-ray diffraction (XRD), UV-vis spectroscopy, Fourier Transform-Infrared Spectroscopy (FTIR), Scanning Electron Microscopy coupled with Energy Dispersive X-ray Spectroscopy (SEM-EDS) and Bright Field Scanning Transmission Electron Microscopy (BFSTEM). The cytogenotoxicity and phytotoxicity assays of AgNPs were assessed by using *Allium* test, Evans blue and 2, 3, 5-triphenyl tetrazolium chloride (TTC) staining, root and stem growth potential, and biomass evaluation. The results revealed that AgNPs were in the size range of 1-15 nm and spherical shape. The biosynthesized AgNPs augment the mitodepressive effect, disruption of cellular metabolism, impairment of root and stem growth, and biomass reduction induced by *C. vitalba* aqueous extracts. These results outline the toxicological profile of the *C. vitalba* extracts, as well as of the phytogenerated AgNPs and provides scientific perspectives on the use of *C. vitalba* extracts as reducing and stabilizing agent for the phytosynthesis of metallic nanoparticles.

Keywords: *Clematis vitalba*, AgNPs, biosynthesis, cytogenotoxicity, phytotoxicity.

INTRODUCTION

Clematis L., one of the best represented genera of the buttercup family (Ranunculaceae), includes about 300 species (He et al. 2019), most climb-

ing plants and shrubs widespread in temperate zones of the northern and southern hemispheres, in mountainous and tropical regions. Over 600 ornamental varieties are commercially cultured worldwide (Weng-Tsai 2003; Woudenberg et al. 2009).

Clematis vitalba L. is a deciduous perennial climber vine which grows in fields and woody areas of Europe, USA, Australia and New Zealand (Bungard 1996; Ogle et al. 2000; Redmond and Stout 2018). In various parts of the world the species *C. vitalba* is known by different common names, such as Old Man's Beard due to its seeds with fluffy heads, Mile-A-Minute based to its high growth rate, or Traveler's Joy, being found along the roads (O'Halloran 2019). Like most buttercups, *C. vitalba* is toxic and irritating, containing protoanemonin lactones and convulsive poisons, but most exposures have resulted in minimal to no toxicity (Duke 1985; Lewis et al. 2020). A synthesis of the compounds identified in *Clematis* species was reported by Da-Cheng (2019), who mentioned the presence of saponin, coumarin, flavonoids, anthocyanins, and alkaloids. In relation to environmental risk, alkaloids and saponins were characterized by Günthardt et al. (2018) as some of the most toxic secondary metabolites. In fact, a large number of papers have shown that buttercups can inhibit mitosis, induce apoptosis and alter the human cell cycle (Naz et al. 2020), but also affect plant cells, being phytotoxic. Thus, the inhibition of root system growth in *Triticum aestivum* L. by ethanolic extracts of *Anemone nemorosa* L. was reported by Ancuceanu et al. (2018). Methanolic extracts from *Anemone reflexa* Steph. & Willd. and *Clematis trichotoma* Nakai showed strong herbicidal activity, inhibiting the growth of barnyardgrass (*Echinochloa crus-galli* (L.) P. Beauv.) seedlings (Kim and Lee 2007).

Phytotoxicity and cytogenotoxicity tests are recommended for assessing the impact of nanoparticles (NPs) on vascular plants. Among the parameters indicated are germination rate, root and stem growth rate, number of leaves, biomass, enzyme activities, photosynthetic rate, mitotic index, i.e. (Roy et al. 2019). The investigation of morphological, physiological and genetic changes in plants under the influence of NPs from natural or anthropogenic sources is still in its infancy (Ogle et al. 2000), from a toxicological perspective the impact proving both positive and negative (RuttkayNedecky et al. 2017).

During the last decades, nanobiotechnology has become an ingenious strategy for green synthesis of NPs. Applying the principle of self-assembly and self-organization through supramolecular interactions and under the action of external stimuli, the bottom-up approach offers the possibility of NPs synthesis in a simple, fast and cost-efficient manner. The use of plant extracts for extracellular synthesis of NPs is currently an eco-friendly alternative to improve their potential impact, as well as to reduce their side effects (Shende et al. 2022; Şuţan et al. 2016). Along with other metallic nanoparticles, biosynthesized silver nanoparticles (AgNPs) have found their utility in medical, ecological, textile, agriculture, food security and other applications (Eswaran et al. 2021; Hassan and El-latif 2018; Prakash 2013; Roy et al. 2017; Shende et al. 2022). Considered an invasive species (Hill et al. 2001) or potentially invasive (Filippin et al. 2009) in some parts of the world, being so common and having a rapid growth rate, and also being rich in novel secondary metabolites such as flavonoids and alkaloids responsible for the reduction of ionic into nanoparticles, *C. vitalba* could become a valuable resource for the biosynthesis of NPs. Moreover, the biomolecules from the *C. vitalba* could act as capping agents, thus increasing the stability and monodispersity of biosynthesized NPs.

Thus, the aim of this study is to emphasize the potential applicability of the extracts of *C. vitalba* in nanobiotechnology, and their impact, prior to and after AgNPs phytosynthesis on cell viability and metabolic activity, in view of highlighting their cytogenotoxic and phytotoxic properties.

MATERIALS AND METHODS

Collection of plant materials

Overground parts of *C. vitalba* plants were collected from 44°51'23.3"N 24°53'17.7"E (GPSMAP® 60CSx), Piteşti, Romania. The voucher specimen no. 2510 was deposited in the Herbarium of Pitesti University Centre, National University of Science and Technology POLITEHNICA Bucharest, Romania.

Decoction method and synthesis of silver nanoparticles

Authenticated plant material was washed insistently with tap water, rinsed with distilled water and dry until constant weight, at room temperature. The dried plants were ground in pulses for 3 min at 4000 RPM and continuously for 10 sec at 10 000 RPM through a laboratory knife mill (Retsch Knife Mill Grindomix GM 200). The aqueous extract of *C. vitalba* was obtained according to the protocol proposed by Muala et al. (2021) with slight modifications. The powdered raw material was extracted in distilled water (1:10 w/v), in a water bath at 95 °C for 15 min and kept 24 hours at room temperature, in the dark conditions. The slurry was filtered through Wattman No.1 paper to obtain crude extracts.

Aqueous extract of *C. vitalba* (Cv) were treated with equal volume of 10^{-3} M $AgNO_3$ and left at room temperature. In order to demonstrate the biosynthesis of AgNPs, as well as to correlate the involvement of secondary metabolites from the extract with the biosynthesis process, the extracts were subjected to Fourier Transform-Infrared Spectroscopy (FTIR) analysis and nanoformulations were subjected to X-ray diffraction (XRD), UV-vis spectroscopy, Scanning Electron Microscopy coupled with Energy Dispersive X-ray Spectroscopy (SEM-EDS) and Bright Field Scanning Transmission Electron Microscopy (BFSTEM). The cytogenotoxicity and phytotoxicity assays of extracts and their nanoformulations were assessed by using *Allium* test, Evans blue and 2, 3, 5-triphenyl tetrazolium chloride (TTC) staining.

Physicochemical characterization of C. vitalba aqueous extract and metallic nanoparticles

Aqueous extract was evaluated for its chemical composition. Fourier transform infrared spectroscopy (FTIR) was made with a FTIR Jasco 6300 spectrometer with an ATR accessory equipped with a diamond crystal (Pike Technologies). The spectra were recorded in the region of 4000-400 cm^{-1}, detector TGS, apodization Cosine. The spectral data were processed with JASCO Spectra Manager II software.

AgNPs biosynthesis (CvAg) was evaluated through color change after 4 h and confirmed by UV-Vis spectroscopy.

Qualitative analysis of compounds in Cv (dilution factor 20x) and CvAg was carried out in the wavelength ranging from 300 to 500 nm and the resolution of 2 nm by using UV-Vis Ocean Optics HR2000+. CvAg sample was centrifuged at 6000 rpm for 15 min and the resuspended sediment in a 10 mg/mL solution was scanned for the characteristic peaks (Kaur et al. 2017).

In order to perform X-ray Diffraction Analysis (XRD), the supernatant was removed, and the sediment was centrifugated twice with distilled water at the same speed and time. The XRD pattern of as-separated NPs was recorded with a Rigaku Ultima IV diffractometer. The experimental conditions were: CuKα radiation, BB geometry, D/teX Ultra detector with graphite monochromator, continuously mode, 2theta range [35^0-900], step 0.05^0, and speed 2^0/min.

Scanning Electron Microscopy coupled with Energy Dispersive X-ray Spectroscopy (SEM-EDS) and Bright Field Scanning Transmission Electron Microscopy (BFSTEM) analyses were performed using the FESEM - HITACHI SU8230 microscope. SEM-EDS was used to confirm the presence of Ag, while STEM was used to investigate particles shape and size distribution. For SEM-EDS, samples of Cv and CvAg were homogenized in the ultrasonic bath (Guyson's Kerry Pulsatron KC2) for 1 min, dropped on the conductive carbon tape (C) and dried for 24 h in the desiccators. In order to enhance the fluorescence data, a sediment sample obtained by CvAg centrifugation was spread on the conductive carbon tape. EDS data have been collected from the conductive carbon tape (in order to extract sample's support contribution from the EDS spectra), from the Cv, CvAg and CvAg sediment. For BFSTEM analysis, CvAg sample was homogenized in the ultrasonic bath for 1 min, dropped on carbon coated nickel STEM grid (Ni-C) and dried for 24 h in the desiccator. Size distribution of biosynthesized AgNPs was analyzed with ImageJ software (Rasband 1997-2018).

Evaluation of cytogenotoxic effects by Allium test

Healthy bulbs of *Allium cepa* L. (2n=16) were provided by a private organic farm. Bulbs with a diameter of about 3 cm were used for cytogenotoxic assessment. The bulbs were incubated with the discoidal stem in contact with distilled water for 48 hours, in the dark, at room temperature (20-22 °C). The bulbs with new roots were transferred for 12, 24 and 48 h in aqueous extracts of *C. vitalba* (Cv12, Cv24 and Cv24) and nanostructured mixture with AgNPs, respectively (CvAg12, CvAg24, CvAg48). Distilled water (C) was used as a negative control and the cytogenotoxic effects were evaluated at appropriate times of 12, 24 and 48 h (C12, C24, C48) of incubation. Microscopic slides were prepared following the protocol exhaustively previous presented (Sutan et al. 2019). About 3000 cells for each sample were evaluated. Mitotic index (MI), distribution of mitosis phases, chromosomal aberrations and nuclear abnormalities in the analyzed cell population were the endpoints of the cytogenotoxic assessment (Şuţan et al. 2020).

Evaluation of cell viability

Cell viability was assessed by performing Evan's blue test, following the protocol proposed by Vijayaraghavareddy et al. (2017) with slight modifications. After the completion of the experimental treatments, 10 freshly harvested roots corresponding to each experimental variant were incubated for 15 min in 2 ml of 0.25% Evan's blue. The roots were rinsed insistently with distilled water and kept in fresh distilled water overnight. Root tips of 5 mm in length were transferred to 2 ml of 1% aqueous SDS solution and kept for 1 h at 50 °C in

water bath. The roots were qualitatively analyzed and the Evan's blue uptake was macro-imaged. For a quantitative estimation of cell viability, the optical density (OD) of the released pigment was read by the spectrophotometer (UV-Vis, T70+) at 600 nm.

Evaluation of mitochondrial activity

The 2,3,5-triphenyl tetrazolium chloride (TTC) staining assay was applied for assessing the metabolic activity of root tip cells. The onion roots were immersed in 0.5% aqueous TTC solution overnight and then extracted into 3 ml of 95% ethanol for 5-15 min, without heating. Due to the instability of TTC to light, the assay was performed in the dark. The absorbance of the extracts was read at 485 nm with a T70 + UV-Vis spectrophotometer (Towill and Mazur 1974; Prajitha and Thoppil 2017).

Assessment of the phytotoxic effect

Phytotoxicity of aqueous extracts and nanostructured mixture were assessed using seeds of *Triticum aestivum* L., Miranda variety. The seeds were soaked in 150 ml distilled water for 2 h. For each experimental variant 10 imbibed seeds were transferred in *C. vitalba* extract with and without phytosynthesized AgNPs for one hour, in the dark, and watered periodically with distilled water. Distilled water was used as negative control. After 4 days, fresh and dry biomass, the length of the roots and stems were evaluated. In order to establish dry biomass, the fresh materials were kept in the oven, at 80 °C, until constant weight was obtained (Azooz et al. 2012).

Statistical interpretation

Three replicates were used to quantify the cytogenotoxic and phytotoxic effects of the extracts and nanostructured mixtures. Statistical analysis of the results was performed using IBM SPSS Statistics 20.0 (2011). Statistical significance and significant differences between variables were determined using variance analysis (One Way ANOVA) and the Ducan test for multiple comparisons, respectively. The values of $P \leq 0.05$ were considered statistically significant. Graphs and tables were compiled based on mean values ± standard error (SE) of several independent experiments. For linear association between variables, Pearson's correlation was significant at the 0.01 level (2-tailed).

RESULTS

Physicochemical characterization of C. vitalba extract prior to and after AgNPs phytosynthesis

The FTIR analysis revealed the band at 3347 cm^{-1} which intensity has almost reduced and shifted to 3359 cm^{-1} in IR spectra of AgNPs. In the case of AgNPs the peaks at 1267 cm^{-1} and at 1046 cm^{-1} are shifted. The strong band at 1636 cm^{-1} existing in the spectrum of *C. vitalba* aqueous extract, are shifted in the FTIR spectrum of the AgNPs as it is shown in Figure 1.

Figure 2 shows a typical metallic Ag XRD pattern, according to ICDD PDF4+ DB04-002-1347. The crystallite size of AgNPs was calculated using Rigaku PDXL2 and Wagner-Halder method (Halder and Wagner, 1966). The obtained value was 10,7±0,4 nm. Furthermore, the biosynthesis of AgNPs was indicated by the visible color shift from greenish-brown to light brown after 2 hours of incubation in the dark, without stirring the mixture (Fig. 3).

The UV-vis spectra of aqueous extracts of *C. vitalba* (Fig. 4A) showed a shoulder peak in the range of 320-330, while the UV-vis spectra of CvAg sample showed a distribution of peaks varying between 400-500 nm, with maximum absorbance at 436 nm (Fig. 4B).

EDS analysis was performed to confirm the presence of Ag. The EDS spectra obtained for the conductive carbon tape, Cv, CvAg and CvAg sedimented on the carbon grid are shown in figure 5. Comparison of the obtained EDS spectra revealed that the aqueous extract of *C. vitalba* contains as majority elements K, Ca, Cl and minority elements such as P, Br, Mg. From analysis of all the superimposed spectra, the presence of Ag can be noticed only in the samples CvAg and CvAg sedimented. Moreover, the EDS pattern did not show any evidence for nitrogen.

In Figure 6A-D the dispersion of biosynthesized AgNPs is represented in BFSTEM at successive magnifications (x20k, x100k, x200k and x500k). The size of the identified particles was below 15 nm, and their shape was relatively spherical (Fig. 6D). It should be noted that a microparticle consisting of AgNPs embedded in a complex biological matrix was identified on the edges of the Ni-C grid and an EDS mapping analysis was performed (Fig. 7).

The analysis of the AgNPs size distribution was performed on the micrograph obtained in BFSTEM (Figure 6D). For the selected area of interest and for the inclusion criterion defined for the range 1-15 nm it was found that AgNPs with domains between 1-10 nm are prevalent.

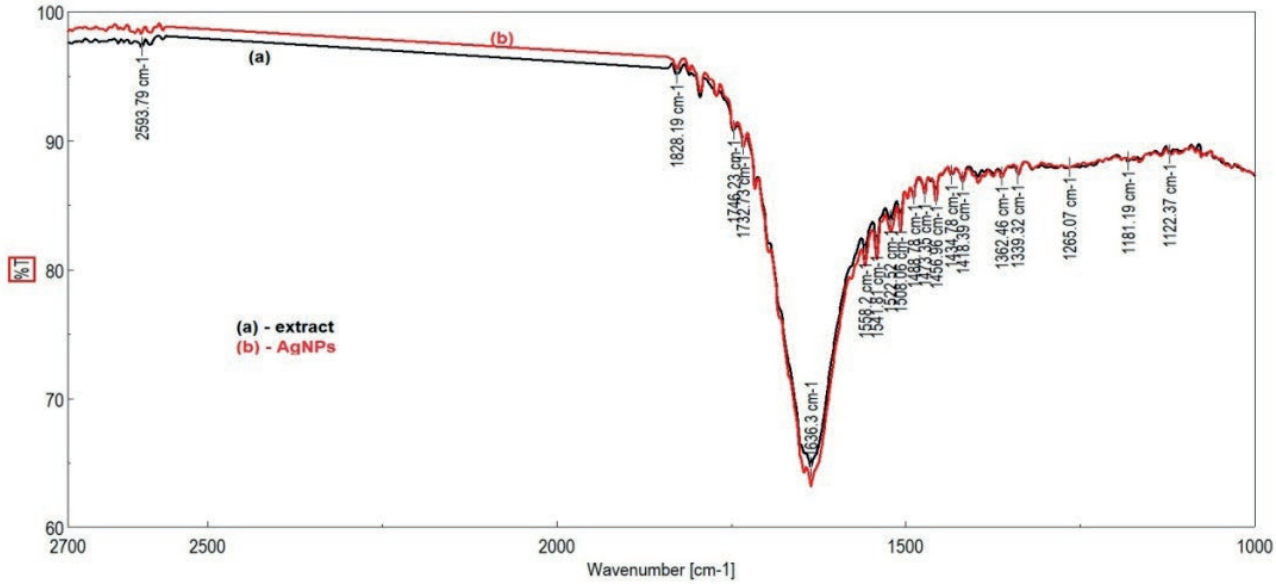

Figure 1. (ATR)-FTIR spectra of *C. vitalba* leaves extract (black) and of AgNPs (red).

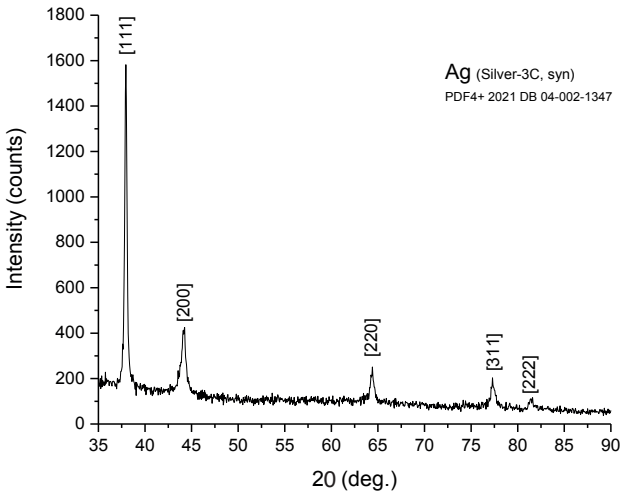

Figure 2. XRD spectra of the phytosynthesized AgNPs using aqueous extract of *C. vitalba.*

Figure 3. Color of *C. vitalba* extract prior (Cv) and after AgNPs phytosynthesis (CvAg).

Cytogenotoxic effects of C. vitalba extract and nanostructured mixture

The effects of *C. vitalba* extracts prior to and after AgNPs biosynthesis on onion meristematic root cells are presented in Table 1. Statistical analysis of the results revealed a significant decrease in MI in the samples defined by aqueous extracts and nanostructured mixtures. The highest MI (8.7%) was recorded for the negative control C12, and the lowest MI (0.6%) was determined in the CvAg48 sample. The Pearson correlation coefficient was -0.87 indicating a significant time dependent inhibition of MI. Nanoformulations with AgNPs determined a severe mitoinhibitory activity, the number of cells identified in the various stages of mitosis being almost zero, after 48 hours from the initiation of treatment.

Suppression of mitosis resulted in a low frequency of chromosomal and nuclear aberrations. However, remarkable differences were noted between the control and the samples defined by *C. vitalba* extracts. Thus, in

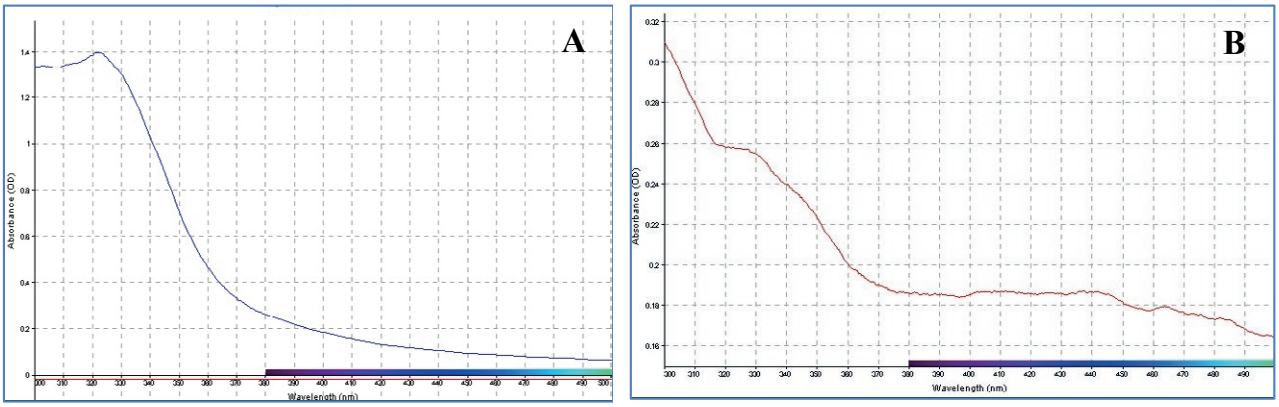

Figure 4. UV-vis spectra of *C. vitalba* prior to (A) and after AgNPs phytosynthesis (B).

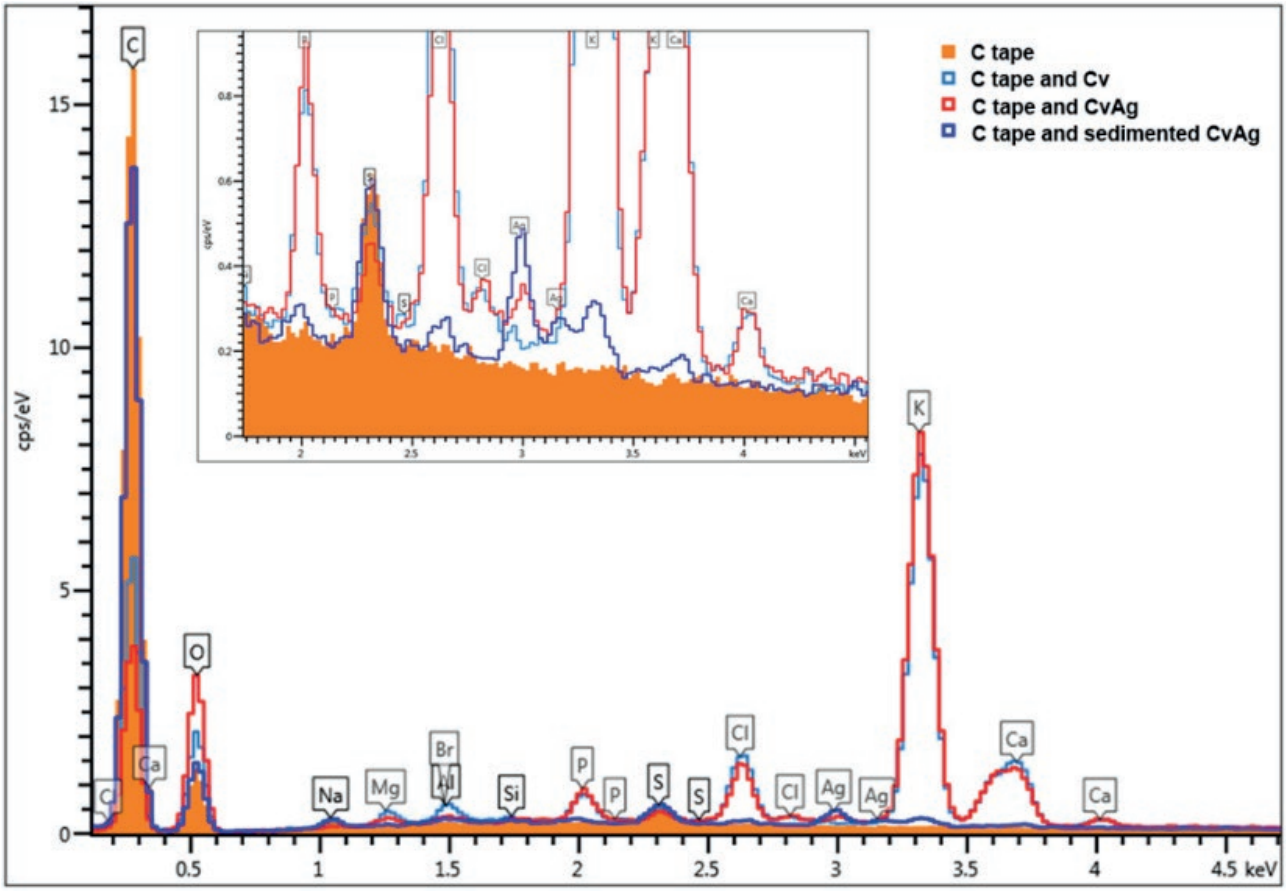

Figure 5. EDS spectra obtained for the conductive carbon tape, Cv, CvAg and CvAg sediment (inset zoom EDS spectra reveal prominent silver peaks).

the control only chromosomal aberrations such as anaphase bridges and very rarely laggards were identified, while *C. vitalba* extracts before and after AgNPs phytosynthesis induced the formation of binucleate and giant cells with displaced nuclei. Additionally, concave plasmolysis was very often revealed by cytological analysis (Fig. 8).

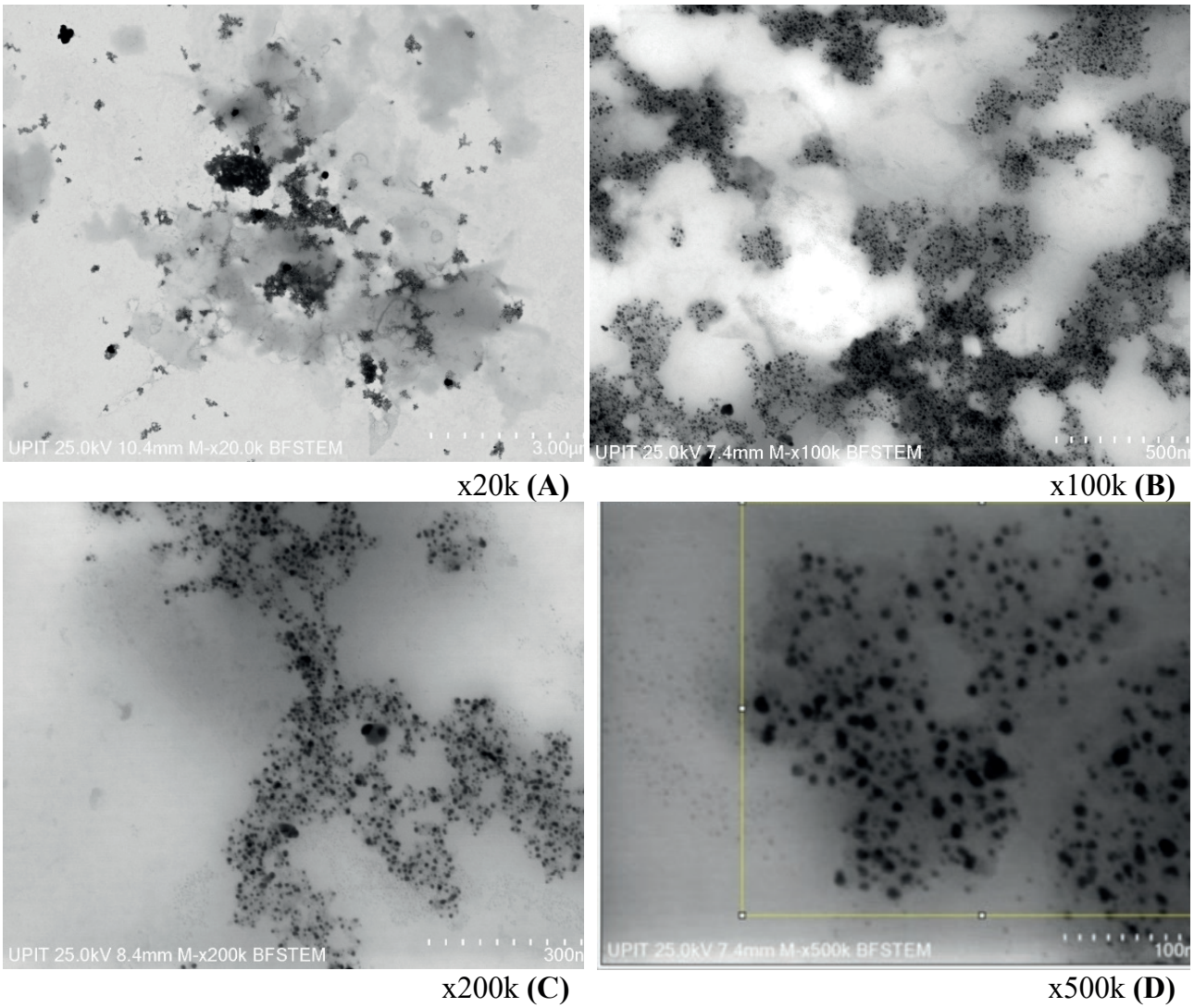

Figure 6. AgNPs dispersion and dimensional analysis on dispersion in BFSTEM.

Evaluation of cell death by Evans blue staining

The permeability of cell membranes in the experimental variants defined by *C. vitalba* aqueous decoction decreased compared to control (Fig. 9). In opposition, incubation of meristematic cells in the CvAg mixture led to an increased uptake of Evans blue, irrespective of treatment duration, suggesting the cytotoxic effect of biosynthesized AgNPs.

Evaluation of viable cells using TTC staining

In Figure 9 is presented the formation of red formazan in meristematic root cells of *A. cepa* and the formazan absorbance. The data suggests that the reduction of TTC by electrons from the mitochondrial electron transport chain (Towill and Mazur 1975) progressively decreased from negative control to aqueous decoction of *C. vitalba*. The absorbance of formazan increased to 0.68 after 12 h from the start of treatment with AgNPs-supplemented extract and remained low after 48 h of incubation.

Assessment of phytotoxicity on T. aestivum

In the Figure 10 is presented the phytotoxicity of *C. vitalba* extract prior to and after AgNPs biosynthesis. The application of *C. vitalba* extract with and without AgNPs

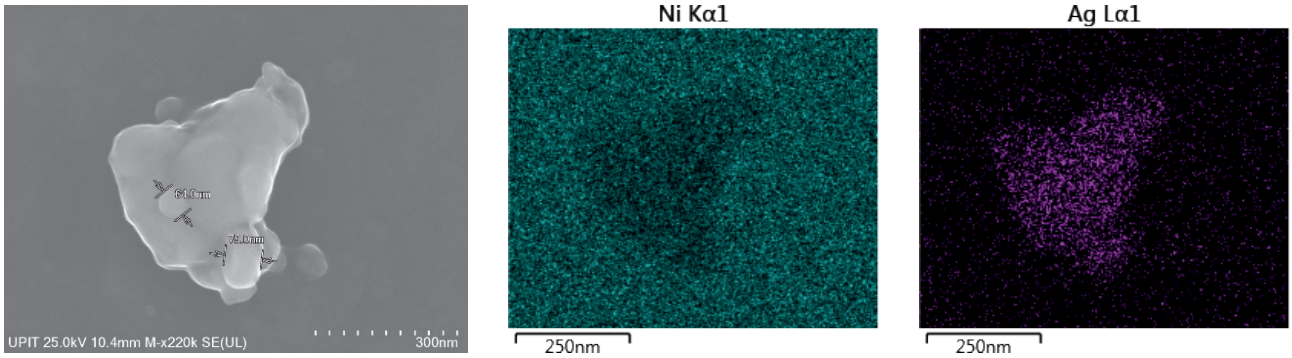

Figure 7. EDS-mapping on the microparticle: Ni grid sample holder (left) and Ag mapping (right).

Table 1. The effects of *C. vitalba* extract and its nanostructured mixture on mitotic index, mitotic cycle and nuclear abnormalities of the *A. cepa* meristematic roots cells (a, b, c, d, e – the interpretation of the significance of the differences by means of the Duncan test, $p < 0.05$).

Experimental variants	MI (%)	Prophase (%)	Metaphase (%)	Anaphase (%)	Telophase (%)	Binucleate cells (%)	Giant cells (%)	Anaphase bridge (%)
C12	8.4±0.7a	35.7±4.4d	27±3.3bc	21.6±3.2a	15.7±0.5abc	0e	0c	15±5.1a
C24	5.5±0.8b	29.2±2.4d	34.6±7ab	18.6±3.4ab	17.7±5.2ab	0.1e	0c	6.7±3.6ab
C48	5.8±1.1b	26.8±5.1d	41.9±1.7a	20±4.6a	11.3±1.4bc	0e	0c	14.8±5.2a
Cv12	2.1±0.1c	62±1.2bc	21.3±1.8c	13.4±1.8abc	3.3±1.6cd	0.2±0.1cd	0c	0b
Cv24	1.7±0.1c	70.9±5.2abc	15.6±1.6c	9.7±1.7bcd	3.8±1.9cd	0.3±0.1bc	0c	0b
Cv48	1.3±0.1c	59.4±6.8c	25.5±4.4bc	8.6±4.8cde	6.5±3.3cd	0.5b	0.1±0.1ab	0b
CvAg12	1.3c	77.8±4.8b	19.6±2.7c	2.6±2.6de	0 d	0.7±0.1a	0.1±0.1ab	0b
CvAg24	1±0.2c	82.2±6.7a	15.2±4.3c	2.6±2.6de	0 d	0.2cd	0.2±0.1a	0b
CvAg48	0.6c	77.8±5.6b	22.2±5.6bc	0e	0 d	0.1±0.1de	0.2±0.1a	0b

on *T. aestivum* seeds had a stimulatory effect on root and stem elongation, and fresh weight compared to control, without significant differences between these variants. The dry biomass of wheat seeds was significantly reduced by AgNPs when compared with negative control.

DISCUSSION

Physicochemical characterization of C. vitalba extract and its nanoformulations

The band at 3347 cm^{-1} revealed by the FTIR analysis corresponded to the -OH groups of phenolic compounds and -NH stretching of the proteins (Borchert et al. 2005; Prakash et al. 2013). The reduced intensity and shifting in IR to 3359 cm^{-1} spectrum of AgNPs indicated the involvement of –OH group in the biosynthesis of AgNPs (Kumar et al. 2016). Similarly, the band at 1636 cm^{-1} revealed for Cv sample was shifted in the FTIR spectrum of the AgNPs, inferring that the –OH group of the phenolic compounds and carboxylate groups of the extract might have bond to silver ions. At the same time, shifting and decreasing bands intensity of peaks 1267 cm^{-1} and at 1046 cm^{-1} found for the sample CvAg are related to the C–O linkages or C=O stretching from phenolic and ceto compounds (Fig. 1).

After 2 hours of incubation in the dark, at room temperature, the reaction mixture changed from greenish-brown to light brown (Fig. 3). The color change of the reaction solution has often been mentioned as a marker of successful AgNPs biosynthesis (Chhatre et al. 2012; Şuţan et al. 2016; Reddy et al. 2021; Lalsangpuii et al. 2022).

The shoulder peak in the range of 320-330 of the UV-Vis spectra of Cv sample (Figure 4), suggests the presence of flavonoids as a major phenolic compound of aqueous decoction of *C. vitalba* (Arabshahi-Delouee and Urooj 2007). These results are in accordance with the method of preparing extracts, knowing that hot water is used for the extraction of phenols and flavonoids (Valencia-Avilés et al. 2018). The maximum absorbance

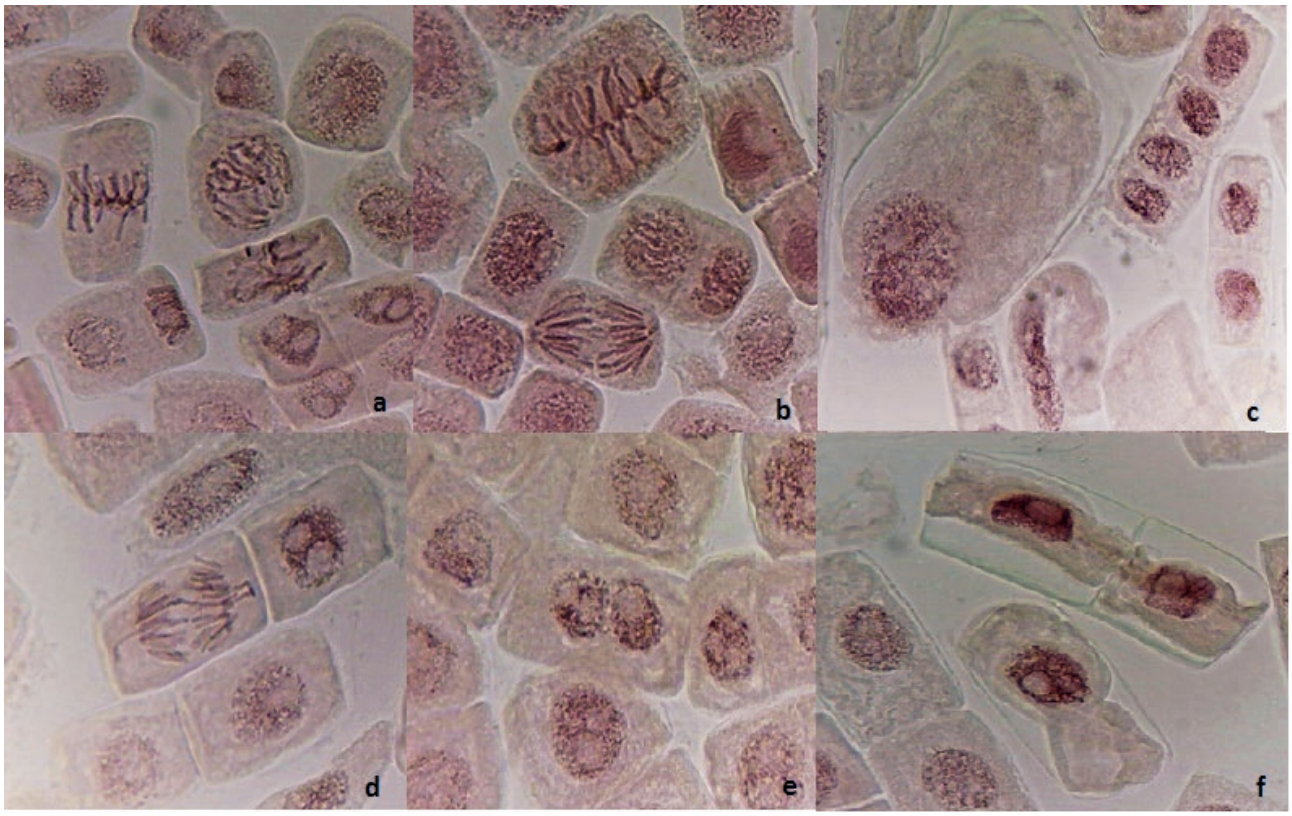

Figure 8. Mitosis, chromosomal aberrations and nuclear abnormalities observed in the root cells of *A. cepa* L. treated with *C. vitalba* L. extracts. (a) - normal prophase, metaphase and telophase (C); (b) – normal metaphase and anaphase (C); (c) - giant cells (CvAg24); (d) – anaphase bridge and laggards (C); (e) – binucleate cell (Cv12); (f) – plasmolysis (Cv48).

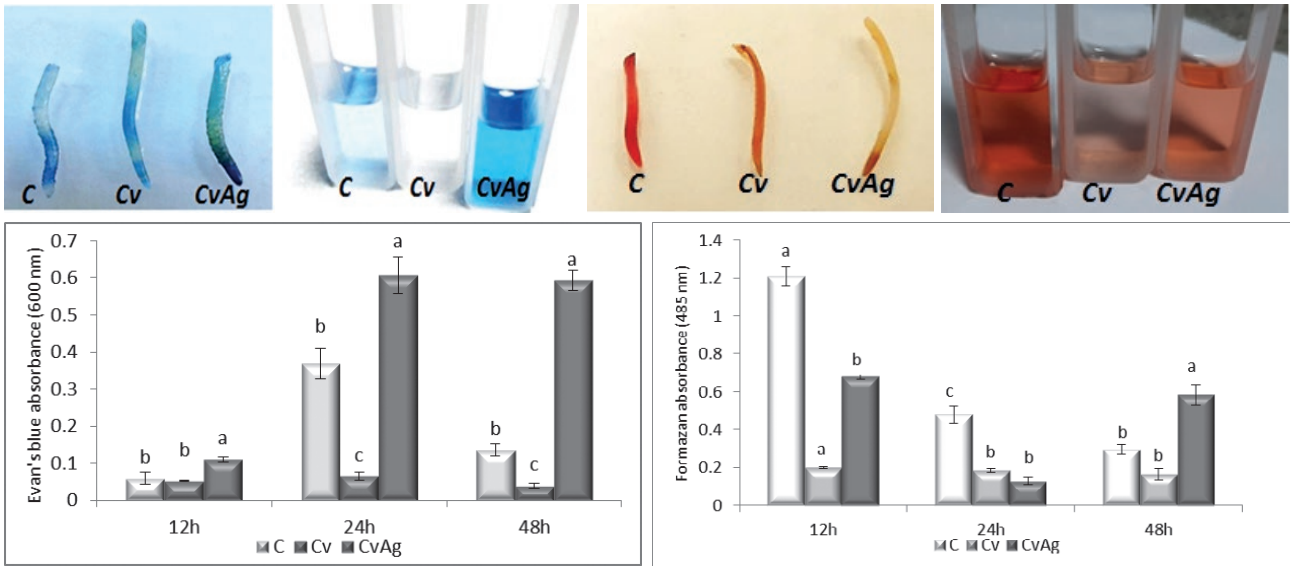

Figure 9. Variation of *A. cepa* meristematic root cell death (left) and root cell viability (right) after treatment with *C. vitalba* aqueous extracts prior to and after AgNPs biosynthesis (a, b, c – the interpretation of the significance of the differences by means of the Duncan test, $p < 0.05$).

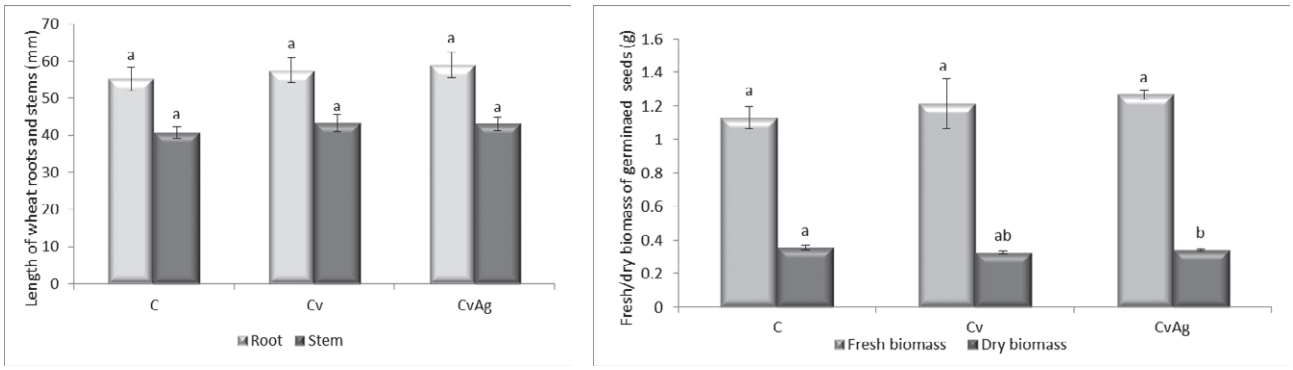

Figure 10. The phytotoxicity of C. *vitalba* extract and its nanostructured mixture on *T. aestivum* seeds: (A) root and stem growth (B) dry and fresh biomass of germinated seeds (a, b, c – the interpretation of the significance of the differences by means of the Duncan test, $p < 0.05$).

at 436 nm characteristic for CvAg sample (Fig. 4B) is an indicator of the presence of AgNPs. The data in the literature suggest that the presence of peaks closer to the wavelength of 400 nm are characteristic of NPs with dimensions of about 10 nm (Martínez-Castañón et al. 2008). Moreover, the position of the peaks specific to AgNPs is also influenced by the shape of the particles, the interaction between them, as well as the density of free electrons and the dispersion medium (Desai et al. 2012; Agnihotri et al. 2014). The data obtained are consistent with the established literature, polyphenols being frequently considered as reducing agents of silver ions (Tyagi et al. 2021).

Some authors appreciate that the absence of ions from $AgNO_3$ initially added to the extract is an indication of their reduction and of the successful AgNPs synthesis (Kambale et al. 2020; Kthiri et al. 2021).

The observed microparticle embedded in a complex biological matrix may be due to the agglomeration of several AgNPs (Taurozzi et al. 2011). The identification of these microparticles suggests the action of secondary metabolites as capping agents for AgNPs (Kambale et al. 2020). A stabilized coating of biosynthesized AgNPs using plant extracts were previously noticed (Jacob et al. 2019). The high free energy from the surface of NPs causes the selective and progressive adsorption of biomolecules on their surface when they come in contact with complex biological liquids (Monopoli et al. 2012). The composition of this biomolecular capping depends on the size, charge, shape of NPs, on the nature of the biological fluids in which NPs are dispersed, hydrophobicity of NPs surface and surface roughness (Piloni et al. 2019; Marichal et al. 2020). Thus, NPs acquire an identity, which must be taken into account in assessing their biological fates and functions (Wypij et al. 2021).

Cytotoxicity, genotoxicity and phytotoxicity of C. vitalba extracts prior to and after AgNPs biosynthesis

The *Allium* test was proposed as a standardized method in environmental monitoring, being a fast, low-cost, sensitive test and having a good correlation with other test systems (Fiskesjö 1985). *A. cepa* is a genetic model frequently used to evaluate the cytogenotoxicity (mitotic index, chromosomal and nuclear abnormalities) and mutagenicity (micronucleus) of chemicals and their mechanism of action on the mitotic apparatus, allowing the detection of clastogenic and/ or aneugenic effects (Wieczerzak et al. 2016; Bonciu et al. 2018).

In our study, the severe inhibition of mitosis can be attributed to the application of the treatment with the whole and undiluted extract of *C. vitalba*, suggesting a high toxicity on onion meristematic cells, even only after 12h. The bioactive compounds of the buttercup family, most of them secondary metabolites, induce cell cycle arrest, apoptosis, and inhibit cell proliferation (Segneanu et al. 2015; Hao et al. 2017). Triterpenoid, saponins, phenolic acids have been mentioned by Łaska et al. (2021) as potent suppressors of HeLa cells growth and proliferation. It has been suggested that active protoanemonin, released by splitting the glycoside ranunculin, can alkylate proteins and DNA (Wink 2010).

Treatment with *C. vitalba* extract and its nanoformulation inhibited mitosis in onion root tips, blocking cells in prophase and significantly reducing the frequency of other phases of mitosis, in a time-dependent manner (Table 1). It is important to note that after 48 hours of incubation in CvAg48, the frequency of anaphase and telophase was zero. These results may be attributed either to suppressing DNA synthesis preventing the cells entering mitosis or to alteration of prophase and prometaphase stages (El-Ghamery et al. 2000). These results confirm the severe cytotoxic effects of the tested extracts and nanoformulations on meristemtic

root cells of *A. cepa*. Recent studies showed the specificity of AgNPs towards ds DNA, to which it binds and determines its destabilization (Pramanik et al. 2016).

Giant cells may be polyploid formed by endomitosis or endoreduplication (Bonciu et al. 2018) or may suggest altered signals for cell growth (Hammann et al. 2020). The cause of binucleate cell formation may be due to inhibition of cytokinesis after telophase (Nefic et al. 2013) or cell plate formation (De Keijzer et al. 2014). However, both types of mitotic abnormalities suggest a disruption of the functioning of the microtubules that make up the mitotic spindle and cell plate, on the basis of which *C. vitalba* decoct can be classified as aneugenic agent.

It has been proved that during plasmolytic process, cortical microtubules and actin microfilaments are subjected to architectural changes depending on the severity of water flow (Lang et al. 2014). Microtubules and actin filaments play important roles in establishing the division plan by forming the preprophase band and by forming the phragmoplast that directs the vesicles to form a new cell wall (Rasmussen et al. 2013). Other studies revealed that some substances allow cell plate initiation, but is ultimately disintegrated and the phragmoplast microtubules break down (Valster and Hepler 1997). Disrupting the organization of these structures may be the cause of nuclear aberrations and mitotic inhibition.

Evans blue staining was applied to assess cell membrane integrity. Damaged cell membranes are unable to exclude dye and cells are stained blue. Based on the direct correlation between extracted Evans blue optical density and cell membrane damage, Evans blue staining is a method used to evaluate the cytotoxicity of external stimuli (Roy et al. 2019).

Geisler-Lee et al. (2013, 2014) found that AgNPs were progressively accumulated in root cells. Following this bioaccumulation, sever cytotoxicity may be due to AgNPs coating developed during the bottom-up approach of their biosynthesis. It has been suggested that coating of AgNPs affects cellular responses and alters cell fate (Riaz Ahmed et al. 2017). Cytotoxicity caused by biosynthesized AgNPs in broth of *Pandanus odorifer* (Forssk.) Kuntze (Panda et al. 2011) or by citrate-stabilized AgNPs were previously mentioned (Gorczyca et al. 2022).

In contrast to the Evans test, TTC is used to assess cell viability. TTC is reduced by the mitochondrial dehydrogenase (active only in the living cells) to red formazan. Therefore, formazan stains only the viable cells and the optical density of the extracted formazan decrease in damaged cells (Roy et al. 2019).

The amount of formazan produced directly relates to mitochondrial electron activity, and is proportional to the amount of oxidative damage. In our study, the results suggest high enzymatic activity following stress (Towill and Mazur 1975) imposed by AgNPs and reduced oxidative damage of respiratory processes, perhaps due to adaptive tolerance capacity (De Ronde and van der Mescht 1997). Furthermore, a non-enzymatic reduction of TTC may have been generated under the conditions of incubating onion roots in CvAg, such as incubation time, temperature and pH (Burdock et al. 2011).

Nanoparticle-induced phytotoxicity can be assessed by morphophysiological (germination rate, root/stem growth potential, biomass, transpiration rate, clorophyll content, water absorbtion capacity, etc.), cellular or molecular changes (Yan and Chen 2019; Heikal and Şuţan 2021).

In our study, improving the growth of roots and stems, but also fresh biomass compared with control may be due to the process of overcompensation hormesis, which is an adaptive response to disruption of homeostasis induced by low levels of stress (Calabrese and Baldwin 2002). Testing the phytotoxicity of different concentrations of uncoated AgNPs with an average size of 13.8 ± 2.5 nm on vegetative growth stages of *T. aestivum*, Cui et al. (2014) reported similar results. The mode of interaction and cytogenotoxic effects of NPs depend on many factors, such as the path of synthesis, concentration, exposure time, species, growth stage, etc. (Cui et al. 2014; Heikal and Şuţan 2021). The particularities of biosynthesized metallic nanoparticles can significantly influence their biological effects. Their cytogenotoxic action depends on numerous factors, such as dosage and exposure duration but also on their chemical composition, surface properties, size and shape. The biosynthesized AgNPs triggered various toxic effects (inhibition of mitosis, disruption of cellular metabolism, impairment of root and stem growth and biomass) that could be attributed to numerous factors, such as dosage and exposure duration but also on their chemical composition, surface properties, size and shape (Heikal and Şuţan, 2021). Furthermore, the presence of a surface coating based on the premise that biosynthesized NPs in *C. vitalba* extracts presents various capping biomolecules that influence their morphology, size and stability, which leads to the diversification of bionano interactions. Thus, further studies comparing the phytotoxicity of NPs with and without surface coating, as well as identification the secondary metabolites bound on their surface and the way of modulating their own bioactivity, should be performed.

CONCLUSIONS

The bottom-up approach of AgNPs biosynthesis was successfully performed using *C. vitalba* aqueous decoc-

tion, which proved to be rich in polyphenols. Phytosyntesized AgNPs had approximately spherical shape, sizes ranging from 1-15 nm. The formation of a biomolecular capping induced changes in the size of the green synthesized AgNPs. Severe mitoinhibitory effects of *C. vitalba* extracts were amplified after phytosynthesis of AgNPs. The biosynthesized AgNPs manifested cytogenotoxicity and phytotoxicity by mitosis suppression, disruption of cellular metabolism, impairment of root and stem growth and biomass. Further studies are required to determine the mechanism of coated and uncoated AgNPs and the effects of coat-type of biosynthesized metallic nanoparticles.

FUNDING

This work was supported by a grant of the Romanian Ministry of Research, Innovation and Digitization, CNCS–UEFISCDI, project number PN-III-P4-ID-PCE-2020-0620, within PNCDI III.

REFERENCES

Agnihotri S, Mukherji S, Mukherji S. 2014. Size-controlled silver nanoparticles synthesized over the range 5–100 nm using the same protocol and their antibacterial efficacy. RSC Adv. 4:3974–3983. doi: 10.1039/C3RA44507K.

Ancuceanu R, Căplănuşi R, Anghel IA, Stoicescu CS, Hovaneţ MV, Dinu M. 2018. Assessment of *Anemone nemorosa* L. toxicity. Acta Med Marisiensis, 64 Supplement 3:7-7.1/2.

Arabshahi-Delouee S, Urooj A. 2007. Application of phenolic extracts from selected plants in fruit juice. Int J Food Prop. 10:479-488. doi: 10.1080/10942910600891279.

Azooz MM, Abou-Elhamd MF, Al-Fredan MA. 2012. Biphasic effect of copper on growth, proline, lipid peroxidation and antioxidant enzyme activities of wheat (*Triticum aestivum* cv. Hasaawi) at early growing stage. Aust J Crop Sci. 6:688–694.

Bonciu E, Firbas P, Fontanetti CS, Wusheng J, Karaismailoğlu MC, Liu D, Menicucci F, Pesnya DS, Popescu A, Romanovsky AV, et al. 2018. An evaluation for the standardization of the *Allium cepa* test as cytotoxicity and genotoxicity assay. Caryologia 71(3):191–209. doi: 10.4236/ajps.2020.111002.

Borchert H, Shevchenko EV, Robert A, Mekis I, Kornowski A, Grubel G, Weller H, 2005. Determination of Nanocrystal Sizes: A Comparison of TEM, SAXS, and XRD Studies of Highly Monodisperse $CoPt_3$ Particles. Langmuir, 21(5):1931–1936. doi: 10.1021/la0477183.

Bungard R. 1996. Ecological and physiological studies of *Clematis vitaba* L. Doctoral (PhD) Theses Lincoln University. https://core.ac.uk/download/pdf/35461632.pdf.

Calabrese EJ, Baldwin LA. 2002. Defining hormesis. Hum Exp Toxicol. 21:91–97. doi: 1191/0960327102ht217oa.

Chhatre A, Solasa P, Sakle S, Thaokar R, Mehra A. 2012. Color and surface plasmon effects in nanoparticle systems: Case of silver nanoparticles prepared by microemulsion route. Colloids Surf. A Physicochem Eng Asp. 404:83-92. doi: 10.1016/j.colsurfa.2012.04.016.

Cui D, Zhang P, Ma Y, He X, Li Y, Zhao Y, Zhang Z. 2014. Phytotoxicity of silver nanoparticles to cucumber (*Cucumis sativus*) and wheat (*Triticum aestivum*). J Zhejiang Univ Sci A 15:662–670. doi: 10.1631/jzus.A1400114.

Da-Cheng H. 2019. Mining chemodiversity from biodiversity: Pharmacophylogeny of Ranunculaceae medicinal plants, In: Da-Cheng H, editor. Ranunculales medicinal plants. Academic Press, p. 35-71.

De Keijzer J, Mulder BM, Janson ME. 2014. Microtubule networks for plant cell division. Syst Synth Biol. 8:187–194. doi: 10.1007/s11693-014-9142-x.

De Ronde JA, van der Mescht A.1997. 2,3,5-triphenyltetrazolium chloride reduction as a measure of drought tolerance and heat tolerance in cotton. S Afr J Sci. 93:431–439.

Desai R, Mankad V, Gupta SK, Jha P. 2012. Size distribution of silver nanoparticles: UV-visible spectroscopic assessment. Nanosci Nanotechnol Lett. 4:30–34. doi: 10.1166/nnl.2012.1278.

Duke JA. 1985. CRC Handbook of medicinal herbs, CRC Press, Boca Raton, Florida.

El-Ghamery AA, Al-Nahas AI, Mansour MM. 2000. The action of atrazine herbicide as an inhibitor of cell division on chromosomes and nucleic acids content in root meristems of *Allium cepa* and *Vicia faba*. Cytologia 65:277-287. doi: 10.1508/cytologia.65.277.

Eswaran A, Muthukrishnan S, Mathaiyan M, Pradeepkumar S, Rani MK, Manogaran P. 2021. Green synthesis, characterization and hepatoprotective activity of silver nanoparticles synthesized from pre-formulated Liv-Pro-08 poly-herbal formulation. Appl Nanosci. doi: 10.1007/s13204-021-01945-x.

Filippin L, Jović J, Cvrković T, Forte V, Clair D, Toševski I, Boudon-Padieu E, Borgo M., Angelini E. 2009. Molecular characteristics of phytoplasmas associated with flavescence dorée in clematis and grape-

vine and preliminary results on the role of *Dictyophara europaea* as a vector. Plant Pathol. 58:826-837. doi:10.1111/j.1365-3059.2009.02092.x.

Fiskesjö G. 1985. The *Allium* test as a standard in environmental monitoring. Hereditas 102:99-112. doi: 10.1111/j.1601-5223.1985.tb00471.x.

Geisler-Lee J, Brooks M, Gerfen JR, Wang Q, Fotis C, Sparer A, Ma X, Berg RH, Geisler M. 2014. Reproductive toxicity and life history study of silver nanoparticle effect, uptake and transport in *Arabidopsis thaliana*. Nanomaterials (Basel) 4:301-318. doi: 10.3390/nano4020301.

Geisler-Lee J, Wang Q, Yao Y, Zhang W, Geisler M, Li K, Huang Y, Chen Y, Kolmakov A, Ma X. 2013. Phytotoxicity, accumulation and transport of silver nanoparticles by *Arabidopsis thaliana*. Nanotoxicology 7:323-37. doi: 10.3390/nano4020301.

Gorczyca A, Pociecha E, Maciejewska-Prończuk J, Kula-Maximenko M, Oćwieja M. 2022. Phytotoxicity of silver nanoparticles and silver ions toward common wheat. Surf Innov. 10(1):48-58. doi: 10.1680/jsuin.20.00094.

Günthardt BF, Hollender J, Hungerbühler K, Scheringer M, Bucheli TD. 2018. Comprehensive toxic plants–phytotoxins database and its application in assessing aquatic micropollution potential. J Agric Food Chem. 66:7577–7588. doi: 10.1021/acs.jafc.8b01639.

Halder NC, Wagner CNJ. 1966. Separation of particle size and lattice strain in integral breadth measurements Acta. Cryst. 20: 312-313. doi: 10.1107/S0365110X66000628.

Hammann A, Ybanez LM, Isla MI. 2020. Potential agricultural use of a sub-product (olive cake) from olive oil industries composting with soil. J Pharm Pharmacogn Res. 8:43-52. doi: 10.56499/jppres19.632_8.1.43.

Hao DC, He CN, Shen J, Xiao PG. 2017. Anticancer chemodiversity of ranunculaceae medicinal plants: Molecular mechanisms and functions. Curr Genomics 18:39–59. doi: 10.2174/1389202917666160803151752.

Hassan SWM, El-latif HHA. 2018. Characterization and applications of the biosynthesized silver nanoparticles by marine *Pseudomonas* sp. H64. J Pure Appl Microbiol. 12:1289-1299. doi: 10.22207/JPAM.12.3.31.

He J, Lyu RD, Yao M, Xie L, Yang ZZ. 2019. *Clematis mae* (Ranunculaceae), a new species of C. sect. Meclatis from Xinjiang, China. PhytoKeys 117:133-142. doi: 10.3897/phytokeys.114.31854.

Heikal Y, Şuţan NA. 2021. Mechanisms of genotoxicity and oxidative stress induced by engineered nanoparticles in plants. In: Khan Z, Ansari MY, Shahwar D (eds) Induced genotoxicity and oxidative stress in plants, Springer, Singapore, p. 151-197.

Hill RL, Wittenburg R, Gourlay AH. 2001. Biology and host range of *Phytomyza vitalbae* and its establishment for the biological control of *Clematis vitalba* in New Zealand. Biocontrol Sci Technol. 11:459–473. doi: 10.1080/09583150120067490.

IBM Corp. Released 2011. IBM SPSS Statistics for Windows, Version 20.0. Armonk, NY: IBM Corp.

Jacob JM, John MS, Jacob A, Abitha P, Kumar SS, Rajan R, Natarajan S, Pugazhendhi A. 2019. Bactericidal coating of paper towels via sustainable biosynthesis of silver nanoparticles using *Ocimum sanctum* leaf extract. Mater Res Express. 6:045401. doi: 10.1088/2053-1591/aafaed.

Kambale EK, Nkanga CI, Mutonkole BPI, Bapolisi AM, Tassa DO, Liesse JM, Krause AWM, Memvanga PB. 2020. Green synthesis of antimicrobial silver nanoparticles using aqueous leaf extracts from three Congolese plant species (*Brillantaisia patula*, *Crossopteryx febrifuga* and *Senna siamea)*. Heliyon 6.e04493. doi: 10.1016/j.heliyon.2020.e04493.

Kaur I, Ellis LJ, Romer I, Tantra R, Carriere M, Allard S, Mayne-L'Hermite M, Minelli C, Unger W, Potthoff A, et al. 2017. Dispersion of nanomaterials in aqueous media: Towards protocol optimization. J Vis Exp. 130:e56074. doi: 10.3791/56074.

Kim KW, Lee DG. 2007. Screening of herbicidal and fungicidal activities from resource plants in Korea. Korean J Weed Sci. 27(3):285-295.

Kthiri A, Hamimed S, Othmani A. 2021. Novel static magnetic field effects on green chemistry biosynthesis of silver nanoparticles in *Saccharomyces cerevisiae*. Sci Rep. 11:20078. doi: 10.1038/s41598-021-99487-3.

Kumar V, Singh DK, Mohan S, Hasan SH. 2016. Photo-induced biosynthesis of silver nanoparticles using aqueous extract of *Erigeron bonariensis* and its catalytic activity against acridine orange. J Photochem Photobiol B: Biol. 155:39-50. doi: 10.1016/j.jphotobiol.2015.12.011.

Lalsangpuii F, Rokhum SL, Nghakliana F, Fakawmi L, Ruatpuia JVL, Laltlanmawii E, Lalfakzuala R, Siama Z. 2022. Green Synthesis of Silver Nanoparticles Using *Spilanthes acmella* Leaf Extract and its Antioxidant-Mediated Ameliorative Activity against Doxorubicin-Induced Toxicity in Dalton's Lymphoma Ascites (DLA)-Bearing Mice. ACS Omega.7(48):44346-44359. doi: 10.1021/acsomega.2c05970.

Lang I, Sassmann S, Schmidt B, Komis G. 2014. Plasmolysis: Loss of turgor and beyond. Plants 3:583-59. doi: 10.3390/plants3040583.

Łaska G, Maciejewska-Turska M, Sieniawska E, Świątek Ł, Pasco DS, Balachandran P., 2021. Extracts from

Pulsatilla patens target cancer-related signaling pathways in HeLa cells. Sci Rep. 11(1):10654. doi: 10.1038/s41598-021-90136-3.

Lewis SN, Balick MJ. 2020. Handbook of poisonous and injurious plants. New York Botanical Garden, Spinger, New York, U.S.A

Marichal L, Klein G, Armengaud J. 2020. Protein corona composition of silica nanoparticles in complex media: Nanoparticle size does not matter. Nanomaterials 10:240. doi: 10.3390/nano10020240.

Martínez-Castañón GA, Niño-Martínez N, Martínez-Gutierrez F. 2008. Synthesis and antibacterial activity of silver nanoparticles with different sizes. J Nanopart Res. 10:1343–1348. doi: 10.1007/s11051-008-9428-6.

Monopoli MP, Aberg C, Salvati A, Dawson KA. 2012. Biomolecular coronas provide the biological identity of nanosized materials. Nat Nanotechnol. 7:779-786. doi: 10.1038/nnano.2012.207.

Muala WCB, Desobgp ZSC, Jong NE. 2021. Optimization of extraction conditions of phenolic compounds from *Cymbopogon citratus* and evaluation of phenolics and aroma profiles of extract. Heliyon 7:e06744. doi: 10.1016/j.heliyon.2021.e06744.

Naz I, Ramchandani S, Khan MR, Yang MH, Ahn KS. 2020. Anticancer potential of raddeanin A, a natural triterpenoid isolated from *Anemone raddeana* Regel. Molecules 25:1035. doi: 10.3390/molecules25051035.

Nefic H, Musanovic J, Metovic A, Kurteshi K. 2013. Chromosomal and nuclear alterations in root tip cells of *Allium cepa* L. induced by alprazolam. Med Arch 67(6):388–392. doi: 10.5455/medarh.2013.67.388-392.

O'Halloran W. 2019. Management of *Clematis vitalba* at 'Suez Pond'. Assessment of monitoring and control using manual methods. Wild Eork, SECAD. https://www.wildwork.ie/wp-content/uploads/2022/01/Management-of-Clematis-vitalba-at-Suez-Pond.pdf. Accessed 3.10. 2023.

Ogle CC, Cock GD, Arnold G, Mickleson N. 2000. Impact of an exotic vine *Clematis vitalba* (F. Ranunculaceae) and of control measures on plant biodiversity in indigenous forest, Taihape, New Zealand. Austral Ecol. 25:539-551. doi: 10.1046/j.1442-9993.2000.01076.x.

Panda KK, Achary VMM, Krishnaveni R, Padhi BK, Sarangi SN, Sahu SN, Panda BB. 2011. *In vitro* biosynthesis and genotoxicity bioassay of silver nanoparticles using plants. Toxicol *In Vitro* 25:1097–1105. doi: 10.1016/j.tiv.2011.03.008.

Piloni A, Wong CK, Chen F, Lord M, Walther A, Stenzel MH. 2019. Surface roughness influences the protein corona formation of glycosylated nanoparticles and alter their cellular uptake. Nanoscale 11:23259–23267. doi: 10.1039/C9NR06835J.

Prajitha V, Thoppil JE. 2017. Cytotoxic and apoptotic activities of extract of *Amaranthus spinosus* L. in *Allium cepa* and human erythrocytes. Cytotechnology 69:123-133. doi: 10.1007/s10616-016-0044-5.

Prakash P, Gnanaprakasam P, Emmanuel R, Arokiyaraj S, Saravanan M. 2013. Green synthesis of silver nanoparticles from leaf extract of *Mimusops elengi* Linn. for enhanced antibacterial activity against multi drug resistant clinical isolates. Colloids Surf B 108:255–259. doi: 10.1016/j.colsurfb.2013.03.017.

Pramanik S, Chatterjee S, Saha A, Devi PS, Kumar GS, 2016. Unraveling the Interaction of Silver Nanoparticles with Mammalian and Bacterial DNA. J Phys Chem B 120(24):5313–5324. doi: 10.1021/acs.jpcb.6b01586.

Rasband WS. 1997-2018. ImageJ, U.S. National Institutes of Health, Bethesda, Maryland, USA, https://imagej.nih.gov/ij/.

Rasmussen CG, Wright AJ, Müller S. 2013. The role of the cytoskeleton and associated proteins in determination of the plant cell division plane. Plant J. 75:258-269. doi: 10.1111/tpj.12177.

Reddy NV, Li H, Hou T. 2021. Phytosynthesis of silver nanoparticles using *Perilla frutescens* leaf extract: Characterization and evaluation of antibacterial, antioxidant, and anticancer activities. Int J Nanomed. 16:15-29. doi: 10.2147/IJN.S265003.

Redmond CM, Stout JC. 2018. Breeding system and pollination ecology of a potentially invasive alien *Clematis vitalba* L. in Ireland. J Plant Ecol. 11:56-63. doi: 10.1093/jpe/rtw137.

Riaz Ahmed KB, Nagy AM, Brown RP, Zhang Q, Malghan SG, Goering PL. 2017. Silver nanoparticles: Significance of physicochemical properties and assay interference on the interpretation of *in vitro* cytotoxicity studies. Toxicol *In Vitro* 38:179–192. doi: 10.1016/j.tiv.2016.10.012.

Roy B, Krishnan SP, Chandrasekaran N, Mukherjee A. 2019. Toxic effects of engineered nanoparticles (metal/metal oxides) on plants using *Allium cepa* as a model system. Compr Anal Chem. 84:125-143. doi: 10.1016/bs.coac.2019.04.009.

Roy P, Das B, Mohanty A, Mohapatra S. 2017. Green synthesis of silver nanoparticles using *Azadirachta indica* leaf extract and its antimicrobial study. Appl Nanosci. 7:843–850. doi: 1007/s13204-017-0621-8.

RuttkayNedecky B, Krystofova O, Nejdl L, Adam V. 2017. Nanoparticles based on essential metals and their phytotoxicity. J Nanobiotechnol. 15:33. doi: 10.1186/s12951-017-0268-3.

Segneanu A-E, Grozescu I, Cziple F, Berki D, Damian D, Niculite CM, Florea A, Leabu M. 2015. *Helleborus purpurascens* - Amino acid and peptide analysis linked to the chemical and antiproliferative properties of the extracted compounds. Molecules 20:22170–2218. doi: 10.3390/molecules201219819.

Shende S, Rajput VD, Gade A, Minkina T, Fedorov Y, Sushkova S, Mandzhieva S, Burachevskaya M, Boldyreva V. 2022. Metal-Based Green Synthesized Nanoparticles: Boon for Sustainable Agriculture and Food Security. IEEE T Nanobiosci., 21(1):44-54. doi: 10.1109/TNB.2021.3089773.

Sutan AN, Vilcoci DS, Fierascu I, Neblea AM, Sutan C, Ducu C, Soare LC, Negrea D, Avramescu SM, Fierascu RC. 2019. Influence of the phytosynthesis of noble metal nanoparticles on the cytotoxic and genotoxic effects of *Aconitum toxicum* Reichenb. leaves alcoholic extract. J Clust Sci. 30:647-660. doi: 10.1007/s10876-019-01524-9.

Şuţan NA, Matei AN, Oprea E, Tecuceanu V, Tătaru LD, Moga SG, Manolescu DS, Topală CM. 2020. Chemical composition, antioxidant and cytogenotoxic effects of *Ligularia sibirica* (L.) Cass. roots and rhizomes extracts. Caryologia 73:83-92. doi: 10.13128/caryologia-116.

Şuţan NA, Fierăscu I, Fierăscu RC, Manolescu DS, Soare CL. 2016. Comparative analytical characterization and *in vitro* cytogenotoxic activity evaluation of *Asplenium scolopendrium* L. leaves and rhizome extracts prior to and after Ag nanoparticles phytosynthesis. Ind Crops Prod. 83:379-386. doi: 10.1016/j.indcrop.2016.01.011.

Şuţan NA, Fierascu I, Şuţan C, Soare LC, Neblea AM, Somoghi R., Fierăscu RC. 2021. *In vitro* mitodepressive activity of phytofabricated silver oxide nanoparticles (Ag_2O-NPs) by leaves extract of *Helleborus odorus* Waldst. & Kit. ex Willd. Mater Lett. 286:129194. doi: 10.1016/j.matlet.2020.129194.

Taurozzi JS, Hackley VA, Wiesner MR. 2011. Ultrasonic dispersion of nanoparticles for environmental, health and safety assessment--issues and recommendations. Nanotoxicology 5:711-729. doi: 10.3109/17435390.2010.528846.

Towill LE, Mazur P. 1975. Studies on reduction of 2,3,5-triphenyltetrazolium chloride as a viability assay for plant tissue cultures. Can J Bot Revue Can Bot. 53:1097–1102.

Tyagi PK, Tyagi S, Gola D, Arya A, Ayatollahi A, Alshehri MM, Sharifi-Rad J. 2021. Ascorbic acid and polyphenols mediated green synthesis of silver nanoparticles from *Tagetes erecta* L. aqueous leaf extract and studied their antioxidant properties. J Nanomater. 6515419. doi: 10.1155/2021/6515419.

Valencia-Avilés E, García-Pérez ME, Garnica-Romo MG, Figueroa-Cárdenas JDD, Meléndez-Herrera E, Salgado-Garciglia R, Martínez-Flores HE. 2018. Antioxidant properties of polyphenolic extracts from *Quercus laurina*, *Quercus crassifolia*, and *Quercus scytophylla* Bark. Antioxidants 7:81. doi:10.3390/antiox7070081.

Valster AH, Hepler PK. 1997. Caffeine inhibition of cytokinesis: effect on the phragmoplast cytoskeleton in living *Tradescantia* stamen hair cells. Protoplasma 196:155–166. doi: 10.1007/BF01279564 .

Vijayaraghavareddy P, Adhinarayanreddy V, Vemanna RS, Sreeman S, Makarla U. 2017. Quantification of membrane damage/cell death using Evan's blue staining technique. Bio Protoc. 7:1-8. doi: 10.21769/BioProtoc.2519.

Weng-Tsai W. 2003. A revision of *Clematis* sect. *Clematis* (Ranunculaceae). J Syst Evol 41:1-62

Wieczerzak M, Namieśnik J, Kudłak B (2016) Bioassays as one of the green chemistry tools for assessing environmental quality: A review. Environ Int. 94:341-361. doi: 10.1016/j.envint.2016.05.017.

Wink M. 2010. Mode of action and toxicology of plant toxins and poisonous plants. Julius Kühn Archiv. 93-112.

Woudenberg JH, Aveskamp MM, de Gruyter J, Spiers AG, Crous PW. 2009. Multiple Didymella teleomorphs are linked to the *Phoma clematidina* morphotype. Persoonia 22:56–62. doi: 10.3767/003158509X427808.

Wypij M, Jędrzejewski T, Trzcińska-Wencel J, Ostrowski M, Rai M, Golińska P. 2021. Green synthesized silver nanoparticles: Antibacterial and anticancer activities, biocompatibility, and analyses of surface-attached proteins. Front Microbiol. 12:632505. doi: 10.3389/fmicb.2021.632505.

Yan A, Chen Z. 2019. Impacts of silver nanoparticles on plants: A focus on the phytotoxicity and underlying mechanism. Int J Mol Sci. 20:1003. doi: 10.3390/ijms20051003.

Finito di stampare da
Logo s.r.l. – Borgoricco (PD) – Italia

OPEN ACCESS POLICY

Caryologia provides immediate open access to its content. Our publisher, Firenze University Press at the University of Florence, complies with the Budapest Open Access Initiative definition of Open Access: By "open access" , we mean the free availability on the public internet, the permission for all users to read, download, copy, distribute, print, search, or link to the full text of the articles, crawl them for indexing, pass them as data to software, or use them for any other lawful purpose, without financial, legal, or technical barriers other than those inseparable from gaining access to the internet itself. The only constraint on reproduction and distribution, and the only role for copyright in this domain is to guarantee the original authors with control over the integrity of their work and the right to be properly acknowledged and cited. We support a greater global exchange of knowledge by making the research published in our journal open to the public and reusable under the terms of a Creative Commons Attribution 4.0 International Public License (CC-BY-4.0). Furthermore, we encourage authors to post their pre-publication manuscript in institutional repositories or on their websites prior to and during the submission process and to post the Publisher's final formatted PDF version after publication without embargo. These practices benefit authors with productive exchanges as well as earlier and greater citation of published work.

PUBLICATION FREQUENCY

Papers will be published online as soon as they are accepted, and tagged with a DOI code. The final full bibliographic record for each article (initial-final page) will be released with the hard copies of *Caryologia*. Manuscripts are accepted at any time through the online submission system.

COPYRIGHT NOTICE

Authors who publish with *Caryologia* agree to the following terms:

- Authors retain the copyright and grant the journal right of first publication with the work simultaneously licensed under a Creative Commons Attribution 4.0 International Public License (CC-BY-4.0) that allows others to share the work with an acknowledgment of the work's authorship and initial publication in Caryologia.
- Authors are able to enter into separate, additional contractual arrangements for the non-exclusive distribution of the journal's published version of the work (e.g., post it to an institutional repository or publish it in a book), with an acknowledgment of its initial publication in this journal.
- Authors are permitted and encouraged to post their work online (e.g., in institutional repositories or on their website) prior to and during the submission process, as it can lead to productive exchanges, as well as earlier and greater citation of published work (See The Effect of Open Access).

PUBLICATION FEES

Open access publishing is not without costs. *Caryologia* therefore levies an article-processing charge of € 150.00 for each article accepted for publication, plus VAT or local taxes where applicable.

We routinely waive charges for authors from low-income countries. For other countries, article-processing charge waivers or discounts are granted on a case-by-case basis to authors with insufficient funds. Authors can request a waiver or discount during the submission process.

PUBLICATION ETHICS

Responsibilities of *Caryologia*'s editors, reviewers, and authors concerning publication ethics and publication malpractice are described in *Caryologia*'s Guidelines on Publication Ethics.

CORRECTIONS AND RETRACTIONS

In accordance with the generally accepted standards of scholarly publishing, *Caryologia* does not alter articles after publication: "Articles that have been published should remain extant, exact and unaltered to the maximum extent possible".

In cases of serious errors or (suspected) misconduct *Caryologia* publishes corrections and retractions (expressions of concern).

Corrections

In cases of serious errors that affect or significantly impair the reader's understanding or evaluation of the article, *Caryologia* publishes a correction note that is linked to the published article. The published article will be left unchanged.

Retractions

In accordance with the "Retraction Guidelines" by the Committee on Publication Ethics (COPE) *Caryologia* will retract a published article if:

- there is clear evidence that the findings are unreliable, either as a result of misconduct (e.g. data fabrication) or honest error (e.g. miscalculation)
- the findings have previously been published elsewhere without proper crossreferencing, permission or justification (i.e. cases of redundant publication)
- it turns out to be an act of plagiarism
- it reports unethical research.

An article is retracted by publishing a retraction notice that is linked to or replaces the retracted article. *Caryologia* will make any effort to clearly identify a retracted article as such.

If an investigation is underway that might result in the retraction of an article *Caryologia* may choose to alert readers by publishing an expression of concern.

COMPLYNG WITH ETHICS OF EXPERIMENTATION

Please ensure that all research reported in submitted papers has been conducted in an ethical and responsible manner, and is in full compliance with all relevant codes of experimentation and legislation. All papers which report in vivo experiments or clinical trials on humans or animals must include a written statement in the Methods section. This should explain that all work was conducted with the formal approval of the local human subject or animal care committees (institutional and national), and that clinical trials have been registered as legislation requires. Authors who do not have formal ethics review committees should include a statement that their study follows the principles of the Declaration of Helsinki

ARCHIVING

Caryologia and Firenze University Press are experimenting a National legal deposition and long-term digital preservation service.

ARTICLE PROCESSING CHARGES

All articles published in *Caryologia* are open access and freely available online, immediately upon publication. This is made possible by an article-processing charge (APC) that covers the range of publishing services we provide. This includes provision of online tools for editors and authors, article production and hosting, liaison with abstracting and indexing services, and customer services. The APC, payable when your manuscript is editorially accepted and before publication, is charged to either you, or your funder, institution or employer.

Open access publishing is not without costs. *Caryologia* therefore levies an article-processing charge of € 150.00 for each article accepted for publication, plus VAT or local taxes where applicable.

FREQUENTLY-ASKED QUESTIONS (FAQ)

Who is responsible for making or arranging the payment?

As the corresponding author of the manuscript you are responsible for making or arranging the payment (for instance, via your institution) upon editorial acceptance of the manuscript.

At which stage is the amount I will need to pay fixed?

The APC payable for an article is agreed as part of the manuscript submission process. The agreed charge will not change, regardless of any change to the journal's APC.

When and how do I pay?

Upon editorial acceptance of an article, the corresponding author (you) will be notified that payment is due.

We advise prompt payment as we are unable to publish accepted articles until payment has been received. Payment can be made by Invoice. Payment is due within 30 days of the manuscript receiving editorial acceptance. Receipts are available on request.

No taxes are included in this charge. If you are resident in any European Union country you have to add Value-Added Tax (VAT) at the rate applicable in the respective country. Institutions that are not based in the EU and are paying your fee on your behalf can have the VAT charge recorded under the EU reverse charge method, this means VAT does not need to be added to the invoice. Such institutions are required to supply us with their VAT registration number. If you are resident in Japan you have to add Japanese Consumption Tax (JCT) at the rate set by the Japanese government.

Can charges be waived if I lack funds?

We consider individual waiver requests for articles in Caryologia on a case-by-case basis and they may be granted in cases of lack of funds. To apply for a waiver please request one during the submission process. A decision on the waiver will normally be made within two working days. Requests made during the review process or after acceptance will not be considered.

I am from a low-income country, do I have to pay an APC?

We will provide a waiver or discount if you are based in a country which is classified by the World Bank as a low-income or a lower-middle-income economy with a gross domestic product (GDP) of less than $200bn. Please request this waiver of discount during submission.

What funding sources are available?

Many funding agencies allow the use of grants to cover APCs. An increasing number of funders and agencies strongly encourage open access publication. For more detailed information and to learn about our support service for authors.

APC waivers for substantial critiques of articles published in OA journals

Where authors are submitting a manuscript that represents a substantial critique of an article previously published in the same fully open access journal, they may apply for a waiver of the article processing charge (APC).

In order to apply for an APC waiver on these grounds, please contact the journal editorial team at the point of submission. Requests will not be considered until a manuscript has been submitted, and will be awarded at the discretion of the editor. Contact details for the journal editorial offices may be found on the journal website.

What is your APC refund policy?

Firenze University Press will refund an article processing charge (APC) if an error on our part has resulted in a failure to publish an article under the open access terms selected by the authors. This may include the failure to make an article openly available on the journal platform, or publication of an article under a different Creative Commons licence from that selected by the author(s). A refund will only be offered if these errors have not been corrected within 30 days of publication.

2023
Vol. 76 – n. 2

Caryologia

International Journal of Cytology, Cytosystematics and Cytogenetics

Table of contents